



Norwegian University of
Science and Technology

Oil Based Solar Concentrator with Heat Storage

Silje Fosseng Duley
Ragnhild Skahjem

Master of Science in Mechanical Engineering

Submission date: June 2016

Supervisor: Ole Jørgen Nydal, EPT

Norwegian University of Science and Technology
Department of Energy and Process Engineering

EPT-M-2016-33
EPT-M-2016-117**MASTER THESIS**

for

Student

Silje Fosseng Duley
Ragnhild Skahjem

Spring 2016

Oil based solar concentrator with heat storage

*Oljebasert solkonsentrator med varmelager***Background and objective**

Several methods for heat collection and heat storage have been tested for concentrating solar systems in a collaboration with several African universities (Ethiopia, Uganda, Tanzania, Mozambique). One option to be explored further is an oil based system. Novel components to be studied in a master thesis work are a new thermostat and a new method for forced thermal stratification in a storage.

The system will be tested in a small scale setup, with electrical heating of the absorber. Upscaling to a larger system will be evaluated based on a computational model. For this purpose, a dynamic model for the whole system will be developed. After qualification and testing, this concept can also be introduced to the collaborating universities in Ethiopia, Uganda, Tanzania, Mozambique.

The objective of the work is to demonstrate an oil based solar heat collection system with an integrated storage based on forced thermal stratification. The work builds on some initial work made in a specialization project.

The work is a collaboration between two master students.

The following tasks are to be considered:

- 1 Evaluate thermostat options and test in a circulation loop
- 2 Design, install and test a storage unit which preserves thermal stratification
- 3 Design, program and test a 1D dynamic incompressible model for the system
- 4 Document the work in a report which includes recommendations for further work

Within 14 days of receiving the written text on the master thesis, the candidate shall submit a research plan for his project to the department.

When the thesis is evaluated, emphasis is put on processing of the results, and that they are presented in tabular and/or graphic form in a clear manner, and that they are analyzed carefully.

The thesis should be formulated as a research report with summary both in English and Norwegian, conclusion, literature references, table of contents etc. During the preparation of the text, the candidate should make an effort to produce a well-structured and easily readable report. In order to ease the evaluation of the thesis, it is important that the cross-references are correct. In the making of the report, strong emphasis should be placed on both a thorough discussion of the results and an orderly presentation.

The candidate is requested to initiate and keep close contact with his/her academic supervisor(s) throughout the working period. The candidate must follow the rules and regulations of NTNU as well as passive directions given by the Department of Energy and Process Engineering.

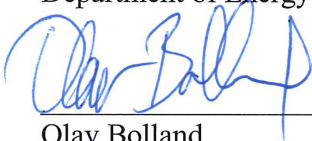
Risk assessment of the candidate's work shall be carried out according to the department's procedures. The risk assessment must be documented and included as part of the final report. Events related to the candidate's work adversely affecting the health, safety or security, must be documented and included as part of the final report. If the documentation on risk assessment represents a large number of pages, the full version is to be submitted electronically to the supervisor and an excerpt is included in the report.

Pursuant to “Regulations concerning the supplementary provisions to the technology study program/Master of Science” at NTNU §20, the Department reserves the permission to utilize all the results and data for teaching and research purposes as well as in future publications.

The final report is to be submitted digitally in DAIM. An executive summary of the thesis including title, student’s name, supervisor's name, year, department name, and NTNU's logo and name, shall be submitted to the department as a separate pdf file. Based on an agreement with the supervisor, the final report and other material and documents may be given to the supervisor in digital format.

- Work to be done in lab (Water power lab, Fluids engineering lab, Thermal engineering lab)
 Field work

Department of Energy and Process Engineering, 13. January 2016



Olav Bolland
Department Head



Ole Jorgen Nydal
Academic Supervisor

Research Advisor:

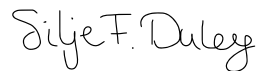
Preface

This is a master thesis written for the Department of Energy and Process Engineering, elaborated at the Norwegian University of Science and Technology in the spring of 2016. The thesis is carried out as a joint effort between two students, and it is an extension of the project work conducted in the fall of 2015.

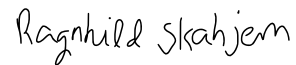
It is a collaboration project with the Ethiopian Institute of Technology in Mekelle, Ethiopia, on developing a concentrated solar thermal energy system with heat storage.

Trondheim, Norway

June 9, 2016



Silje Fosseng Duley



Ragnhild Skahjem

Acknowledgment

First of all we would like to express a sincere gratitude to our supervisor, Ole Jørgen Nydal, for the continuous support, enthusiasm and guidance that he has provided throughout the work with this thesis.

Besides our supervisor, we would like to thank Paul Svendsen, Benjamin Foss Hansen, Marius Laukholm and Markus Jensen for their immense assistance in the laboratory, and for always having a solution to the challenges faced during the experimental work. A sincere thanks also goes to Nicolas La Forgia and Carl Otto Gjelsvik, for their support and encouragement during the work with this thesis.

Additionally, we would like to thank Asfafaw Haileselassie Tesfay. The field study carried out in Mekelle would not have been possible if it was not for his tremendous support.

Silje Fosseng Duley & Ragnhild Skahjem

Abstract

A test system for storing solar thermal energy in the form of hot oil is constructed and tested. The motivation for the work is the need for a thermal energy storage which provides heat, from solar concentrators, for food preparation after sunset. The work is part of a collaboration project with a group of universities in Ethiopia, Uganda, Tanzania and Mozambique, focusing on renewable energy systems for off-grid communities.

Latent heat storage methods can be attractive for cooking purposes, as heat is available at a constant temperature (the phase change temperature). A similar benefit can also be obtained with a sensible heat storage, provided thermal stratification can be established. Natural stratification can be possible in vertical containers, where hot and cold volumes can be naturally separated if the density gradient is stable. However, as natural stratification can easily be disrupted due to the internal flow conditions, the objective of this work was to investigate a forced stratification method. This was done by separating the cold and the hot oil with a piston in a horizontal pipe. The piston moves as hot oil enters the storage inlet, and will be available for usage by exploiting manual valves.

To control the temperature from the concentrator into the storage a thermostat is needed. At a given temperature, the thermostat will divert the flow from a circulation loop, and direct it through the concentrator to the storage. Three principles were considered for the thermostat. The first was based on an edge welded bellows containing an evaporating liquid which expands and opens a valve. This showed acceptable opening times but too slow closing times, non-equilibrium effects were therefore prominent. The second was based on expansion of a gas volume connected to a small diameter bellows. This was unsuccessful due to the mechanical resistance of the bellows, in addition to the compressibility of the gas. In the third case, a linear solenoid actuator was used to operate the valve, triggered by a thermostat switch. This solution worked as expected, but is more complex and does require power.

A test system with electrical heating of the absorber pipe, instead of solar heating, was constructed and the concept was successfully demonstrated with the solenoid actuator. However, due to the material of the piston used, made of thermoplastic, the temperature in the system had to be adjusted based on its physical properties. Hence, high oil temperatures could not be tested. Nevertheless, focus was on demonstrating the principles of the system setups, which was accomplished. The test system shows the feasibility of a solar heat collection system which can charge and discharge a thermal oil storage unit at a constant temperature.

A 1D dynamic network model was programmed. The thermostat was implemented in the network as a switch between the flow rate in the two connected outlet pipes, and the storage was implemented with a dynamic separating section representing the position of the moving piston. The loss coefficients for the different parts of the system were tuned, and acceptable comparisons with experimental measurements were obtained.

A test setup with solar heating was tested at Mekelle University in Ethiopia. However, due to the duration of the study, and difficulties with the manufacturing of required components, there were issues with demonstrating the principles of the system.

Sammendrag

Et testsystem for lagring av solenergi i form av varm olje er konstruert og testet. Motivasjonen for arbeidet er behovet for et termisk energilager som gir varme fra en solkonsentrator, for tilberedning av mat etter solnedgang. Arbeidet er en del av et samarbeidsprosjekt med en gruppe universiteter i Etiopia, Uganda, Tanzania og Mosambik. Prosjektet har fokus rettet mot fornybare energisystemer for samfunn i avsidesliggende områder, hvor strømmettet ikke er tilgjengelig.

Latente varmelagringsmetoder kan være attraktivt for matlagingsformål, da varme er tilgjengelig ved en konstant temperatur (faseforandringstemperaturen). Om termisk stratifisering kan opprettholdes i lageret, kan en tilsvarende fordel oppnås med følbare varmelagring. Naturlig stratifisering er oppnåelig i vertikale beholdere, hvor varmt og kaldt kan separeres dersom tetthetsgradient er stabil. Ettersom naturlig stratifisering lett kan forstyrres av interne strømninger, er målet med dette arbeidet å undersøke lagring ved tvungen stratifisering. Dette gjøres ved å skille kald og varm olje med et stempel i et horisontalt lager. Stempelet beveger seg når varm olje strømmer inn ved innløpet til lageret, og er tilgjengelig for bruk ved hjelp av manuelle ventiler i systemet.

For å kontrollere temperaturen i oljen fra konsentratoren til lageret, vil en termostat være nødvendig. Når en gitt temperatur er oppnådd, vil termostaten avlede oljestrømmen fra en sirkulasjonskrets, og sørge for at strømmingen går via konsentratoren til varmelageret. Tre termostatkonsepter ble vurdert. Det første konseptet var basert på en sveiset belg som inneholdt en fordampende væske, som ekspanderer og dermed åpner en ventil. Ventilen ble åpnet med akseptabel temperaturrespons, mens temperaturresponsen for stengeprosessen var for langsom. Ikke-likevektseffekter syntes derfor å være fremtredende. Det andre konseptet var basert på ekspansjon av et gassvolum som var koblet til en belg med liten diameter. Dette var mislykket grunnet den mekaniske motstanden i belgen, i tillegg til kompressibiliteten av gassen. Det tredje konseptet var basert på en magnetventil, hvor dens låse-/frigjøringsmekanisme, utløst av en termostadbryter, ble benyttet for å operere ventilen. Denne løsningen virket som forventet, men var mer komplisert i tillegg til at den krever strømforsyning.

Et testsystem med elektrisk oppvarming av absorberingsrøret, i stedet for solvarme, ble konstruert og konseptet ble demonstrert ved bruk av magnetventilen. Da stempelet var lagd av termoplast, kunne systemet ikke testes ved høye temperaturer. Testsystemet demonstrerte prinsippet av et solfangersystem, som kan fylle og tømme en termisk oljelagringsenhet ved en konstant temperatur.

En 1D dynamisk nettverksmodell ble programmert. Termostaten ble implementert i nettverket som en bryter mellom oljestrømmen til de to tilkoblede utløpsrørene. Lageret ble anordnet med en dynamisk separasjonsseksjon, som representerer bevegelsen til stempelet. Tapskoeffisientene for de forskjellige delene av systemet ble innstilt, og akseptable sammenligninger med de eksperimentelle målingene ble oppnådd.

Et testoppsett basert på solvarme ble testet ved Mekelle University i Etiopia. På grunn av varigheten av studiet, og vanskeligheter med å fremstille nødvendige komponenter, var det problemer med å demonstrere prinsippene ved systemet.

Contents

| | |
|--|-----------|
| Preface | i |
| Acknowledgment | ii |
| Abstract | iii |
| 1 Introduction | 1 |
| 1.1 Background | 1 |
| 1.2 Objective | 1 |
| 1.3 Scope | 2 |
| 2 Theory | 3 |
| 2.1 Solar Cooker | 3 |
| 2.1.1 Direct Solar Cookers | 3 |
| 2.1.2 Indirect Solar Cookers | 4 |
| 2.2 Temperature Responsive Devices | 4 |
| 2.2.1 Thermostat Concepts of This Research | 5 |
| 2.3 Thermal Energy Storage | 7 |
| 2.3.1 Sensible Heat Storage | 7 |
| 2.3.2 Latent Heat Storage | 8 |
| 2.3.3 Thermochemical Heat Storage | 9 |
| 2.4 Literature Review | 9 |
| 3 Thermostat & Storage | 13 |
| 3.1 Liquid Filled Bellows | 13 |
| 3.1.1 Liquids - Working Mediums | 15 |
| 3.2 Design of the Thermostat | 16 |
| 3.3 Design Improvements | 17 |
| 3.4 Gas Filled Bellows | 18 |
| 3.5 Linear Solenoid Actuator | 18 |
| 3.5.1 Design of the Thermostat | 20 |

| | | |
|----------|--|-----------|
| 3.6 | Storage | 21 |
| 3.6.1 | Heat Transfer and Storing Medium | 22 |
| 3.6.2 | Piston - Physical Barrier in Storage | 22 |
| 4 | Experiments With Bellows | 25 |
| 4.1 | Preliminary Testing - Liquid Filled Bellows | 25 |
| 4.2 | Data Acquisition With LabVIEW | 26 |
| 4.3 | System Setup - Oil Bath | 27 |
| 4.4 | Experimental Method | 27 |
| 4.4.1 | Observations | 28 |
| 4.4.2 | Results | 29 |
| 4.4.3 | Discussion | 30 |
| 4.5 | System Setup - Circulating Oil System | 31 |
| 4.6 | Experimental Method | 32 |
| 4.6.1 | Observations | 36 |
| 4.6.2 | Results | 37 |
| 4.7 | Discussion and Comparison of The Experiments | 54 |
| 4.8 | Procedure With The Gas Filled Bellows | 56 |
| 4.8.1 | Results | 60 |
| 4.8.2 | Discussion | 61 |
| 5 | Experiments - Complete System Setup | 63 |
| 5.1 | System Setup | 63 |
| 5.1.1 | Data Acquisition With LabVIEW | 66 |
| 5.2 | Experimental Method | 68 |
| 5.2.1 | Observations of The System | 70 |
| 5.2.2 | Results | 73 |
| 5.3 | Discussion and Comparison of The Experiments | 83 |
| 6 | Dynamic Simulation | 86 |
| 6.1 | Equations for Fluid Flow and Heat Transfer | 86 |
| 6.1.1 | Simplifications | 87 |
| 6.1.2 | The Mathematical Model | 88 |
| 6.2 | 1D Dynamic Model | 89 |
| 6.2.1 | Discretized Energy Equation | 89 |
| 6.2.2 | Pipe Network Analysis | 90 |
| 6.2.3 | Implementation | 92 |
| 6.3 | Simulation of The Experimental Work With The Complete System | 95 |

| | | |
|----------|---|---------------|
| 6.3.1 | Network Setup | 95 |
| 6.3.2 | Simulation Results | 98 |
| 6.3.3 | Discussion | 103 |
| 7 | Field Work at Mekelle University, Ethiopia | 105 |
| 7.1 | The Motivation | 105 |
| 7.2 | System Components, Material And Equipment | 106 |
| 7.3 | System Setup | 108 |
| 7.3.1 | Data Acquisition With Pico Data Logger | 113 |
| 7.4 | Experimental Method | 114 |
| 7.4.1 | Observations of The System | 114 |
| 7.4.2 | Results | 115 |
| 7.5 | Discussion | 115 |
| 8 | Conclusions and Recommendations for Further Work | 118 |
| 8.1 | Conclusions | 118 |
| 8.2 | Recommendations for Further Work | 122 |
| | Bibliography | 125 |
| I | Appendices | II |
| A | The Liquids Inside The Bellows | III |
| B | Duratherm 630 | XIII |
| C | Weldon Racing Pumps | XIX |
| D | The Bellows | XXI |
| E | The Gas Bellows | XXIV |
| F | The Solenoid | XXVIII |
| G | Capillary Thermostat | XXXI |
| H | Risk Assessment | XXXIII |

List of Figures

| | | |
|------|---|----|
| 2.1 | Graph Displaying Temperature and Supplied Heat in a Latent Heat Storage | 8 |
| 3.1 | A Sketch of the Bellows | 15 |
| 3.2 | A Picture of an Expanded and Compressed Bellows in the Thermostat Configuration (Oil Bath Experiment) | 15 |
| 3.3 | Picture of the Liquids Tested Inside the Bellows. | 16 |
| 3.4 | Design of the Thermostat | 17 |
| 3.5 | Cross Section of a Solenoid with and Without a Permanent Magnet | 19 |
| 3.6 | Picture of the Solenoid Taken from Above and from the Side | 20 |
| 3.7 | Picture of the Solenoid in the Latched and Unlatched Position | 21 |
| 3.8 | Picture of the Sensible Heat Storage Half Charged with Thermal Oil | 21 |
| 3.9 | Picture of the Stainless Steel and POM (Thermoplastic) Pistons Used Inside the Storage | 23 |
| 4.1 | Representation of the Logging Setup in the Experiments with the Bellows | 26 |
| 4.2 | The Oil Bath Represented by an Insulated Steel Tank Filled with Oil | 27 |
| 4.3 | Plot of the Heat Cycles in the Third Oil Bath Experiment | 30 |
| 4.4 | The Circulating Oil System Setup | 32 |
| 4.5 | An Illustration of the Thermostat in the Circulating oil System at Different Oil Temperatures. | 33 |
| 4.6 | Plot Showing Vapor Pressure Curves for Several Liquids | 35 |
| 4.7 | The Vacuum Pump System Setup | 36 |
| 4.8 | Plot of the Circulating Oil Experiment - Test 1 (Second Experiment) | 39 |
| 4.9 | Plot of the Circulating Oil Experiment (Internal Vacuum) - Test 2 (Second Experiment) | 40 |
| 4.10 | Plot of the Circulating Oil System - Test 3 | 43 |
| 4.11 | Picture of the Bellows Inside the Confining Tunnel, After Parts of the Tunnel Has Been Cutoff | 45 |
| 4.12 | Illustration of the Initial Position of the Bellows in the Third Experiment with Ethanol | 46 |
| 4.13 | Plot of the Circulating Oil System - Test 4 | 47 |
| 4.14 | Plot of the Circulating Oil System - Test 5 | 48 |
| 4.15 | Plot of the Circulating Oil System - Test 6 | 49 |

| | | |
|------|--|-----|
| 4.16 | Plot of the Circulating Oil System - Test 7 (First Experiment) | 51 |
| 4.17 | Plot of the Circulating Oil System - Test 7 (Second Experiment) | 52 |
| 4.18 | Plot of the Circulating Oil System - Test 8 (Third Experiment) | 52 |
| 4.19 | Finding the Displacement Volume of the Bellows as it Expands 2.50 cm. | 57 |
| 4.20 | Plot of the Copper Coil Dimensions for Given Gas Bellows Parameters. | 58 |
| 4.21 | The Gas Bellows System Setup | 59 |
| 5.1 | Picture of the Circulating Oil Based System Setup Containing an Application Unit and a Storage. | 64 |
| 5.2 | Simple Sketch of the Circulating Oil System, Including Locations and Specifications for Pipes, Thermocouples and Valves | 66 |
| 5.3 | Picture Showing the Arrangement of the Valves in Case 1 | 67 |
| 5.4 | A Screen Shot Visualizing the Experimental Data Acquisition Setup in LabVIEW. | 68 |
| 5.5 | The Magnet Ball Travelling on the Outside of the Storage | 70 |
| 5.6 | Pictures of the Storage Taken by a Thermal Camera | 71 |
| 5.7 | Pictures of the POM Piston in an Oil Bath and the PEEK Piston Inside the Storage | 72 |
| 5.8 | Plots of the First and Second Experiment Conducted with the Solenoid. The Temperature of the Thermostat Was Set to 90°C in LabVIEW | 74 |
| 5.9 | Plots of the Third Experiment Conducted with the Solenoid. The Temperature of the Thermostat Was Set to 110°C in LabVIEW | 78 |
| 5.10 | Plots of the Fourth Experiment Conducted with the Solenoid. The Temperature of the Thermostat Was Set to 130°C in LabVIEW | 79 |
| 5.11 | Plots of the Fifth Experiment Conducted with the Solenoid. The Temperature of the Thermostat Was Set to 130°C in LabVIEW | 82 |
| 6.1 | Illustration of the Piston in the Storage | 90 |
| 6.2 | Illustration of Branch Connections | 91 |
| 6.3 | Flow Conservation Through the Thermostat | 92 |
| 6.4 | Storage with a Dividing Piston | 92 |
| 6.5 | Flowchart of the Model | 94 |
| 6.6 | The System Setup in the Model | 95 |
| 6.7 | Simulation Results from Test 1 | 98 |
| 6.8 | Simulation Results from Test 4 | 100 |
| 6.9 | Comparison of the Numerical and Experimental Results | 101 |
| 6.10 | Graphical Visualization of the Simulation Results | 103 |
| 7.1 | Components Utilized in the System Constructed at Mekelle University | 107 |
| 7.2 | Machines Utilized During Construction of the System at Mekelle University | 108 |
| 7.3 | Critical Components Affecting the Quality of the System Constructed at Mekelle University | 109 |

| | | |
|------|--|-----|
| 7.4 | The Circulating Oil Based System Setup at Mekelle University | 109 |
| 7.5 | The Electronic Board Connected to the Solenoid | 111 |
| 7.6 | The Pump and the Specifications of the PV Panel Used | 112 |
| 7.7 | The Thermostat Solution and Offset Parabolic Dish with Receiver Utilized at Mekelle University | 112 |
| 7.8 | The Data Acquisition With Pico Data Logger | 113 |
| 7.9 | Plot of the Heating Process in the Second Experiment Conducted at Mekelle University . . . | 115 |
| 7.10 | Plot of the Third Experiment Conducted at Mekelle University | 116 |

List of Tables

| | | |
|------|---|----|
| 3.1 | Material Properties for the Different Piston Materials Utilized | 22 |
| 4.1 | Temperatures of Interest - Experiments With the Liquid Filled Bellows in the Oil Bath | 28 |
| 4.2 | Temperatures Measured at the Surface of the Bellows in the Oil Bath Experiments | 29 |
| 4.3 | Temperatures of Interest - Experiments With the Liquid Filled Bellows in the Circulating Oil System | 37 |
| 4.4 | Test 1 - Temperatures Measured at the Surface of the Bellows in the Circulating Oil Experiments | 38 |
| 4.5 | Test 2 - Temperatures Measured at the Surface of the Bellows in the Circulating Oil Experiments (Internal Vacuum) | 40 |
| 4.6 | Temperatures of Interest - Experiments With the Liquid Filled Bellows in the Circulating Oil System | 42 |
| 4.7 | Test 3 - Temperatures Measured at the Surface of an Antifreeze Filled Bellows in a Circulating Oil System. It Was Used a Spring With $k = 0.7 \text{ N/mm}$ | 43 |
| 4.8 | Test 4 - Temperatures Measured at the Surface of an Ethanol Filled Bellows in a Circulating Oil System | 46 |
| 4.9 | Test 5 and Test 6 - Temperatures Measured at the Surface of an Ethanol Filled Bellows in a Circulating Oil System, Without the Presence of a Return Spring | 47 |
| 4.10 | Test 7 and Test 8 - Temperatures Measured at the Surface of a 1,2-Propylene Glycol Diacetate Filled Bellows in a Circulating Oil System | 51 |
| 4.11 | Comparison of the Temperature Intervals Required to Open and Close Port 3 in the Experiments With the Liquid Filled Bellows | 55 |
| 5.1 | Valve Arrangements in the Complete System Setup | 66 |
| 5.2 | Temperatures of Interest - Complete System Setup | 69 |
| 5.3 | Time Intervals and Critical Temperatures in Test 1 - Complete System Setup | 73 |
| 5.4 | Time Intervals and Critical Temperatures in Test 2 - Complete System Setup | 78 |
| 5.5 | Time Intervals and Critical Temperatures in Test 3 - Complete System Setup | 80 |
| 5.6 | Time Intervals and Critical Temperatures in Test 4 - Complete System Setup | 81 |

| | | |
|-----|--|-----|
| 5.7 | Comparison of the Experiments Conducted on the Complete System Setup | 83 |
| 6.1 | Boundary Conditions and Parameters Applied to the Entire System. | 96 |
| 6.2 | Initial Network Setup | 97 |
| 6.3 | Temperatures of Interest- Simulation Test 1 2 nd Experiment | 99 |
| 6.4 | Temperatures of Interest- Simulation Test 4 | 100 |
| 7.1 | Measured Temperatures - Sytem Setup in Mekelle | 113 |

Nomenclature

| | |
|-----------|--|
| ϕ | dissipation [W/m^3] |
| ρ | density [kg/m^3] |
| A_r | cross-sectional area [m^2] |
| A_s | surface area [m^2] |
| c_p | specific heat capacity at constant pressure [J/kgK] |
| I | index of flow direction |
| q'' | heat flux [W/m^2] |
| Q_v | volumetric heat source term [W/m^3] |
| r_b | radius of pipe [m] |
| r_i | inner radius of pipe [m] |
| r_o | outer radius of pipe [m] |
| r_s | outer radius of storage [m] |
| T_i | temperature at r_i [$^{\circ}C$] |
| T_o | temperature at r_o [$^{\circ}C$] |
| T_{air} | ambient air temperature [$^{\circ}C$] |
| u_p | mean velocity in the longitudinal direction in the pipes [m/s] |
| u_s | mean velocity in the longitudinal direction in the storage [m/s] |
| 1D | one dimension |
| e | internal energy [J/kg] |
| h | heat transfer coefficient [W/m^2K] |

| | |
|---|---|
| k | thermal conductivity [W/mK] |
| p | pressure [N/m^2] |
| t | time [s] |
| U | overall heat transfer coefficient [W/m^2K] |
| u | mean velocity in the longitudinal direction [m/s] |

Chapter 1

Introduction

The work with the master's thesis is an extension of the project work carried out in the fall of 2015. This opening chapter will present the background of the study, together with its objective and scope.

1.1 Background

Many of the Sub-Saharan African countries are heavily dependent on firewood for food preparation. Approximately 80 % of the population has this as their main source of energy, embedded in the fact that they live in remote areas, out of reach of the electrical grid (IEA [2015]). The use is not sustainable and it cause high indoor smoke pollution (Belward et al. [2011]). This have a negative impact on people's health, mainly affecting women and children who spends most of the time with the food preparations. Deforestation is also an emerging problem, and is increasing along with the population (Nydal [2014]). Small-scale concentrated solar thermal energy can provide a clean and sustainable alternative for firewood. With the generous amount of sunshine spread over the African continent, the utilization of a concentrated solar energy system with heat storage could have great potential.

The small-scale system should be a stand-alone unit, and due to its application purpose, it should be produced and maintained by simple means. A low-cost and robust system is therefore required. The system must be safe to handle, and it should be able to operate at high temperatures (Nydal [2014]). Demonstration will be conducted on an oil based heat collection system with an integrated storage based on forced thermal stratification. The system will use a pump to provide circulation in the system, and oil for sensible heat storage.

1.2 Objective

The objective of this master's thesis was to demonstrate and test an oil based solar collection system with an integrated heat storage, based on forced thermal stratification. The oil based system could substitute

firewood as an energy source in developing countries, and should therefore be robust, low-cost and easy to maintain.

1.3 Scope

Experimental work will be conducted to develop a self-regulating oil system, in terms of controlling the direction of the oil in the system. The regulation will be obtained by a thermostat. Three different thermostat solutions will be tested; a liquid filled bellows, a gas filled bellows and a solenoid. Experimental testing will be carried out in a stationary oil system and in a pump driven circulating oil system. Duratherm 630 will be used as the heat transfer medium.

In the circulating oil system, a storage unit based on forced thermal stratification will be constructed, integrated, and tested. The thermal stratification will be ensured by a piston. Three different piston materials will be tested; stainless steel, POM and PEEK (thermoplastics). The system will be tested with both electrical heating and with concentrated solar energy heating.

A computational model will be developed as a simplified dynamic 1D model. It will be derived from the numerical integration of conservation equations of mass and energy (for the oil). A finite difference approach will be used, with an upstream first order scheme, integrated explicit in time. The model shall be designed as a network of pipes connected to each other. A mathematical approximation of the thermostat and the storage will also be implemented into the model. The simulation results will be compared with measured data from the experiments.

After qualifying and testing, the system will be constructed and tested at The University of Mekelle, at The Ethiopian Institute of Technology.

Chapter 2

Theory

This chapter will present different types of solar cookers, thermostat solutions, thermal storage solutions and numerical approaches. A brief introduction of the different concepts will be conducted, before a literature review will be presented.

2.1 Solar Cooker

A solar cooker is a device that utilize solar energy for food preparation, and is usually classified into direct and indirect systems. A direct solar cooker utilize the solar radiation directly in the cooking process, whereas an indirect solar cooker separates the solar energy receiver from the cooking area ([Cuce and Cuce \[2013\]](#)).

2.1.1 Direct Solar Cookers

There are essentially three different categories of direct solar cookers. The most common type is a box cooker, which is non-concentrating. A box cooker consist of an inner box covered with plastic or clear glass, a reflector and insulation ([Srinivasan \[2013\]](#)). It can reach temperatures up to 140°C and is relatively easy to construct. To reach higher temperatures a more concentrated focus point is necessary. Panel cookers use flat panels which reflect and focus the radiation. They are easy and cheap to make, but do not obtain high temperatures when the sun is hidden behind clouds. The system is also unstable in high wind. With a parabolic solar cooker, the temperature can reach 180°C. However, it is a system that requires more precision from the user, and exactness during the construction process to focus the sunlight ([Mussard \[2013\]](#)). A concern with parabolic solar cooker is related to safety issues. To prepare the food the user is enticed to access the focal point of the dish ([Kaasjager and Moeys \[2012\]](#)). With a direct solar cooker, the user can only prepare food outside during the sunny parts of the day.

2.1.2 Indirect Solar Cookers

An indirect solar cooker utilizes a heat transfer medium to transport the collected energy from the receiver to the cooking application. Heat transfer mediums can be solids, liquids and gasses. There are many considerations when selecting the appropriate heat transfer medium. Temperature-dependent properties as density, specific heat capacity, heat conductivity and kinematic viscosity influence the heat transfer rate between the medium and the surface, which affect the efficiency of the solar cooker (Kilger). Vapor pressure and flash point affects the suitable operating temperature range. Corrosive activity towards metals and alloys is also important regarding the duration of the system.

Heat transfer mediums in liquid or gas state can be carried from the receiver to the application by a pump or by self-circulation. The principles of a self-circulation system are the density difference in cold and hot mediums. Density differences cause variation in the gravity forces which induce buoyancy-driven flow, also called natural convection. These principles are widely used in solar hot water tanks (Mussard [2013]).

2.2 Temperature Responsive Devices

A thermostat is a heat controlling device, which senses the temperature of a given system, and thus has the ability of regulating the system heat. There are a variety of thermostat solutions available on the market, where type, size, price and sensors are some of the varying factors. Some of the thermostat concepts which could be used in an oil based system are thermal actuators, thermally activated valves, and temperature controllers; consisting of a thermostat and a valve. In all of these thermostat concepts, temperature change alone can be exploited to operate a given device.

A thermal actuator consists of a solid material, for example wax, which is sealed in the actuator (Therm-Omega-Tech [2014]). As a result of temperature increase, the wax will change phase from solid to liquid. Consequently, since the volume of the liquid will be greater than the volume of the solid, a piston will start to move and extend equivalent. In the opposite case, when the temperature is being reduced, the piston will retract if a return spring is acting on the piston. The temperature interval, which the phase transition and obtained piston motion occurs over, is small (Therm-Omega-Tech [2014]). Hence, the thermal actuator will provide precise control of a device at a particular temperature.

A thermally activated valve is based on a similar concept as the thermal actuator, where phase transition from solid to liquid works as the driving mechanism. However, what distinguishes them is that this type of control device contains valve components. Depending on the application, the thermally activated valve will have two to four ports, where three ports will be required if one need a thermal diverter valve (Rostra-Vernatherm [2014]). Hence, the valve contains one inlet port and two outlet ports. As a result, when a preset temperature level is reached, the flow will be diverted from the one outlet to the other.

Companies such as ThermOmegaTech, Rostra Vernatherm and Senior Aerospace delivers these types of heat controlling devices. However, they come with some limitations. The actuators manufactured by

ThermOmegaTech can not handle more than between 121.1°C and 132.2°C (with a maximum temperature exposure of 149°C). Rostra Vernatherm does manufacture actuators and activated valves in which can tolerate temperatures up to 199°C, however, they comprise rubber components which will break down at 200°C. Senior Aerospace manufacture actuators meeting higher temperature demands, however, all of their actuator products are custom designed, tested to meet the specific design requirements of each customer and application. Unfortunately, they do not have resources available to custom design a part for low volume or one-off requirements.

Thermostat controllers consisting of a thermostat and a valve, which can meet high temperature demands, can be delivered by a company named Clorius Controls. Their thermostat is a thermal actuator, consisting of a liquid filled sensor, which can operate in the area between -30°C up to 280°C (Clorius-Controls [n.d.]). For instance, at temperatures between 140°C and 200°C, paraffin will be the sensing liquid. Onto the thermostat a three-way control valve can be fixed. The function of the three-way valve is similar to that of the thermally activated valves containing three ports. This type of temperature controlling device can be used to regulate cold/hot water, steam or oil in heating as well as in cooling systems. Nevertheless, even if this concept can handle high temperatures, it is too expensive to utilize in a small-scale concentrated solar energy system.

2.2.1 Thermostat Concepts of This Research

The thermostat concept chosen for the system was based on three different approaches; phase transition, superheated gas and electromagnets. The theory behind the different approaches will be reviewed in the following paragraphs.

Phase Transitions - Evaporation & Condensation

While evaporation represents the transition from a liquid to a gas, condensation represents the opposite. The difference between evaporation and condensation is that while a molecule is being emitted from a surface in the evaporation process, it is being absorbed by the surface in the condensation process (Barrett and Clement [1991]). The surface is defined as the interface (at saturation state) between respectively a liquid and a vapor. If, for instance, a closed system is being exposed to a temperature increase and decrease around the same temperature, where the pressure will increase and decrease accordingly along the same curve, the rates of evaporation and condensation would be in equilibrium. However, there are some factors in which can limit these processes. For instance, the presence of a noncondensable gas, e.g. air in a given system, will in the condensation process accumulate on the interface, and thus build up a noncondensable layer. An accumulation limiting the diffusion of vapor through the layer (Barrett and Clement [1991]). This phenomenon can be better understood by looking at a study conducted by (Minkowycz and Sparrow [1966]), which illustrates the effect the presence of a noncondensable gas will have on the condensation process in a given system. The study shows that more than a 50 percent reduction in the heat transfer would be persistent if a mass fraction as small as 0.5 percent of the noncondensable gas would be present in the

system. Additionally, when increasing the amount of the noncondensable gas, the result was a correspondingly decrease in the condensation heat flux. What also emerged from the study was that when the noncondensable mass fraction was held constant (e.g. closed system), the reduction in heat transfer would become greater with an increased difference between the bulk-to-wall temperatures. Minkowycz and Sparrow's results also showed that the effect of the noncondensable gas became significantly enhanced when the bulk saturation temperature (thus the pressure level in the system) was decreased. The reason why the system experienced such substantial reductions in heat transfer, even though there was such an insignificant concentration of noncondensable gas in the system, was due to what happens at the moment when the condensation process is being initiated. When the vapor is being carried towards the interface, the convective flow carrying it will also bring the noncondensable gas. At the interface, impermeable for noncondensable gases, a noncondensable gas accumulation will therefore be introduced, producing a noncondensable layer. The accumulation of the noncondensable gas at the interface will provide an accompanying reduction in the partial pressure of the vapor (at the interface). The outcome being a lower saturation temperature at which the condensation process will occur. Thus, the reduced heat transfer rate is a result of the diffusional resistance of the vapor and the noncondensable gas mixture. Minkowycz and Sparrow also conducted a study on a system containing a noncondensable gas and a superheated vapor. They discovered that the presence of the noncondensable gas had the identical effects as what was observed in the saturated mixture system.

When it comes to the evaporation process, the effect of a noncondensable gas is likely to be of less importance. The noncondensable gas will during this process, in contrast with the condensation process, be carried away from the interface, instead of accumulating on it ([Peterson and Kageyama \[1993\]](#)).

Chapter 3 will review how this concept could be applied to a liquid filled bellows, and Chapter 4 will get a better understanding of how this theory can be applied to what was observed in the experiments.

Superheated Gas

The superheated gas principle arises from experimental results acquired by Joseph Louis Gay-Lussac, in 1802. He observed that equal volumes of real gases, at a given temperature increase, under an isobaric pressure condition (constant pressure condition), would cause the gases to expand the same volume ([Benedict \[1984\]](#)). The gases he studied included oxygen, nitrogen, hydrogen, carbon dioxide and air.

In Chapter 3 we will review how this concept could be demonstrated with a gas filled bellows, and in Chapter 4 the observations made during the experiments will be reviewed.

Electromagnets

Electromagnets are coils of wire which behaves like bar magnets. When an electric current is being sent through the coil, electromagnetism is produced ([Electronics \[2016\]](#)). This occurs due to a magnetic field that is being created when the current is being passed through the coil/conductor. Thus, giving the conductor a distinct north and south pole. The poles are determined based on the direction of the electric current. This

phenomenon is what one of our thermostat solutions are based upon, the linear solenoid, at which will be carried out in more detail in Chapter 3.

2.3 Thermal Energy Storage

Solar energy is a highly intermittent energy source. Consequently, there will be imbalance between energy supply and users demand. An efficient and economical heat storage is therefore crucial to effective and broad the utilization of solar energy for thermal applications. Thermal energy can be stored as sensible heat, latent heat or as thermochemical heat. This study will focus on high temperature thermal storage solutions, required for cooking applications.

2.3.1 Sensible Heat Storage

Sensible heat is related to temperature variations in a medium without a phase change being present. Thermal energy is accumulated as a result of an increasing temperature in the storage medium. The amount of energy stored can be represented as:

$$Q = \int_{T_1}^{T_2} mC_p dT \quad (2.1)$$

where C_p is the specific heat, T_1 is the initial temperature, T_2 is the final temperature and m is the mass of the material.

Sensible heat can be stored in liquids (water, oil, molten salt) and in solids (rocks, metals) (Cárdenas and León [2013]). A sensible heat storage (SHS) is the simplest and least expensive form of storing thermal energy. However, a disadvantage with SHS is its inability to release energy at a constant temperature.

For a low temperature liquid media storage, water is the most common storage medium. It has a high heat capacity and is cheap and available. However, water is not suitable for high temperature storing due to its boiling point. The most common alternative in solar power systems are oil and molten salt. However, the heat capacity is only about 25-50 % compared to water (Hasnain [1998]). A storage could also be based on solid mediums, where for instance stones and bricks are readily available and at a low cost. The most efficient solid as storing medium, but also the more expensive one, is cast iron. Cast iron exceed the energy stored per volume compared to water (Hasnain [1998]). For high temperature storage in solids, inorganic salt or metals are suitable. However, these materials are often expensive.

Natural & Forced Thermal Stratification

A sensible heat storage containing a liquid can be based on either natural or forced thermal stratification. If the density gradient is stable, natural stratification can be achieved (Bahnfleth and Musser [1998]), and can be exploited in vertical containers where hot and cold volumes of the liquid are naturally separated. However, natural stratification can easily be disrupted due to internal flow conditions. Hence, if a stable density

gradient will be difficult to obtain, forced stratification can be a substitute. This form of stratification can be achieved in a horizontal pipe, where a physical barrier (e.g. a piston) can provide separation between the hot and the cold volumes.

2.3.2 Latent Heat Storage

A latent heat storage (LHS) utilize phase change. Latent heat is energy released or absorbed during these processes, without change in temperature. Even though the liquid-vapor phase change has a higher energy storage potential, the solid-liquid or solid-solid phase change are most commonly used. This is due to the practical problems of storing vapor.

Figure 2.1 illustrates the principles of a latent heat storage. As the material is heated the temperature increase until it reaches phase change temperature. At this point, the material absorbs large amounts of heat energy in order to carry out the phase transition. The cooling process is opposite and releases a large amount of heat during the process. Hence, it is possible to extract the stored energy as heat at a constant temperature, equal to the phase change temperature (Cárdenas and León [2013]). The amount of energy stored can be represented as:

$$Q = \int_{T_1}^{T_m} mC_p dT + ma_m \Delta h_m + \int_{T_m}^{T_2} mC_p dT \quad (2.2)$$

where C_p is the specific heat, T_1 is the initial temperature, T_2 is the final temperature, T_m is the melting temperature, m is the mass of the material, a_m is the fraction melted, Δh_m is the heat of fusion per unit mass(J/kg).

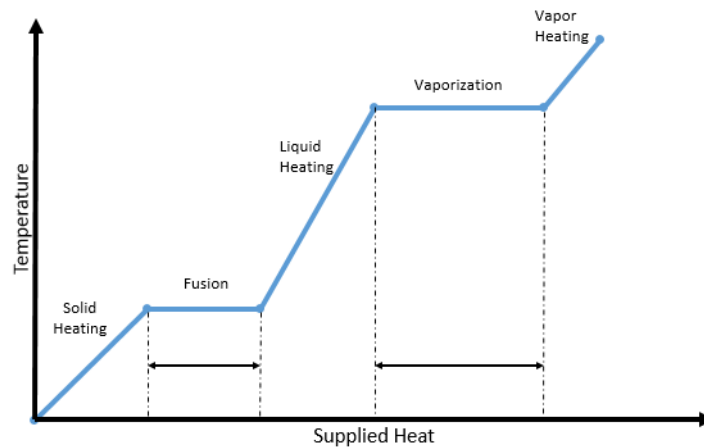


Figure 2.1: Graph shows the correlations between temperature and supplied heat during heating and phase change (Cárdenas and León [2013]).

A latent heat storage often requires less volume of storage material compared to a sensible heat storage. However, for a LHS to work efficiently for food preparation applications, the phase changing material(PCM) requires a high melting point. Nitrate salts are suitable for these purposes, but there are some challenges

with the low thermal conductivity of these materials. Thus, a challenge which results in low power density (W/m^3) during the charging/discharging processes (Laing et al. [2009]).

2.3.3 Thermochemical Heat Storage

A thermochemical heat storage (THS) take advantage of the energy stored in chemical compounds. The principle is represented in Equation 2.3. When the right amount of heat is added to compound AB, it will break into two compounds which can be stored separately. A reverse process will free almost the same amount of heat that was required to separate them (Aydin et al. [2015]).



THS has almost negligible losses during the storing process, compared to SHS and LHS which requires insulation. THS is a relatively new technology, but has great potential.

2.4 Literature Review

Kaasjager and Moeys tested a hot plate solar cooker with electricity generation in 2012 (Kaasjager and Moeys [2012]). The cooker used a parabolic trough mirror to reflect and concentrate the solar radiation. Evacuated tubes absorbed the reflected light and a heat pipe transported the energy to the hot plate. The evacuated tubes were designed to absorb the sunlight and provide vacuum insulation for the heat pipe, which was inserted in the center of the evacuated tube. The heat pipe was a hollow cylinder with a small amount of water inside. The system is about 2 m long and mounted at an angle of 20° . When the water inside the heat pipe evaporated, it moved at high speed as gas towards the condenser, which were clamped under the aluminum hot plate. The condensed water flows back to the evaporation side by means of gravity. The cooker was tested by boiling three liters of water in a pot placed at the hot plate. The temperature measured in the adiabatic part, between the condenser and the evaporation area, reached 175°C as the water heated and 200°C during boiling. Without a pot at the hot plate, the system reached over 250°C . The parabolic trough needed focusing adjustments every twenty minutes, but the system was not heavy and could be lifted by one person. A thermoelectric generator was connected to the hot plate and could combine cooking with electrical generation. The evacuated tube can be bought relatively cheap, but demand maintenance to ensure vacuum in the pipe.

In 2012, Maxime Mussard tested a self-circulating system at NTNU with oil as the heat transfer medium. The test showed great abilities for thermal oil as a heat transfer medium. A challenge in the study was overheating of the oil, which reduced the durability. By increasing the diameter of the absorber pipe, the reduction of the friction increased the flow rate, and gave a lower temperature in the absorber. This was at the expense of higher thermal losses. His worked showed many advantages for the concept of a self-circulating

system, such as absent of a pump and self-regulation of the temperature. However, a self-circulating loop will have a slower flow rate than a pump driven system, and the heat transfer will therefore be weaker.

An oil based storage system based on natural thermal stratification was tested at NTNU in 2014. The study was performed by Alejandro de la Vega Fernández ([Fernández \[2014\]](#)), and was based on a similar system to the one carried out through this Master's work. The aim of Fernández's study was to observe the stratifying effect of the oil flowing into the storage, in which was controlled by a manual valve. He illustrated the temperatures of the oil in the storage by the use of a thermal camera. The images taken with this camera, however, visualized the temperature distribution on the surface of the heat storage tank, and thus not the actual temperature distribution of the oil. The images could be interpreted as if stratification was reached; however, the author concludes that this was not the case. Natural thermal stratification therefore does not seem to have been achieved. To obtain stratification, it is important that the incoming hot fluid is maintained at a constant temperature, which can be difficult to achieve in a solar energy storage [Dincer and Rosen \[2002\]](#). An alternative to natural stratification could be to use forced stratification. In addition, the temperatures of the oil in the storage, illustrating whether thermal stratification is achieved or not, should be based on another concept than a thermal camera. For instance, it is possible to use thermocouples as control points inside the storage, not causing any interference with the oil flow.

A study conducted at Cal Poly Physics in 2009, tested a thermal storage designed for cooking application ([Rapp \[2010\]](#)). Their objectives were to decrease complexity and reduce costs for a solar cooking technology with thermal storage. They designed a storage using sand as the storing medium. The storage was directly heated by sun irradiation, and the hot plate was located at the top of the storage. After 9 hours of heating, the temperature at the top of the storage, near the cooking plate, was about 350°C. 14 hours of cooling gave a temperature around 250°C. Further recommendation from the experiment was to insert a thermal conduit in the storing medium to give a faster distribution of heat in the storage.

A study conducted at Bahir Dar university investigated a combination of NaNO₃ and KNO₃ as the PCM in a LHS ([Wagari and Aman](#)). A combination of 60% NaNO₃ and 40% KNO₃ was concluded as the most promising combination, with a melting point at 225.38°C. 1 kg of the PCM had a charging time of 50 minutes and a discharging time of 4.5 hours from 300°C down to 100°C. These results suggest that LHS can be used for high temperature storage, including cooking applications.

In 2014, Tesfay tested a small-scale high temperature tracking concentrator with heat storage at NTNU and at Mekelle University. Solar salt(40 % KNO₃ and 60% NaNO₃) was used as the PCM with a melting point at 210-220°C. Steam was applied as the heat transfer medium, and the heat transfer process was governed by natural circulation boiling-condensation between the boiler and a stove ([Tefay et al. \[2014\]](#)). The system utilized an automatically tracking mechanism, governed by a motor and gear, controlled the major axis of the collector (east-west) assisted by a secondary (north-south) manual adjuster. The setup for the tracking mechanism was a rather large construction. High pressure was required in the heat transfer loop when utilizing steam as the heat transfer medium. This gave some safety concerns, but was manageable

as long as the heat transfer loop was small. Tesfay raised concerns regarding accessibility of the chemical required for the thermal storage in some parts of Africa.

In 2013, Mussard tested a self-circulating liquid based solar collector with heat storage (Mussard [2013]). In his study, he compared an oil- and salt ($NANO_3 - KNO_3$) storage with an aluminum- and salt based heat storage. The research showed that a large volume of oil was more efficient than an aluminum based heat storage. He also tested the high temperature thermal storage potential of sensible and latent heat based systems at NTNU. He concluded that latent heat showed greater potential than a sensible heat storage at the temperature range of 180 to 250°C. A latent heat storage requires less volume and therefore less energy to preheat to operational temperature and it is cheaper to insulate.

It does not seem to be many thermostat solutions tested on a system similar to the one constructed in this research. Thus, the thermostat concept is still a field requiring further research. However, one thermostat solution that has been tested at NTNU before is a bimetallic-type thermostat, which was constructed to control the heat in an oil based system. This type of thermostat contains a strip, in which comprises two materials, each having different thermal expansion coefficients. The two metals are welded together to become one bimetallic unit/blade (HVAC-Specialist [2011]). The bimetallic unit is securely anchored at one edge, and connected to a contact point on the other edge. The contact point will be closed/joined as long as the temperature in the system is below a certain temperature. The metals are arranged so that the one with the largest expansion coefficient is placed at the bottom of the unit. As the temperature rises to a certain level the the metal at the bottom will start to expand, causing the blade to become disconnected from the contact point. When the temperature eventually drops, the blade will cool down and cause the contact points to be joined back together. Temperature changes could therefore make this type of thermostat capable of regulating e.g. oil flow in a system. However, attempts based on this concept failed and was not published.

There are numerous of commercial software that provides solution for fluid dynamics with heat transfer systems. TRNSYS is a commercial software which provides transient system simulation with a modular structure. It is used for renewable energy engineering and provides feasible solution for solar systems (Duffy et al. [2009]). It allows the user to benefit from available add-on components and create their own user-written components.

Karidewa Nyeinga conducted a study based on a dynamic model for small scale concentrated solar energy system with heat storage in 2012 (Nyeinga [2012]). The aim of the study was to develop an analysis tool for concentrated solar system with integrated heat storage units. The model was constructed with a rock bed heat storage, using air as the heat carrier. The model was based on numerical integration of a set of conservation equations for mass, momentum and energy of the heat carriers, the walls and the rocks. An implicit time integration was used and the model predicted temperatures of the air, rock bed and wall during time along the heat storage. The model also provided the velocity, density and pressure of the air.

Comparison of the experimental work and the model predictions showed that the system worked well and had realistic results. More measurement from the experiments was recommended to do further validations, but the numerical model functioned as a design tool for concentrated solar system with integrated heat storage units.

Three-dimensional heat transfer simulations were conducted to simulate a high-temperature sensible thermal storage, using a commercial software, COMSOL, by Likhendra Prasad et al. in 2013. Heat transfer fluid was sent through multi-tubes embedded in a cylindrical configuration utilizing concrete and cast steel as storing mediums (Prasad et al. [2013]). Number of embedded tubes were optimized based on charging time using a finite element approach in COMSOL. The model assumed a fully developed, laminar, unsteady and incompressible flow and utilized conservation equation for mass and energy. Initial- and boundary condition were provided to the model. The model results were in good agreement with data reported in the literature, and could provide predictions for different designs and materials of the storage.

Chapter 3

Thermostat & Storage

The oil based system requires a temperature responsive device, which can regulate the direction of the oil flow. A thermostat concept with this functionality was therefore going to be constructed. As the system is mainly intended for people living in remote areas, the thermostat solution should as a consequence be based on simple means. The different solutions which have been focused on in this thesis, and which have been tested in the laboratory, are based on three different approaches; phase transitions, superheated gas and electromagnets (require power supply). Two different bellows and a solenoid were used in terms of utilizing these methods.

This chapter will look at the properties of the chosen bellows and solenoid, and how they were incorporated into the design of the thermostat. After the different thermostat solutions have been reviewed, the sensible thermal heat storage will be presented. The storage is a critical component in the concentrated solar energy system, and the different pistons utilized to obtain forced stratification in the storage will be described.

3.1 Liquid Filled Bellows

In the first thermostat concept was based on a liquid filled bellows. The bellows would exploit evaporation and condensation to become expanded and compressed. Thus, when incorporated into a configuration containing ports, it would hold the same features as a thermally activated valve in the system. Before looking at how the bellows was incorporated into a thermostat design, the general properties of bellows will be reviewed. Thereafter, the choice of bellows for the system will be presented.

The bellows can be thought of as a combination of a spring and a piston. As a piston the bellows can exploit internal or external pressure changes and convert it into an applied force ([Sigma-Netics \[2015\]](#)). Whereas as a spring, the bellows is capable of deflecting elastically and exert a counter force as a response to an inflicted force. Additionally, the bellows will due to its spring features expel linearity effects and hysteresis (negligible as long as deflection is kept below the elastic limit). Holding the properties of both a spring and a piston makes the bellows very flexible.

The bellows can therefore be taken advantage of in many situations, for instance in fluid handling, sensing and actuation applications. The flexibility of the bellows, however, will create some design challenges. Depending on how a given bellows is loaded, it will behave in a certain way. For instance, when the bellows is being compressed under an axial load, it will have one set of lifecycle, pressure and stroke characteristics, whereas when it is expanded due to an internal pressure this set will be completely different.

There are many different bellows available on the market, where the manufacturing methods and materials are the varying factors. The method and material chosen, determines how long the bellows will be functional in a given field ([Sigma-Netics \[2015\]](#)). Bellows are manufactured by methods including seamless hydroformed bellows, seam-welded formed bellows, edge-welded bellows and electro-formed bellows ([Sigma-Netics \[2015\]](#)). Additionally, the different metals in which are common to use are brass, bronze, beryllium copper, monel, stainless steel and nickel. For the purpose of this work an edge-welded stainless steel bellows was chosen. Even though edge-welding is somewhat more expensive than the other manufacturing methods, it has the ability of offering the smallest package sizes available, for a given set of stroke and life cycle requirements. The reason for having stainless steel as the material (347 SST) would also ensure a bellows with a high quality tensile strength (making it easier to maximize its stroke as well as reducing its package size). Stainless steel also tolerates high operating temperatures. As bellows made in stainless steel material is often used in applications such as for example electrical interrupters and industrial controls, it was believed that it could also work efficiently in a high temperature operating system like the one carried out in this research. The bellows chosen was custom made and produced by the American company Metal Flex. It had an inside and outside diameter of respectively 13.72 mm and 34.30 mm, together with a working stroke of 7.62 cm. The stroke size was unnecessarily large, as the required stroke for the bellows was approximately 2.5 cm, a distance at which will become evident when the design of the thermostat is being carried out in one of the next sections. The spring rate of the bellows was approximately 0.368 N/mm. A technical drawing of the bellows, with further information regarding its properties, can be found available in [Appendix D](#).

The objective was to design a bellows capable of regulating the oil flow in the system. As the bellows exploit phase transition, its expansion and contraction features would therefore be embedded in the liquid inside (see [Figure 3.1](#)). A bellows based on this phenomenon would as a consequence provide a thermostat solution independent of external power supply. Rather, thermal energy would be converted into mechanical by exploiting the phase transition behaviour of the liquid. Consequently, when incorporated into a configuration containing ports, it would hold the same features as a thermally activated valve in the system. When choosing to have a thermostat solution based on a bellows, it is important that the expansion and contraction processes (the phase transition processes) are in equilibrium. This due to the fact that the bellows should ensure that oil flowing through one inlet port of the thermostat configuration, should leave through one out of two outlet ports. Hence, depending on the temperature of the oil. For the purpose of the system we are constructing, i.e. cooking application, it is important that the oil (sent to the stove) is sufficiently hot for a desirable heat output to be achieved. The same principle applies for the opposite case; the stove is being switched off, thus

the heat should be shut off immediately.

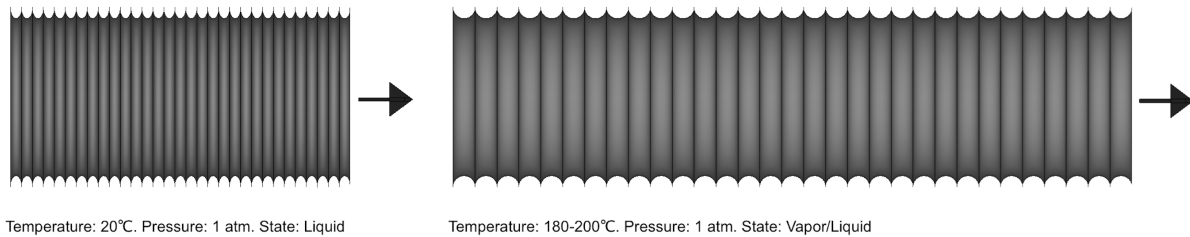
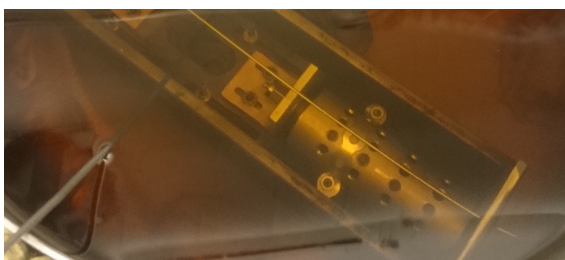


Figure 3.1: A Sketch of the Bellows

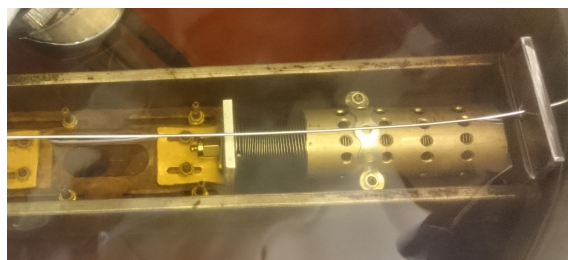
The desired temperature of the oil, 180-200°C, should be the instance at which the bellows reacts. Thus, corresponding to the boiling temperature of the liquid inside the bellows. As the liquid starts to boil/evaporate, bellows expansion will be initiated, causing a change in the direction of the oil flow. The bellows expansion should therefore introduce a gradual transition from what will be referred to as the bellows initial and final position. When the oil in the system cools down again, thus below the desired temperature, the vapor inside the bellows would start to condense, resulting in bellows contraction. Thus, the bellows expansion indicates heat supply, whereas the bellows contraction represents a stoppage in heat supply. This is illustrated in respectively Figure 3.2a and 3.2b. The outlet open in Figure 3.2a will be referred to as port 2, whereas the outlet open in Figure 3.2b will be referred to as port 3. The oil inlet will be referred to as port 1 (located underneath the bellows in the figures). Further description of the thermostat design, and how the bellows was incorporated into it, will be carried out in one of the next sections.

3.1.1 Liquids - Working Mediums

There were conducted experiments with three different liquids inside the bellows. Antifreeze from Wilhelmsen Chemicals, ethanol from Kemetyl and 1,2-Propylene glycol diacetate from Merck. See picture of the three liquids in Figure 3.3. What distinguishes the three liquids from each other is that while antifreeze and ethanol



(a) The bellows in its initial position - open port 2



(b) The bellows after expansion - open port 3

Figure 3.2: A picture of an expanded and compressed bellows in the thermostat configuration (oil bath experiment). Figure a): The boiling point of the liquid has not been reached, thus port 2 is open. Figure b): Boiling has been initiated. Hence, the two pictures shows the transition from an open port 2 to an open port 3. Port 1 is located underneath the bellows (inside the confining tunnel).

both are multi-component liquids, 1,2-Propylene glycol diacetate is a one-component liquid. The two first liquids are also easy accessible and inexpensive, while the one-component liquid is special ordered (thus not readily accessible) and somewhat more expensive. They were chosen based on their different boiling points at an atmospheric pressure condition; 164°C for antifreeze, 78°C for ethanol and $190\text{-}191^{\circ}\text{C}$ for 1,2-Propylene glycol diacetate. Additionally, 1,2-Propylene glycol diacetate was tested because of its purity. It was desirable to observe whether this would have any implications on the features of the bellows. Additional information regarding the liquids can be found in Appendix A.



(a) Picture of the ethanol and the 1,2-Propylene glycol diacetate used inside the bellows



(b) Picture of the antifreeze used inside the bellows

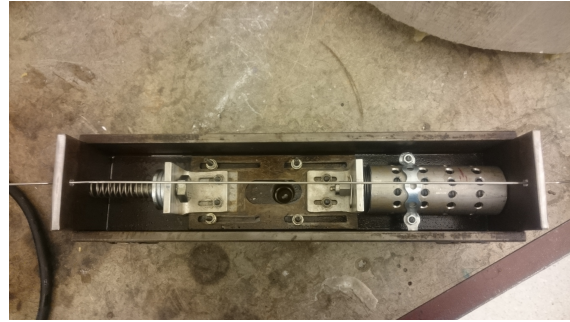
Figure 3.3: Picture of the liquids tested inside the bellows.

3.2 Design of the Thermostat

The thermostat constructed was comprising a bellows, three ports and a return spring (compression spring). The design became as shown in Figure 3.4a. Five steel plates; two short and three long, gave the thermostat its rectangular shape. Three holes (15 mm.) were drilled in the bottom plate, representing the three ports; one inlet port and two outlet ports. The remaining steel plates were welded onto the bottom plate. The rectangular box was comprising a compression spring, washers, 90 degrees brackets, bolts, and a bellows inside a confining tunnel. The bellows was located above port 1. Port 2 was located in the middle section of the plate, and port 3 was located underneath the 90 degree bracket connected to the spring. In a complete system setup these ports would be connected to pipes. Depending on the temperature of the oil, the flow entering through port 1 would leave through port 2 or port 3. Figure 4.4b in Chapter 4 illustrates this in more detail. A thin steel plate with sliding ability and with an oval opening zone in the middle section, fixed with bolts to the bottom plate, would ensure a gradual transition between port 2 and port 3. The distance



(a) First version of the thermostat



(b) Upgraded version of the thermostat

Figure 3.4: The design of the thermostat. Figure a: Shows a thermostat configuration comprising steel plates adjusted into a rectangular shape, surrounding a spring, two washers, two 90 degrees brackets, bolts and a bellows inside a confining tunnel. Figure b: Showing a similar thermostat design as in Figure a, but with an additional washer and a new tunnel equipped with several holes. Figure a and b: The tunnel restricts the bellows movement to the longitudinal direction. There were three ports in the bottom plate; one inlet port and two outlet ports. The inlet port was located underneath the bellows, and the two outlet ports in respectively the middle section (as visualized) and underneath the bracket connected to the spring.

between the ports were approximately 2.0 cm. Therefore, the opening zone in the sliding plate would have to be this distance plus the diameter of a port. Hence, the opening zone had a length of 3.5 cm. It was reasonable to assume negligible oil penetration in-between the sliding plate and the bottom plate, as the gap between was sufficiently thin.

Two different compression springs would be tested during the experimental work; one with a spring rate of $k = 0.237$ N/mm (weaker than the bellows), and another with a spring rate of $k = 0.7$ N/mm (stronger than the bellows). However, it will be the first spring that will be used primarily. Hence, when the other spring is to be used this will be specified. The purpose of the tunnel was to restrict the bellows expansion and contraction to the longitudinal direction. There were also two 90 degrees brackets, one connected to the spring and the other to the bellows. Both brackets were attached to a thin steel plate. The thin plate could slide back and forth along the bottom plate, moving accordingly to what happened inside the bellows.

3.3 Design Improvements

After some preliminary tests of the thermostat were conducted, it was seen as necessary to do some upgrades. The tunnel was not confining enough, and experiments indicated that its length had to be extended. In addition to this, the confining tunnel was equipped with several holes to ensure better heat transfer between the oil and the bellows.

The spring is an important element in the system due to its ability to exert return force towards the bellows. Any under-pressure inside the bellows will be eliminated if the spring has an adequate amount of force toward the bellows at its initial position. Observations from the preliminary tests revealed that the bellows moved too early, thus the spring needed an enhanced arrangement. The bracket connected to the spring was therefore rearranged, and an additional washer was supplied. Figure 3.4 illustrates these adjustments. The rearrangement caused the bellows to have an initial position in a further distance from

port 2 (approximately 4 mm instead of 2 mm). It became evident that this bellows arrangement was favorable due to gas impurities/air causing the bellows to expand at lower system temperatures. Observations which will be reviewed in Chapter 4.

3.4 Gas Filled Bellows

The second thermostat concept would exploit expansion of a gas volume connected to a small diameter bellows. Hence, the bellows would utilize superheated gas to become expanded in a given thermostat design, where the gas volume would be in direct contact with the oil. How the size and configuration of the gas volume was decided, will be reviewed in detail in the Chapter 4. The bellows, ordered from the same company as the previous one, was also edge-welded and made in stainless steel. The bellows had an inside and outside diameter of respectively 6.55 mm and 15.11 mm, together with a working stroke of 2.54 cm. The spring rate of the bellows was approximately 0.403 N/mm. Further information regarding its characteristics can be studied in Appendix E. The bellows was, however, not going to be fixed into the thermostat structure, as was done with the liquid filled bellows. This was because of the size of of the gas volume connected to it, which would have required reconfiguration of the thermostat. For the purpose of the testing it was therefore easier to have the bellows in a separated system. How the setup was constructed will be reviewed in detail in Chapter 4.

3.5 Linear Solenoid Actuator

The last thermostat concept tested was based on a linear solenoid actuator (henceforth referred to as solenoid). In this section the mechanical principles of the solenoid will be reviewed in detail, where information presented has been based on a data sheet written by a company named RS Components ([RS-Components](#)).

A solenoid is a device which consists of a coil (becomes an electromagnet) with an associated iron circuit. This forms the fixed part of the solenoid. When the coil is being energized, a moving iron plunger will be pulled into it. If the solenoid contains an integrated permanent magnet, it is referred to as a latching solenoid. This was the type of solenoid that was going to be exploited in the last thermostat concept. What distinguishes this solenoid from the ones without an integrated permanent magnet is that it is capable of maintaining a continuous hold after power has been disconnected, and it can operate on pulse signals. In addition, it offers no self-heating. However, to obtain proper operation, electrical polarity is important for this type of solenoid.

The plunger in the latching solenoid will be pulled into the coil or released from it, depending on the direction of the current. In the pull operation an activation pulse ensures that the coil is being energized. The plunger will at this instance be pulled into the coil and maintain at this position due to the attraction force of the permanent magnet. This force is present without any power applied to the coil. Additionally, it increases on short strokes. In the pull operation, the magnetic force from the coil, in addition to the small pull

force from the permanent magnet, results in a higher overall pulling force. The duration of the pulse will be dependent on the size of the solenoid, its stroke and/or the weight of a physical load. 80-150 ms is normally sufficient. In the push/release operation, the attraction force from the permanent magnet will be cancelled as a result of the coil being energized with reversed polarity. The plunger will at this instance be free from the magnetic effect of the coil, and thus become released from the permanent magnet. The separation will require some assistance from an external mechanism, for example a return spring. It is important that the external release mechanism has an adequate force, and that the amplitude of the releasing voltage is applied correctly. The duration of the releasing pulse will depend on the inductance of the coil, and/or the force of the external releasing mechanism. Normally, 30-60 ms will be required. An illustration of the cross sections of a solenoid with and without a permanent magnet is shown in Figure 3.5.

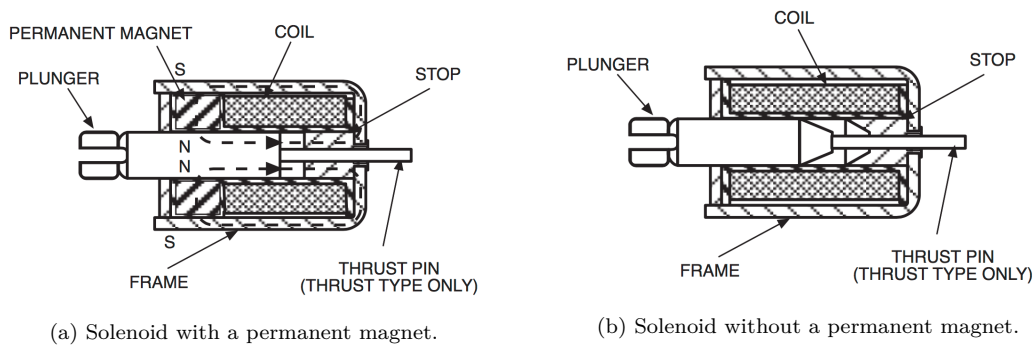


Figure 3.5: Cross section of a solenoid with and without a permanent magnet.

The latching solenoid chosen for the purpose of this research (ordered from RS Components), had a working stroke of 20 mm, and was requiring 12 V dc and 80 W. Further information regarding the solenoid can be found in Appendix F. Compared to the bellows, the solenoid would be based on a thermostat concept dependent on power supply. However, as it can operate on pulse signals, the amount will be small. For remote areas, 12 V PV panels could contribute with power supply during day time, and small battery-packages could provide power stability after sunset.

To control the instance when the solenoid should become energized, a temperature sensor will be necessary. This type of sensor will need to contain a switch, where the conductors of the solenoid (positive and negative) can be connected. For instance, a capillary thermostat can be used. This type of sensor was tested, and how it works and how the solenoid operates together with it, will be reviewed in Chapter 7. The chapter in which concerns the field study carried out in Ethiopia. The experiments conducted in the laboratory at NTNU, which will be reviewed in Chapter 5, were based on another approach. The setup constructed in the laboratory was using a programmable software named LabVIEW, where a sensor containing a switch was programmed to ensure operation of the solenoid. LabVIEW will be introduced in Chapter 3.

3.5.1 Design of the Thermostat

The design of the thermostat with the solenoid was almost identical to the one used with the liquid filled bellows, only a few changes had to be done with the original design. The solenoid was incorporated into the thermostat configuration as visualized in Figure 3.6. The solenoid was fixed, with assistance from an additional bracket, to the 90 degree bracket at the right hand side of the thermostat. The added bracket was arranged with a bended top part, where the external end configuration of the plunger was attached (with a pin), and was directly connected to the 90 degree bracket with a bolt. This was the bolt ensuring safe motion of the compression spring in the thermostat design with the bellows (see Figure 3.4). The spring would, however, need to be located at a higher position in the new design. This was due to the additional bracket, which had to be longer than the 90 degree bracket to accommodate the solenoids position. Therefore, the spring was located in a position where it could exert a horizontal force directly onto the center point of the added bracket (see Figure 3.6b). The spring was maintaining a stable horizontal arrangement due to a bolt fixed in the wall of the thermostat. The arrangement of the solenoid, caused the initial position of the spring to be somewhat compressed. In Chapter 5 it will become evident why some adjustments would have to be done with the spring, so that the solenoid could operate without problems. The spring ($k = 0.237 \text{ N/mm}$) functioned as the external releasing mechanism in this thermostat design. Where the bellows once had been located there was instead added a supporting stick. See Figure 3.6a. The supporting stick ensured that the solenoid would be stopped after 15 mm (maximum stroke of 20 mm). This was the diameter of the ports, and a longer stroke than this would not be required. Additionally, it was favorable since a shorter stroke would provide a higher overall pulling force.



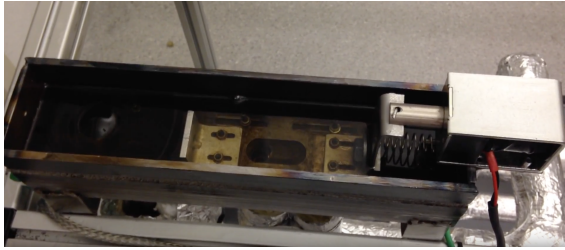
(a) Picture of the solenoid taken from above. Where the bellows once was located, there has been added a supporting stick instead. The supporting stick ensured that only a 15 mm stroke was required (diameter of the ports), and a higher overall pulling force could therefore be obtained.



(b) Picture of the solenoid from the side, showing the position of the solenoid and the compression spring. An extra bracket (bended at the top), fixed to the original 90 degree bracket at the right hand side of the thermostat, was providing a connection point for the solenoid. The external end configuration of the plunger was attached with a pin to the bended part of this bracket.

Figure 3.6: Picture of the solenoid taken from above and from the side.

The latched and unlatched arrangements of the solenoid were as illustrated in Figure 3.7. In the unlatched position the oil was below a set temperature, and would therefore flow through port 2. In the latched position a set temperature was reached, causing the oil to flow through port 3.



(a) Picture of the solenoid in the unlatched position.



(b) Picture of the solenoid in the latched position.

Figure 3.7: Picture of the solenoid in the latched and unlatched position. In the unlatched position the oil was below a set temperature, and would therefore flow through port 2. In the latched position a set temperature was reached, causing the oil to flow through port 3.

3.6 Storage

The complete system setup included a sensible heat storage, based on forced stratification. A thermal oil would be the heat transfer and storing medium. When the oil in the system reached the desired temperature, it would be sent directly to the storage. By achieving forced stratification the storage can charge and discharge at a constant temperature, which is attractive for cooking purposes.

The storage was divided by a piston into two sections; one cold and one hot. The piston would work as the physical barrier between these sections to ensure thermal stratification. The piston will be described in more detail in one of the next sections. The storage could easily be charged and discharged, by the means of manual valves and the thermostat. During charging, heated oil was sent into the hot side of the storage, causing the piston to move toward the cold side. Cold oil would then be sent into the system from the cold side of the storage. When discharging the storage, cold oil was sent into the cold side of the storage, the piston was sent towards the hot side and hot oil was sent into the system from the hot side. The capacity of the storage and the period in which it can store hot oil, depends on the volume and the insulation of the storage. Figure 3.8 illustrate the pistons position, and the cold and hot sides of the storage when half charged.

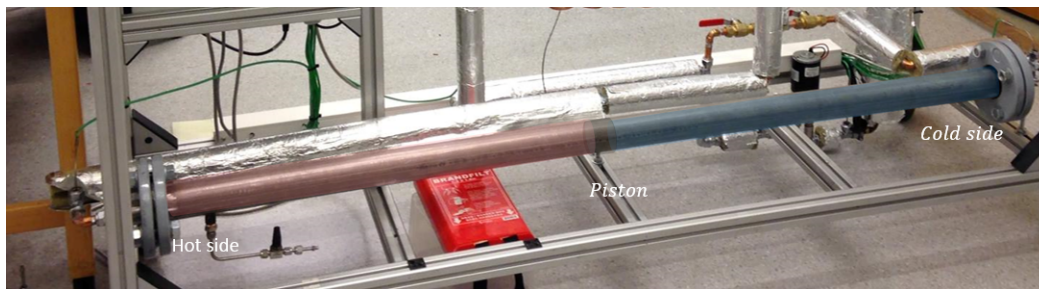


Figure 3.8: Picture of the storage half charged. The piston separates the hot and cold side, where red color indicates the hot side and blue color indicated the cold side. This picture is taken before the storage was insulated.

The storage used in the experiments carried out at NTNU was a stainless steel pipe. It had an outer diameter of 59.5 mm, an inner diameter of ~ 56 mm, and a length of 1.7 m. Each end of the storage was arranged with flanged pipe-ends, where two flanges could work as an interconnection between the storage

and a given copper pipe. The storage was well insulated with rock wool pipe insulation, having a thickness of ~ 50 mm.

3.6.1 Heat Transfer and Storing Medium

Duratherm 630 was the thermal oil used as the heat transfer and storing medium in the system. The oil is an environmental friendly fluid that offers high temperature stability up to 332°C . The heat capacity is in the range between 1.971 [kJ/kgK] at 38°C and 0.645 at 260°C . For further information about the liquid see Appendix B.

3.6.2 Piston - Physical Barrier in Storage

The piston was the device separating the hot and the cold oil in the storage. To avoid leakage between the hot and the cold side, the piston was designed to have a diameter as close as possible to the inner diameter of the storage. It was beneficial with a material with low thermal conductivity, so that the heat transfer between the hot and the cold oil would be small. It was also desirable with a low-density material, and a material causing low friction forces, so that the piston could slide as smoothly as possible inside the storage. As the storage would be charged with oil at temperatures up to 200°C , it was important that the piston material could handle high temperatures.

Three different piston materials were tested; stainless steel, polyoxymethylene (POM) and polyetheretherketone (PEEK). Table 3.1 shows the properties of the different material.

Table 3.1: Material properties for the different pistons
(* Properties from AZO, (**) Properties from Bagges [2016]

| Properties for the pistons tested in the storage | | | |
|--|--------------------|------------|------------|
| | Stainless Steel(*) | POM(**) | PEEK(**) |
| Outer Diameter [mm] | 55.3 | 55.4 | 55.6 |
| Length [mm] | 30.4 | 80 | 80 |
| Density [kg/m^3] | 7850 | 1410 | 1310 |
| Thermal conductivity [W/mK] | 14 | 0.231 | 3.48 |
| Service Temperature [$^{\circ}\text{C}$] | -273 to 925 | -60 to 100 | -40 to 260 |

Stainless Steel

The first piston tested was made of stainless steel, designed as a hollow cylinder. Stainless steel has a relatively low thermal conductivity, compared to other metals (e.g. copper). However, compared to POM

and PEEK, it has the highest value. The density value of stainless steel is quite high, but by making the piston hollow, the weight was reduced. The material is cheap and easily accessible, which is beneficial.

The piston had an outer diameter of 55.3 mm and a length of 30.4 mm. For the piston to move as smoothly as possible, the edges were rounded to some extent. Figure 3.9a shows a picture of the stainless steel piston. In terms of tracking the pistons movement inside the storage, a metal plate with an attached magnet was connected to one side of the piston. When the piston moved, a small magnetic ball would run along the outside of the storage following the piston. See Figure 5.5 in Chapter 5.

POM - Thermoplastic

The second piston was made as a solid cylinder in POM, which is an engineering thermoplastic offering good sliding properties (Bagges [2016]). The material has low density and low thermal conductivity, which is desirable. However, as can be observed in Table 3.1, the material can only operate at temperature up to 100°C. Therefore, it will not be possible to use this type of material in a high temperature storage. Nevertheless, as the objective was on demonstrating the principles of the system setup, a piston made in this material could be used. It was also desirable to observe how a piston made of plastic would slide compared to a metal piston.

The piston was made with an outer diameter of 55.4 mm and a length of 80.0 mm. The length was increased, compared to the first piston, to decrease the possibility of tilting inside the storage. Additionally, a longer piston could be favorable with regards to leakage. Figure 3.9b shows a picture of the piston. In the middle of the piston, a lowering was made, and a magnet was attached. Hence, the piston could be tracked with a magnet ball.



(a) Picture of the piston made of stainless steel



(b) Picture of the piston made of POM (thermoplastic)

Figure 3.9: Picture of the stainless steel and POM (thermoplastic) pistons used inside the storage.

PEEK - Thermoplastic

The third piston tested was made as a solid cylinder in PEEK. PEEK is an engineering thermoplastic, as POM, and can operate at temperatures up to 260°C, and has good sliding properties. As shown in Table 3.1, this material also has relatively low thermal conductivity and density. The piston was made almost identical to the POM piston, where a 0.2 mm increase in the diameter was the only difference between the

two. Therefore, it had an an outer radius of 55.6 mm and a length of 80.0 mm. A drawback with this material is that it is expensive.

Chapter 4

Experiments With Bellows

Experiments with the thermostat concept utilizing a liquid filled bellows was tested in two different system setups; in a stationary oil bath and in a circulating oil system. The bellows was tested with three different liquids as the working medium, to observe its expansion and contraction with different internal environments. The liquids tested were antifreeze, ethanol and 1,2-Propylene glycol diacetate. The filling of the bellows was based on three different approaches, as a result of observations made during the experiments. After the experiments with the liquid filled bellows, experiments with a gas bellows was carried out. The bellows was incorporated onto a device containing a large air volume, at which was to be superheated. The gas bellows could then become expanded and compressed, by exploiting this physical phenomenon. In this chapter the experiments will be reviewed in detail, where focus has been on the temperatures causing expansion and contraction of the two bellows. The results will be presented in terms of graphs and tables.

Prior to the experiments a risk assessment was conducted and carried out according to the procedures of the Department of Energy and Process Engineering. The risk assessment was documented and approved in advance of the experimental work. Approval with signatures can be found in Appendix H. The risk assessment conducted applies to the experiments carried out in Chapter 5 as well.

4.1 Preliminary Testing - Liquid Filled Bellows

There was conducted a preliminary test of the thermostat before it was arranged into the oil system. The test was based on safety measures, to gather experience on how the thermostat design would respond to expansion and contraction of the bellows, without the risk this could inflict in a heated oil system. A water based system was arranged, and the bellows was filled with a liquid with lower boiling temperature than water, at atmospheric pressure. Ethanol was therefore chosen, due to its boiling point at 78.5°C at atmospheric pressure. The test showed that the bellows was performing satisfactory, thus the expansion and contraction occurred without any disruptive implications on the thermostat. It was therefore decided to proceed with the oil based experiments.

4.2 Data Acquisition With LabVIEW

The two different experimental setups were a stationary oil bath system and a circulating oil system. An electrical heating element of 2000 W was in both systems utilized in terms of heating the oil. Two temperature sensors/thermocouples (Type K), calibrated before the experimental testing, worked as measuring devices. One measured the temperature of the oil in the region close to the bellows, and the other measured the temperature at the bellows surface. The thermocouples recorded the temperatures based on two different measurement methods. One of the thermocouples was connected to a regular monitoring instrument and the other to a data acquisition (DAQ) device; converting analog information into digital data. The DAQ device was connected to a computer running a programmable software, LabVIEW, which was used to record the measured system temperatures at a user defined time interval.

National Instruments supplied the necessary instrumentation used in the DAQ system (chassis: NI cDAQ-9172, module: NI-9211, and thermocouple: Type K). LabVIEW visualized temperature change per time unit graphically, and the system setup was arranged as illustrated in Figure 4.1.

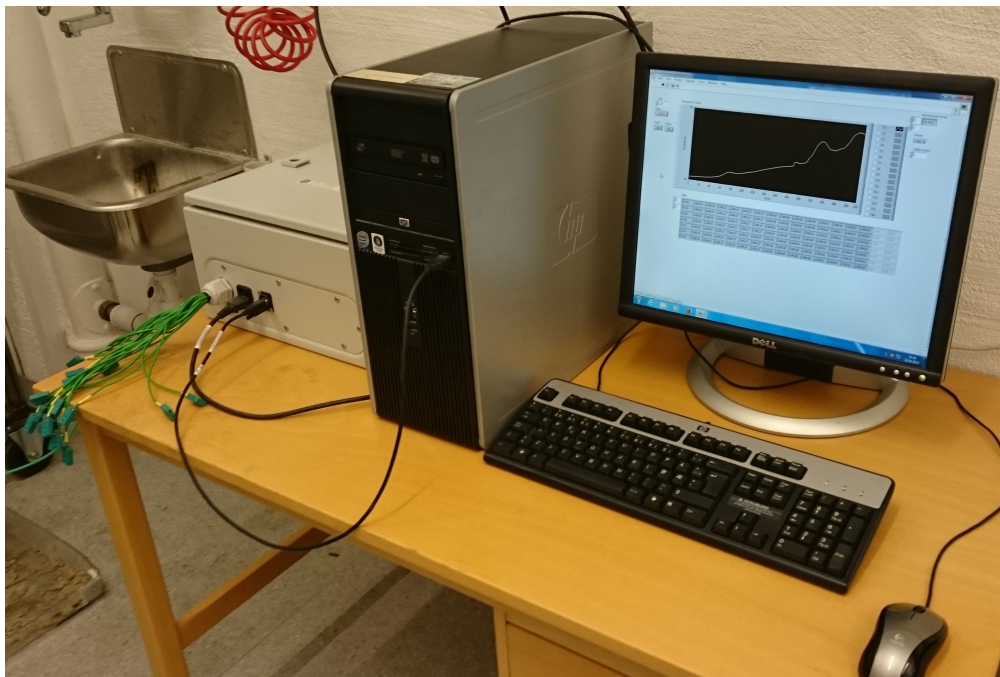
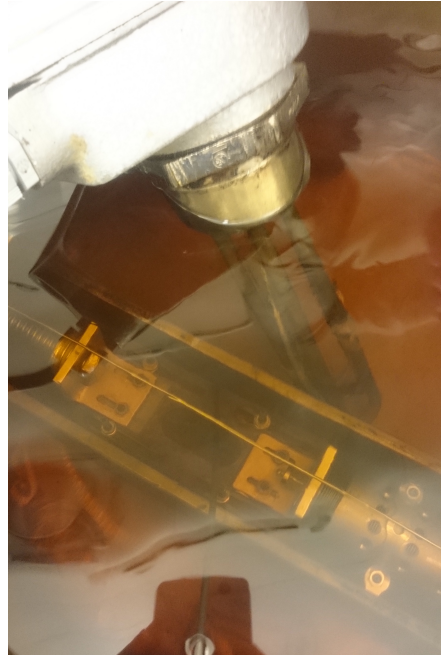


Figure 4.1: Representation of the logging setup where temperature changes are visualized per time unit. Thermocouples worked as temperature sensors, and a DAQ device worked as the transmission channel between the oil based system and a computer.

The reason for having two thermocouples in the thermostat was so that we could always double check the measured temperatures in the system. Additionally, it was desirable to observe the temperature of the oil against the temperature at the bellows surface.



(a) The oil bath



(b) Thermostat submerged in the oil bath

Figure 4.2: The oil bath represented by an insulated steel tank filled with oil. The heating element is in direct contact with the oil, located next to the immersed thermostat. Two thermocouples measure the temperature of the oil and the bellows.

4.3 System Setup - Oil Bath

The first experiments conducted was in an oil bath. See Figure 4.2. The thermostat was immersed in a well-insulated tank (comprised of one layer of rockwool insulation, thickness ~ 60 mm) together with a heating element of approximately 2000 W. Two thermocouples were present to measure the temperatures of the oil and the surface of bellows. A total amount of 23 liters of oil were required to run the oil bath experiments, due to observations made of the heating element. As can be observed in Figure 4.2b, the heating element was sufficiently submerged in oil during the testing. This was done as a safety measure to prevent unfortunate smoke from any part not completely submerged (a smoke in which was discovered in preliminary testing of the heating element). An adequate amount of oil was therefore needed in the tank to ensure safe behavior of the system setup, with no surface tension between the oil and the elements.

4.4 Experimental Method

The experimental method was based on the procedures for filling the bellows. The filling was based on two different approaches, and arose as a result of the observations made during the experimental testing.

- Method 1 - Filling took place under atmospheric pressure. The bellows was contracted completely, becoming as small as about 3.5 cm, and filled with liquid until it was full (11.0 cm long). This required a total amount of 51.9 mL.

- Method 2 - Similar to the first method. However, this time the bellows was lowered into a bath of liquid, with an aim to reduce the amount of air inside. The cap was therefore attached to the nozzle while the bellows was still fully immersed. In advance of this we cleaned the outside surface area of the bellows with ethanol, before heating it in the oven to dry. Thus to ensure no unfortunate oil penetration into the bellows.

The results from the experiments will be presented in terms of plots. Temperatures of interest will be the ones represented in Table 4.1.

Table 4.1: Temperatures of Interest - Experiments With the Liquid Filled Bellows in the Oil Bath

| Temperature instances of interest | |
|-----------------------------------|--|
| T_1 | First bellows expansion; a small movement of approximately 2.50 mm (observed with both filling methods). The expansion could be initiated due to the presence of gas impurities/air inside the bellows. An additional assumption could be based on the penetration ability of the antifreeze, as a result of the welded composition of the bellows (small cavities). |
| T_2 | The temperature representing the end of the first bellows expansion. |
| T_3 | Second bellows expansion; the liquid has reached its boiling point (atmospheric pressure condition). This expansion represents the instance at which the spring is becoming gradually compressed. An upcoming large expansion is initiated, resulting in a gradual change in the direction of the oil flow; flow regulation from port 2 to port 3. |
| T_4 | The temperature representing that port 3 is fully open and port 2 is fully closed. |
| T_5 | The temperature instance in which the bellows is contracted back into a position where port 3 is fully closed and port 2 is fully open. |

Before reviewing the experimental results, the observations made of the system during the experiments will be reviewed.

4.4.1 Observations

The experiments conducted in the oil bath were the first to illustrate the behavior of the oil, Duratherm 630, and the thermostat. The density of Duratherm 630 changes considerably with the gradual change in temperature (see Appendix B). During the experiments, as the oil was being heated, this was observed through oil expansion. We started out with an oil temperature of approximately 23°C, ending up at temperatures in the range of 180°C and 190°C. The result of this was approximately 1.5 liters excess oil that had to be removed, to maintain the original oil level in the tank. The volume amount of oil present in the tank was small enough to suggest that static pressure forces on the bellows would not impact the results. Additionally, a decrease in density will also reduce the static pressure even further.

The gradual change in viscosity also resulted in a system containing different temperature layers. Measurements indicated that the surface temperature of the oil was about 10°C higher than the temperature in the bottom section of the oil bath. Due to this, it was important to stir in the oil frequently to obtain a smooth temperature distribution. Nevertheless, the experiments showed a 4°C temperature difference between the oil (in the region close to the bellows) and the bellows. This could have been a result of the uneven temperature distribution. However, the heat capacity of stainless steel, which is the material of the bellows, is low and could therefore be the reason for the temperature difference. The temperature difference was observed even when consecutively heat cycles were performed.

After the first experiment was conducted one could observe some color changes in the oil. The unused oil had a light color, which was clear and easy to see through (neutral color; cooking oil), but after a couple of experiments had been carried out, the color became darker. This did not cause any obstacles to the further experiments. Smoke development from the oil was also observed as its surface temperature surpassed 100°C. Sufficient ventilation was therefore necessary.

4.4.2 Results

In the first experiment, the first version of the thermostat was used together with Method 1 for filling the bellows. In the two following experiments, the upgraded version of the thermostat was used together with filling Method 2. Table 4.2 contains a range of temperatures corresponding to the expansion and contraction processes of an antifreeze-filled bellows during these experiments. All temperatures are measured at the bellows surface. The results from the third experiment are also visualized graphically in Figure 4.3. The instances of evaporation and condensation of antifreeze are highlighted in the graph.

Table 4.2: Temperatures measured at the surface of the bellows in the oil bath experiments

| The oil bath experiments | | | | | | |
|--|----------------------------|----------------------------|--------------|----------------------------|--------------|--------------|
| | 1 st experiment | 2 nd experiment | | 3 rd experiment | | |
| | Heat cycle 1 | Heat cycle 1 | Heat cycle 2 | Heat cycle 1 | Heat cycle 2 | Heat cycle 3 |
| T ₁ ^(a) | 105.0 | 110.0 | - | 110.0 | - | - |
| T ₂ ^(a) | 113.0 | 122.0 | - | 122.0 | - | - |
| T ₃ - start to open port 3 | 161.0 | 173.0 | 167.0 | 174.0 | 171.0 | 171.0 |
| T ₄ - port 3 fully open (port 2 fully closed) | 175.0 | 182.0 | 178.0 | 184.0 | 182.0 | 181.0 |
| T ₅ - port 2 fully open (port 3 fully closed) | 140.0 | 140.0 | 140.0 | 140.0 | 140.0 | 140.0 |

(a) T₁ represents the first bellows expansion, and T₂ the temperature at which this bellows expansion is completed. This expansion was believed to be due to disturbing factors inside the bellows (e.g. gas impurities/air).

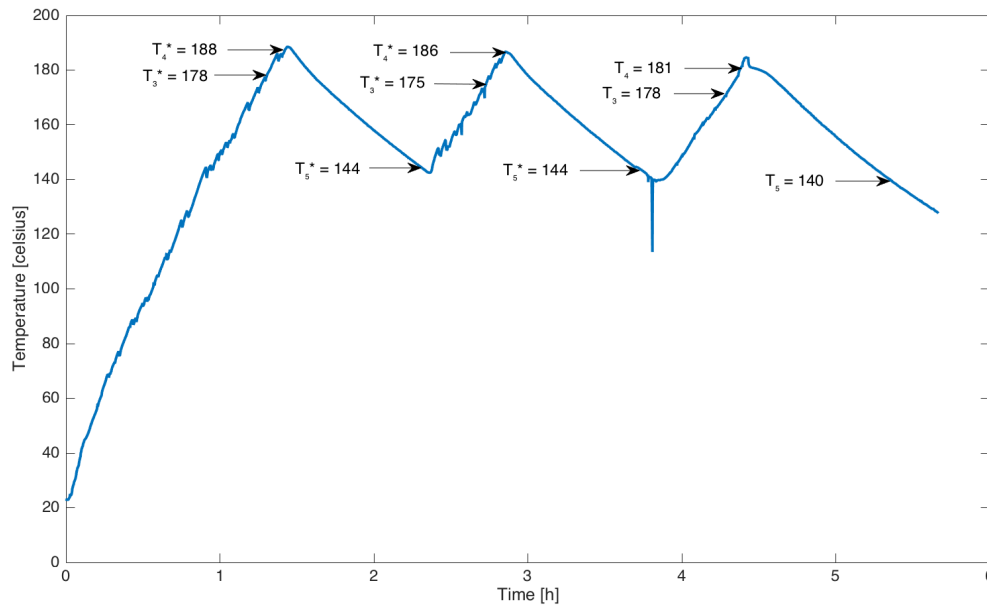


Figure 4.3: Plot of the heat cycles in the third oil bath experiment. Highlighted temperatures represent bellows expansion and contraction. T_3 and T_4 indicates the beginning and the end of the bellows expansion, and T_5 represents the end of the bellows contraction. Temperatures are marked with '*', representing that they are measured in the oil region close to the bellows. The downward spike between heat cycle two and heat cycle three represent a change in the placement of the two thermocouples.

In the first two heat cycles the temperatures were measured in the oil region close to the bellows (marked with '*'). The graphic results, when compared to the tabulated results, shows that the temperatures in this oil region were constantly about 4°C above the bellows surface temperature at the same time. In the third heat cycle the temperatures were measured at the bellows surface, thus representing the same as those tabulated. The downward spike between heat cycle two and heat cycle three hence represents a change in placement of the two thermocouples.

About 1 hour and 20 minutes were required before the temperature in the oil bath was high enough for the antifreeze to start boiling. The evaporation process, T_3 to T_4 , required a 10°C temperature interval, whereas a 40°C interval was needed for the condensation process, T_4 to T_5 , to be completed. The evaporation process took about 8 minutes, whereas the condensation process required approximately 50 minutes.

4.4.3 Discussion

The reason for conducting adjustments with the thermostat after the first experiment was conducted, was due to the bellows expansion between T_1 and T_2 . In the first experiment this expansion resulted in an emerging change in the oils flow direction, hence some oil was escaping through port 3 at a too early instance. As can be observed in Table 4.2, this was not an issue in the following experiments.

Consecutively heating in the second and third experiment illustrated that the bellows expansion between T_3 and T_4 occurred earlier in the subsequent heat cycles. This could be a result of a more even temperature

distribution in the oil region close to the bellows. In addition, the heat capacity of the bellows material could have its contribution, as the bellows in the subsequent heat cycles would be in a more uniform temperature environment, and thus it would be possible to heat it faster. However, T_5 remains the same in all the experiments. The change from filling Method 1 to filling Method 2 did not have any impact on the elimination of, as believed, air impurities inside the bellows. The condensation rate in all the experiments is less efficient compared to the evaporation rate.

The results from the oil bath experiments showed a 4°C temperature difference between the oil and the bellows, even with consecutively heat cycles. This could be an indication of an ineffective heat transfer system. It is possible that the oil does not manage to penetrate into the bellows cavities in an efficient manner, resulting in inadequate heat convection onto the total surface area of the bellows.

The experiments required several hours to complete, making them very time consuming. The time interval for the condensation process was affected by the heating element and its ability to cool down while being immersed in the heated oil environment. The time intervals are however not observed as a system limitation. It is the temperature intervals and the responsiveness of the bellows that will be the decisive factors, concerning the thermostatic functionality of the bellows. The limitation of the system is embedded in the phase transition processes inside the bellows. When the oil was hot enough for the bellows to expand this occurred on a relatively short temperature interval. An interval in which was not observed in the condensation process. As the bellows is the controlling valve in the system, it is important that these processes are occurring symmetrically and on a short temperature interval. It became desirable to try understanding whether the condensation process could be enhanced in a circulating oil system. A system in which is also more representative to the complete system setup (including a storage). The oil bath system therefore became more of a preliminary testing setup, before a complete pipe system was finished constructed.

4.5 System Setup - Circulating Oil System

Experiments on a circulating oil system became the sequel to the oil bath experiments. The objective of these experiments was to observe whether it could be possible to enhance the condensation process in a circulating oil system. The experiments will be reviewed in detail and they will be divided into two separated parts. In the first part, the same bellows as in the last oil bath experiments has been used (filling Method 2), and in the second part the bellows was filled by utilizing filling Method 3.

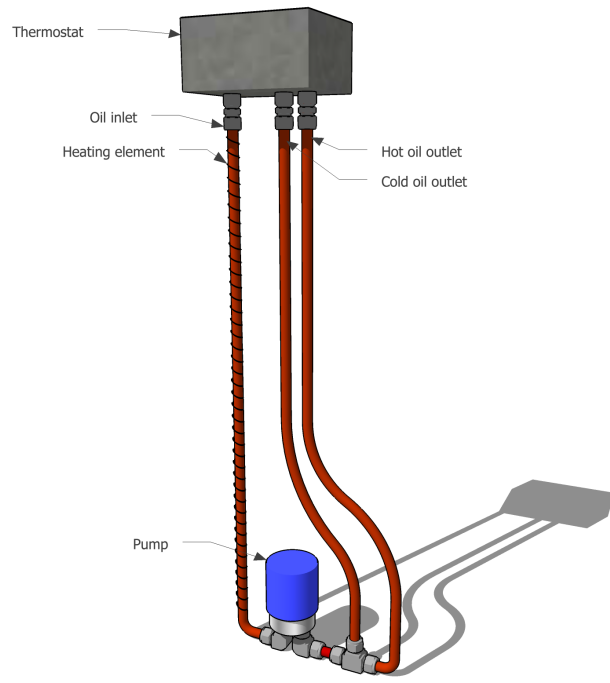
Before the experiments could be carried out, an oil based rig had to be constructed. Figure 4.4 visualizes the system setup. The setup contained three long pipes, one inlet pipe (pipe 1) surrounded by a heat cable, and two outlet pipes (respectively pipe 2 and pipe 3). The pipes were connected to the three ports in the bottom section of the thermostat. A pump was integrated into the system together with a shorter pipe working as an intermediary between the pump and the two outlet pipes. The pump capacity rate was 1.89 liters/min. Further information regarding the pump used in the experiment can be studied in Appendix C.

The whole system was then mounted on a tripod and filled with oil. Oil was filled into the system until the thermostat was half full, thus covering the whole surface area of the bellows.

The pipes in the system setup comprised the same outside diameter, 15 mm, and were all sufficiently insulated in advance of the experiments. The outlet pipes were insulated with one layer of rockwool pipe insulation, thickness 20 mm, and the inlet pipe, surrounded by the heating cable, was covered with a ceramic fiber blanket insulation, thickness 80 mm. A weak conductive material was also used in terms of separating the thermostat and the tripod from being in direct contact. This was done to avoid any heat loss due to heat conduction in the tripod. Additionally, as for the oil bath experiments, two thermocouples were attached to measure the temperatures of the oil and the bellows.



(a) The circulating oil system.



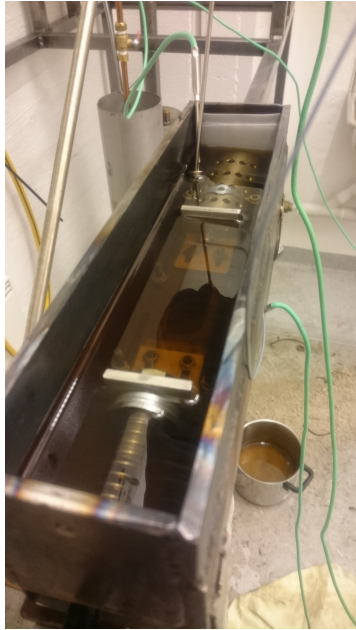
(b) A sketch of the circulating oil system.

Figure 4.4: The circulating oil system setup. Oil is being pumped through the system and heated by an electric heating element. The oil flows through the inlet pipe into the thermostat where the bellows is located. The bellows regulates in which of the outlet pipes the flow will go next.

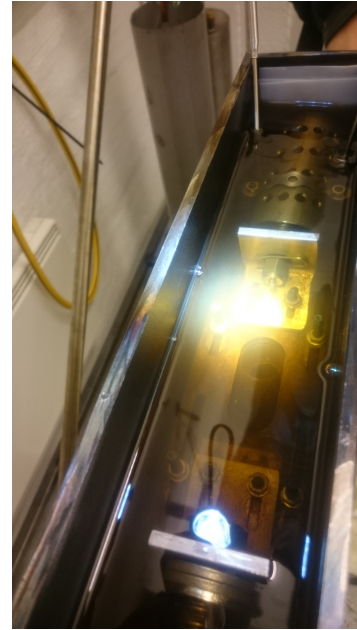
Pictures illustrating the initial and final position of the bellows are represented in Figure 4.5b and Figure 4.5c.

4.6 Experimental Method

The experimental method for the circulating oil experiments, as for the oil bath experiments, was based on the procedure for filling of the bellows. While one filling method had been rejected, Method 1, Method 2 was still desirable to test in the circulating oil system. A third filling method was, however, initiated based on observations made during the experiments:



(a) The bellows in its initial position, before the heating element has been turned on. The two thermocouples can be observed in the area where the bellows is located. Teflon films are added in the end section of the thermostat.



(b) The initial position of the bellows at the instance before the second expansion, as a result of the boiling of the liquid inside. All of the oil entering into the thermostat leaves through port 2.



(c) The bellows has expanded to its final position. The liquid inside has reached its boiling temperature, causing vapor formation inside the bellows. The oil entering the thermostat is now leaving through port 3.

Figure 4.5: An illustration of the thermostat in the circulating oil system at different oil temperatures.

- Method 3 - Observations from the first conducted experiments with the circulating oil system gave rise to a third filling method. The motivation for introducing this method was to reduce the amount of air inside the bellows. The bellows was therefore connected to a vacuum pump before filling. Introducing a liquid into a vacuum (pressure meter reading less than 1 mbar) would cause the liquid to boil immediately. The bellows was in addition filled with less liquid than in the first filling methods, 20.0 mL instead of 51.9 mL. The result was then a shorter bellows length, 6.5 cm instead of 11.0 cm. The ratio between the amount of liquid added and the length of the bellows suggested that it contained a sufficient amount of vapor. Having this condition inside could also have an enhancement effect on the condensation process. An increased condensing surface, as a result of the increased number of molecules in the vapor phase, would as a consequence also increase the number of collisions of vapor molecules onto the liquid surface (Halpern [n.d.]).

Internal Vacuum - Filling Method 3

Before a setup with a vacuum pump was constructed, the vacuum pump was tested on a glass flask containing water. The vacuum pump was connected to the flask's exit point. Water boils at 100°C with a vapor pressure of 1.013 bar (1 atm). The flask was initially at an atmospheric pressure condition at 25°C (workplace temperature). The vacuum pump was then turned on. A measuring device illustrated the gradual pressure decrease that was taking place inside the flask, eventually causing water to evaporate. The vacuum pump managed to reduce the pressure to approximately 1 mbar, hence introducing what can be approximated to an internal vacuum in the flask.

Introducing an internal vacuum condition in the bellows was desirable since the removal of air could enhance the condensation process. Having only pure antifreeze inside could additionally result in a bellows following the characteristic of a vapor pressure curve more accurate. The vapor pressure curve for antifreeze was not readily available, but its curve would probably follow a similar characteristic as the ones illustrated in Figure 4.6. The curves show that as the vapor pressure increases to an atmospheric condition and above, the result is a more temperature sensitive system, which in our case applies to the bellows.

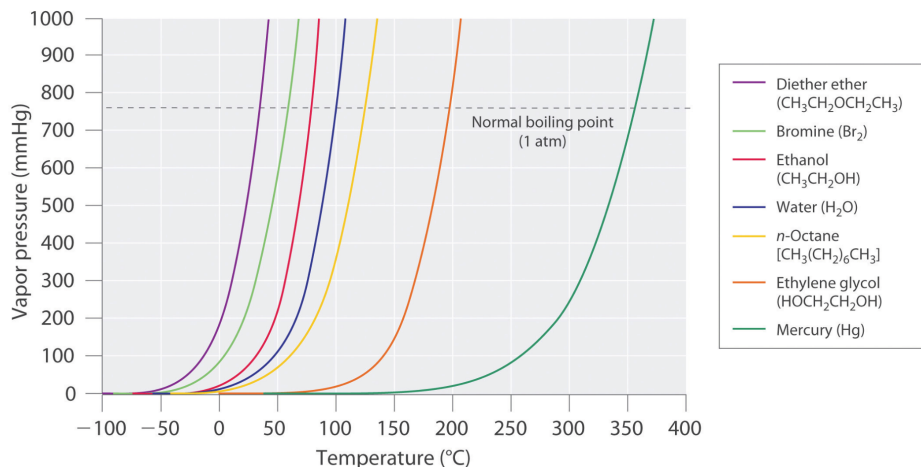


Figure 4.6: Plot showing vapor pressure curves for several liquids, (Halpern [n.d.]). The vapor pressure curve for antifreeze is not part of the plot, but a similar characteristic could have been represented close to Ethylene glycol curve, due to the boiling point at atmospheric pressure.

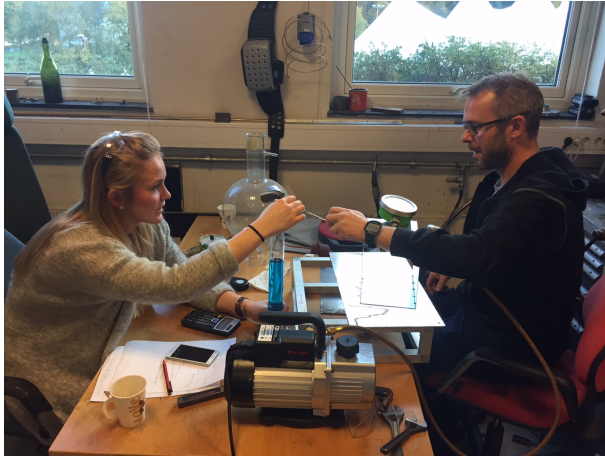
Vacuum Pump Setup

The vacuum pump setup is visualized in Figure 4.7. The system contained small diameter pipes connecting the components together. Three pipe outlets were connected to respectively the bellows, a test tube with antifreeze and a vacuum pump. There were two valves in the system, ensuring that the bellows was either drained by the vacuum pump or filled with antifreeze from the test tube. A pressure meter was measuring the pressure in the system while the vacuum pump was connected.

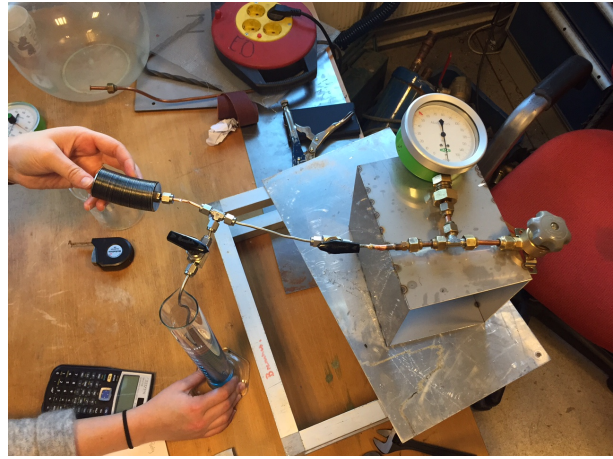
The valve connected from the pipe outlet to the test tube was closed while the valve connected to the pipe outlet to the vacuum pump was open. At the instance the vacuum pump was switched on, the pressure meter started to show a decrease in the pressure in the system. When the pressure was read to be less than 1 mbar, the valve was closed and the vacuum pump was disconnected. The bellows with the internal vacuum inside had a measured length of 3.50 cm, as represented in Figure 4.7b. The valve to the test tube with antifreeze was then gradually opened, causing the liquid to flow into the bellows. When 20.0 mL had been extracted from the test tube the valve was closed (see Figure 4.7c). The bellows ended up at a final length of 6.50 cm. The outlet pipe connected to the bellows was then squished with a pipe crimping tool. The crimping tool ensured that no air entered the bellows after it was disconnected with pincers. The effect of the crimping tool is visualized in Figure 4.7d.

The results from the experiments will be presented as plots, where the temperatures in Table 4.3 will be the ones of interest (same numbering as for the oil bath experiments):

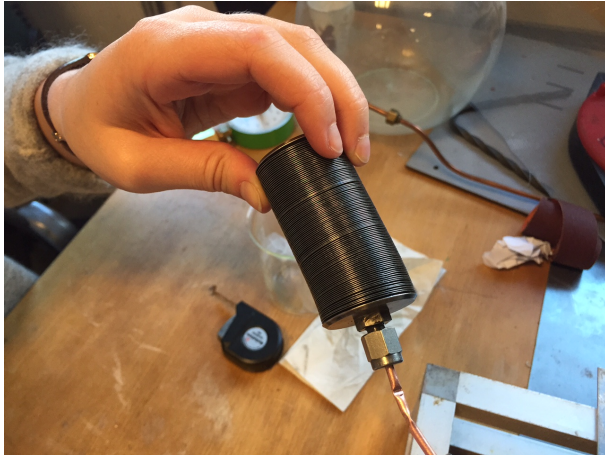
Before reviewing the experimental results, the observations made of the system during the experimental testing will be reviewed.



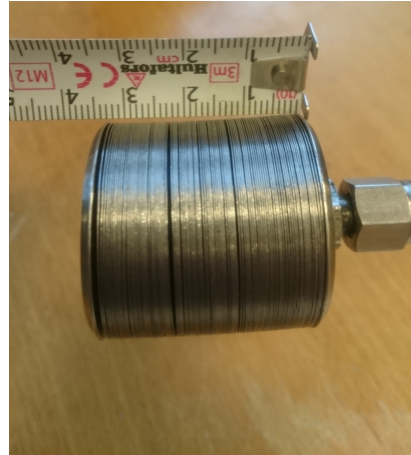
(a) The setup constructed to fill the bellows by utilizing a vacuum pump. The vacuum pump is presented in the foreground. The remaining of the system is visualized in Figure 4.7c.



(b) An illustration of the complete system setup without the vacuum pump. The vacuum pump has been disconnected, and the bellows has been filled with 20.0 mL of antifreeze. The bellows has expanded from a length of 3.5 cm (vacuum) to a final length of 6.5 cm (liquid and vapor).



(c) Closeup picture of the bellows from Figure 4.7c.



(d) Internal vacuum introduced in the bellows.

Figure 4.7: The vacuum pump system setup. The bellows was filled with antifreeze after an internal vacuum had been introduced. These figures aims to illustrate this filling procedure.

4.6.1 Observations

Due to a system requiring sufficiently less amounts of oil, compared to what was required in the oil bath experiments, the large viscosity change in Duratherm 630 was not observed as an issue. However, the experiments showed a more efficient overall heat transfer rate between the oil and the bellows. The experiments indicated that the bellows, on average, had a surface temperature of about 2°C above the temperature of the oil. The reason why this was observed could have been a result of the arrangement of the thermostat in the system. The thermostat was no longer immersed in the oil, but rather it was now in direct contact with the surrounding environment (see Figure 4.4). It was therefore reasonable to assume more heat losses from the thermostat in these experiments as a result of heat conduction through its walls, together with heat

Table 4.3: Temperatures of Interest - Experiments With the Liquid Filled Bellows in the Circulating Oil System

| Temperature instances of interest | |
|-----------------------------------|--|
| T ₁ | First bellows expansion; a movement of about 4.75 cm, not causing any change in the flow pattern. The bellows moves inside the confining tunnel due to its decreased initial length. It is expanding until the compression spring exerts force towards it. It seems like the expansion could be a result of the characteristics of a vapor pressure curve. |
| T ₂ | The temperature representing the end of the first bellows expansion. |
| T ₃ | Second bellows expansion; the liquid has reached its boiling point (atmospheric pressure condition). This expansion represents the instance at which the spring is becoming gradually compressed. An upcoming large expansion is initiated, resulting in a gradual change in the direction of the oil flow; flow regulation from port 2 to port 3. |
| T ₄ | The temperature representing that port 3 is fully open and port 2 is fully closed. |
| T ₅ | The temperature instance in which the bellows is contracted back into a position where port 3 is fully closed and port 2 is fully open. |

convection from the surface of the oil to the surroundings.

4.6.2 Results

In this section the results from the experiments will be presented. Based on the filling procedure of the bellows, the liquid inside and some other factor they have been divided into the following parts:

- Test 1 - Experiments utilizing filling Method 2 and antifreeze as the liquid inside the bellows
- Test 2 - Experiments utilizing filling Method 3 and antifreeze as the liquid inside the bellows
- Test 3 - Experiments utilizing filling Method 3, antifreeze as the liquid inside the bellows, and the stronger compression spring ($k = 0.7 \text{ N/mm}$)
- Test 4 - Experiments utilizing filling Method 3 and ethanol as the liquid inside the bellows
- Test 5 - Experiments utilizing filling Method 3, ethanol as the liquid inside the bellows, and without a spring being present
- Test 6 - Experiments utilizing filling Method 3, ethanol as the liquid inside the bellows, and with the back part of the bellows being fixed to the confining tunnel
- Test 7 - Experiments utilizing filling Method 3 and 1,2-Propylene glycol diacetate as the liquid inside the bellows

- Test 8 - Experiments utilizing filling Method 3, 1,2-Propylene glycol diacetate as the liquid inside the bellows, and the stronger compression spring ($k = 0.7 \text{ N/mm}$)

Test 1

Two experiments were conducted with the bellows from the final oil bath experiments, hence based on filling Method 2. The experiments were both carried out with one heat cycle, believed as adequate due to the observations made. The only difference between the experiments were the presence of insulating Teflon films, at which was added before the second experiment was conducted. The motivation for using the Teflon films was to separate the back part of the bellows from one of the short walls in the thermostat configuration (which the bellows was normally in direct contact with). See Figure 4.5a). The aim was to observe whether these films would enhance the condensation rate, as the walls of the thermostat were hot and thus would cool down at a slower rate compared to the surrounding oil.

Table 4.4 contains the important temperature results from the experiments. The second experiment can also be found visualized graphically in Figure 4.8.

Table 4.4: Test 1 - Temperatures Measured at the Surface of the Bellows in the Circulating Oil Experiments

| Test 1 - Circulating oil experiments | | |
|--|----------------------------|----------------------------|
| | 1 st experiment | 2 nd experiment |
| T ₁ ^(a) | 100.0 | 100.0 |
| T ₂ ^(a) | 110.0 | 110.0 |
| T ₃ - start to open port 3 | 159.0 | 158.0 |
| T ₄ - port 3 fully open (port 2 fully closed) | 171.0 | 170.0 |
| T ₅ - port 2 fully open (port 3 fully closed) | 140.0 | 140.0 |

(a) T₁ represents the first bellows expansion, and T₂ the temperature at which this bellows expansion is completed. This expansion was believed to be due to disturbing factors inside the bellows (e.g. gas impurities/air).

The results in Table 4.4 illustrates two experiments with virtually the same results. Therefore, the Teflon films did not have any visible effect on the processes inside the bellows. The early expansion between T₁ and T₂ does not affect the flow pattern and can therefore be ignored. The bellows expansion, T₃ to T₄, in both experiments required a temperature interval of about 10°C, and the bellows contraction, T₄ to T₅, an interval of approximately 30°C.

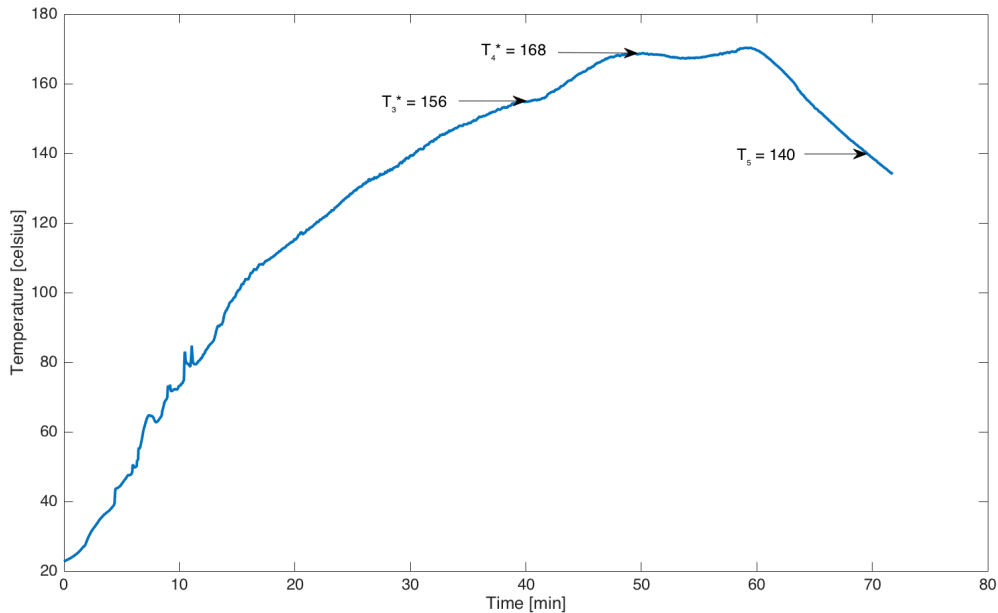


Figure 4.8: Plot of one of the circulating oil experiments - Test 1 (second experiment). Highlighted temperatures represent bellows expansion and contraction. T_3 and T_4 indicates the beginning and the end of the bellows expansion, and T_5 represents the end of the bellows contraction. Temperatures marked with '*', represents that they are measured in the oil region close to the bellows. The inclination after T_4^* represents a change in the placement of the two thermocouples.

Discussion

The results represent a system where the temperatures of the oil and the surface of the bellows were more closely correlated (when compared with the oil bath experiments). The bellows temperature in the experiments was about 2°C higher than the temperature of the oil. The expansion of the bellows also occurred at a lower temperature than in the oil bath experiments, which could be a result of an enhanced overall heat transfer rate. Consequently, causing the liquid to boil at an earlier instance. However, the bellows contraction (antifreeze condensation) was still observed as too inefficient. Some improvements of the condition inside the bellows was therefore initiated. The aim was to this time use a vacuum pump to eliminate the air inside the bellows, by introducing an internal vacuum before filling.

Test 2

This test will illustrate the results obtained with filling Method 3. The motivation for carrying out this experiment was to observe whether pure antifreeze inside the bellows, without the presence of air, could have any implications on the condensation process. Table 4.5 contains the important temperature results from the experiments. There were conducted two experiments, the first with one heat cycle and the second with two. The second experiment is represented graphically in Figure 4.9.

Table 4.5: Test 2 - Temperatures Measured at the Surface of the Bellows in the Circulating Oil Experiments (Internal Vacuum)

| Test 2 - circulating oil experiments | | | |
|---|----------------------------|----------------------------|--------------|
| | 1 st experiment | 2 nd experiment | |
| | Heat cycle 1 | Heat cycle 1 | Heat cycle 2 |
| $T_1^{(a)}$ | 140.0 | 140.0 | - |
| $T_2^{(a)}$ | 157.0 | 157.0 | - |
| T_3 - start to open port 3 | 164.0 | 164.5 | 164.5 |
| T_4 - port 3 fully open (port 2 fully closed) | 173.0 | 174.5 | 174.5 |
| T_5 - port 2 fully open (port 3 fully closed) | 149.5 | 150.0 | 150.0 |

(a) T_1 represents the first bellows expansion, and T_2 the temperature at which this bellows expansion was completed. This expansion was believed to be a result of the characteristics of a vapor pressure curve.

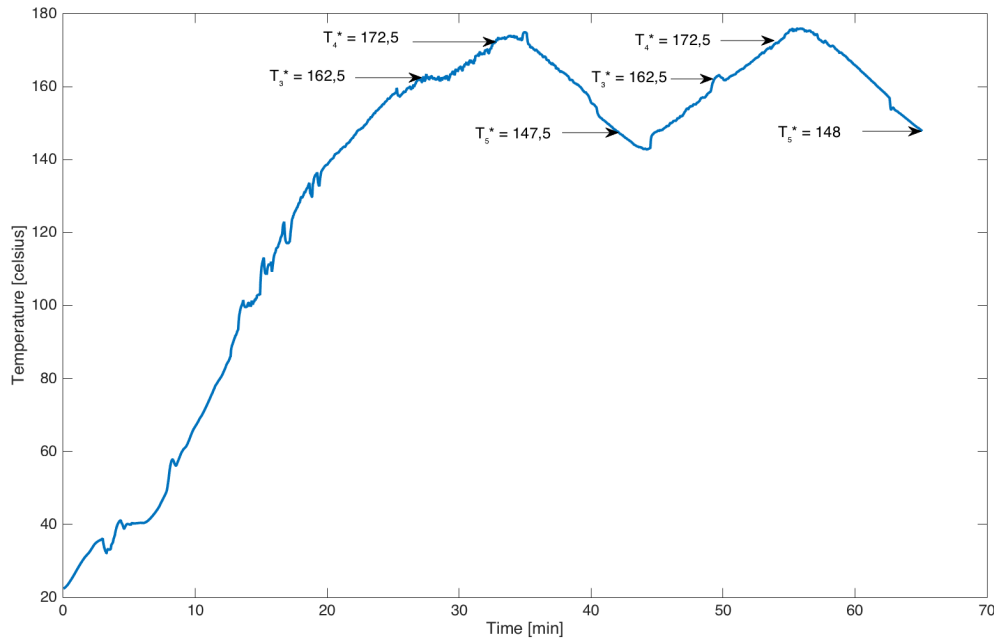


Figure 4.9: Plot of the circulating oil experiment where an internal vacuum was introduced in the bellows before filled with antifreeze. Highlighted temperatures represent bellows expansion and contraction. T_3 and T_4 indicates the beginning and the end of the bellows expansion, and T_5 represents the end of the bellows contraction. Temperatures are marked with '*', representing that they are measured in the oil region close to the bellows.

The results represented in Table 4.5 shows a bellows expansion when air impurities seem to have been eliminated. To justify this statement, the bellows appear to follow the characteristic vapor pressure curve, illustrated in Figure 4.6. From 20°C until 140°C, T_1 , the bellows expansion could be thought of as negligible, which corresponds to the near zero slope. From T_1 to 157°C, T_2 , the bellows started to expand gradually. This could be a response corresponding to the emerging slope of the curve. Due to the decreased length of the bellows this expansion occurred gradually inside the confining tunnel, until the bellows was stopped by the compression spring ($k = 0.237$ N/mm). From T_2 to 164.5°C, T_3 , a pressure build-up was initiated inside the

bellows, to overcome the force exerted by the spring. T_3 to 174.5°C , T_4 , represents the final bellows expansion. The bellows expands somehow gradually on this interval too, but with some more pronounced stepwise motion. This could be a result of many small pressure build-ups inside the bellows during the expansion process, due to the features of the spring (the spring force increases as the spring is being compressed towards its permissible clamped length). The bellows contraction was occurring from T_4 to 150.0°C , T_5 .

Discussion

The results from these experiments represents an enhanced system. The condensation process was improved, and the early bellows expansion, expected to be a result of air impurities, was no longer observed. Consequently, if the inside of the bellows this time only contained pure antifreeze, the characteristic vapor pressure curve could therefore be used in terms of understanding the physical processes inside. However, the condensation process still deviated from the evaporation process. From the description of condensation and evaporation processes in Chapter 3, even small mass fraction (0.5 percentage) of air in the system could have serious implications on this phenomenon. Regardless of this, air should not be present inside the bellows after an internal vacuum had been introduced. However, the vacuum pump system setup with its many interconnecting parts could result in some minor leakage somewhere in the system. In addition, antifreeze is also a liquid that could be a limiting factor in itself. It is an inexpensive multi-component liquid, and thus it would be interesting to test a pure one-component/homogeneous liquid to see whether this could have any implications on bellows features. Consequently, some further enhancements of the thermostat will be necessary before it can be utilized in a complete system.

Introduction - Test 3 to Test 7

The bellows valve-controlling behavior did not show efficient enough in the experiments with antifreeze. The temperature intervals were not short enough, and the evaporation and condensation processes inside the bellows did not seem to be in equilibrium. The most efficient experiment with the bellows that was conducted, resulted in a bellows expanding on a 10°C temperature interval, and a bellows contraction on a 25°C interval. However, these results are not efficient enough when the objective is to utilize the bellows as a control switch in the system. Despite this, it was decided to continue the work with the bellows. The motivation based on the fact that the bellows offers a thermostatic concept exploiting a physical phenomenon, which makes it independent of power supply. If there could be a possibility of the bellows being more functional, for example, by using another type of liquid and/or compression spring, it would be interesting to test this before continuing work with other control device solutions. The further work with the bellows will be carried out in the following sections, to observe if an enhancement of the bellows expansion and contraction could be realized by conducting some minor adjustments with the internal environment in the bellows, as well as the external.

In contrast to the previously conducted experiments with the bellows, there were also made some minor

changes concerning which temperatures to collect during the experiments. The reason for this was to try to obtain a better understanding of the condensation process inside the bellows. Additionally, as we are only utilizing filling Method 3, the information behind each collected temperature has been adjusted to fit this filling methods believed impact on the bellows sensitivity. All temperatures are still measured at the surface of the bellows, and the temperatures of interest are represented in Table 4.6.

Table 4.6: Temperatures of Interest - Experiments With the Liquid Filled Bellows in the Circulating Oil System

| Temperature instances of interest | |
|-----------------------------------|--|
| T_1 | First bellows expansion; a movement of about 4.75 cm, not causing any change in the flow pattern. The bellows moves inside the confining tunnel due to its decreased initial length. It is expanding until the compression spring exerts force towards it. The gradual bellows expansion that is being initiated seems to occur due to the condition inside being at the steeper part of the vapor pressure curve. |
| T_2 | initialization of the second bellows expansion where port 2 is being gradually closed and port 3 gradually opened. The condition inside the bellows is now moving towards the steepest part of the vapor pressure curve, thus from an atmospheric pressure condition and above. |
| T_3 | End of the second bellows expansion. |
| T_4 | initialization of the bellows contraction causing a gradual closing of port 3 and a gradual opening of port 2. |
| T_5 | The temperature instance when the bellows is compressed back into a position where port 3 is fully closed and port 2 is fully opened. |

Test 3

It was desirable to do an experiment with a compression spring with a higher spring rate, $k = 0.7 \text{ N/mm}$, to observe if this could have an enhanced effect on the motions of the bellows. A stronger spring (stronger than the bellows) could cause an increased internal pressure inside the bellows, resulting in a delayed expansion, and in addition making it more temperature sensitive. The characteristic vapor pressure curves of several liquids, as visualized in Figure 4.6, show that as the pressure increases the curves as a response to this becomes steeper. Hence, causing the system to obtain a more temperature sensitive state when entering into this region. The results from the experiment is presented in Table 4.7, and graphically in Figure 4.10.

Table 4.7: Test 3 - Temperatures Measured at the Surface of an Antifreeze Filled Bellows in a Circulating Oil System. It Was Used a Spring With $k = 0.7 \text{ N/mm}$

| Bellows filled with antifreeze - stronger spring experiment | | |
|---|--------------|--------------|
| | Heat cycle 1 | Heat cycle 2 |
| $T_1^{(a)}$ | 140.0 | 145.0 |
| T_2 - opening of port 3 is initiated | 165.0 | 165.0 |
| T_3 - port 3 fully open (port 2 fully closed) | 185.0 | 185.0 |
| T_4 - closing of port 3 is initiated | 172.0 | 172.0 |
| T_5 - port 2 fully open (port 3 fully closed) | 149.0 | 149.0 |

(a) T_1 represents the first bellows expansion. This expansion was believed to be a result of the characteristics of a vapor pressure curve.

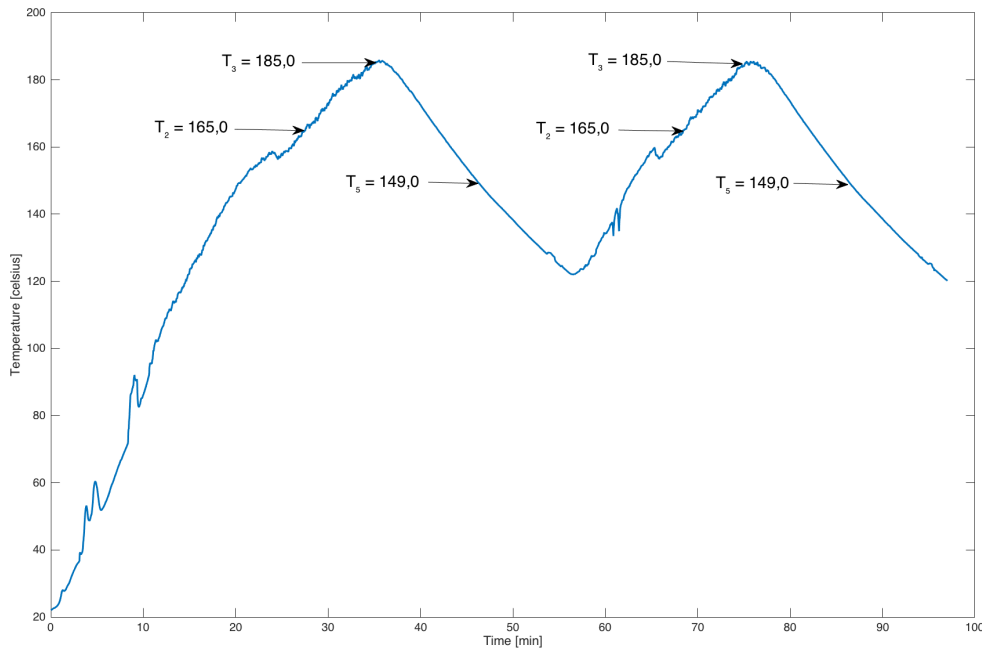


Figure 4.10: Plot of the circulating oil system with an antifreeze filled bellows, and with a stronger spring ($k = 0.7 \text{ N/mm}$) in the thermostat. Highlighted temperatures represent bellows expansion and contraction. T_2 and T_3 indicates the beginning and the end of the bellows expansion, and T_5 represents the end of the bellows contraction. All the temperatures are measured at the surface of the bellows.

The bellows expansion, T_2 to T_3 , required a 20°C temperature interval, and the contraction process, T_3 to T_5 , a 36°C interval. This illustrates an increase in 10°C in both the expansion and contraction process, compared to earlier obtained results. A 13°C temperature interval, T_3 to T_4 , was also required before the contraction process was initiated. Thus, when the bellows expansion processes ended at 185°C , the contraction process would not start before the surface temperature of the bellows had dropped to 172°C . Prior to this, the bellows would stay stationary. After the first heat cycle was completed, the oil system

was cooled down until 125°C was reached; the instance at which the bellows was back at its initial position. Hence, a 15°C lower temperature compared to when the first heat cycle was initiated. Additionally, the small peaks occurring prior T_2 in both of the heat cycles, at about 157°C , represents a small oil penetration through port 3.

Discussion

The stronger spring did not show any improvement on the bellows expansion and contraction processes. The aim for testing with a stronger spring, $k = 0.7 \text{ N/mm}$, was to observe if it could be possible to obtain a higher pressure condition inside the bellows, with a desire to obtain a more temperature sensitive bellows. Consequently, making the expansion and contraction processes occurring on a shorter temperature interval than before as a result of the higher pressure condition. The bellows and its internal pressure could then be at an even steeper part of the vapor pressure curve (above the atmospheric pressure condition) than what was obtained with the weaker spring, $k = 0.237 \text{ N/mm}$. The stronger spring did, however, not cause the bellows expansion at T_2 to occur at a later temperature stage, even with a higher pressure condition inside. The same was observed at the temperature instance when the bellows was compressed back into its initial position at T_5 . Both T_2 and T_5 were unchanged even though a compression spring with a stronger spring rate was used. This could, however, seem like a comprehensible behavior as we are moving along the steepest part of the vapor pressure curve, and the temperatures vary insignificantly in this area. Nevertheless, this would only have been the case if temperature T_3 had been unchanged as well. The same temperature interval should be obtained independent of the spring. The experiment required a 10°C additional temperature interval, compared to the previously conducted experiments, on both the expansion and contraction processes of the bellows. The stronger spring did not make the bellows more temperature sensitive, on the contrary, it made it less temperature sensitive, and as a consequence of this also less efficient. Thus, the bellows did not manage to overcome the force of the spring, and rather it delayed its motion.

When it comes to the temperature introducing the bellows contraction process, T_4 , we can observe that the bellows requires a 13°C decrease in temperature, and consequently a decrease in pressure, before the condensation process inside the bellows is being initiated. From the theory behind phase transitions reviewed in Chapter 2, this could be understood to represent a system containing air/gas impurities. If there are small percentages of air inside the bellows, it requires the saturation pressure to decrease due to the diffusional resistance on the interface. If this is the case, the bellows offers some distinct limitations in terms of being used as a controlling valve in this type of system.

Test 4, Test 5 and Test 6

Based on the results obtained above, it was decided to proceed with another liquid inside the bellows. The bellows was therefore drained, rinsed with water and dried before it was filled with ethanol. Ethanol, boiling at 78°C at atmospheric pressure, was tested inside the bellows to observe whether a liquid boiling at a

lower temperature could have any positive impact on the bellows features. The final bellows solution should, however, be able to regulate the oil flow at high temperatures, 180 - 200°C, in which would not be possible if a liquid boiling at a significantly lower temperature was to be used. However, if it would result in bellows expansion and contraction requiring shorter temperature intervals, the next step would be to try come up with a solution to adjust the bellows to the high temperature system.

Before the experiment was initiated, there was done some minor enhancement of the confining tunnel. A small section of the metal was cutoff, as it was believed that this could result in a more efficient overall oil penetration on the surface of the bellows. Figure 4.11 shows an illustration of the bellows inside the confining tunnel, after this cutoff had been conducted.



Figure 4.11: Picture of the bellows inside the confining tunnel, after parts of the tunnel has been cutoff. It was believed that this could result in a more efficient overall oil penetration on the surface of the bellows.

There were conducted three different experiments with the ethanol filled bellows. The strong spring ($k = 0.7 \text{ N/mm}$) was rejected after the experiment with antifreeze was carried out, based on the results from this experiment. Therefore, the following three bellows experiments with ethanol were carried out:

- The first experiment was conducted by using the weak spring ($k = 0.237 \text{ N/mm}$).
- The second experiment was conducted without any spring present in the thermostat. In the contraction process it was therefore necessary to assist the bellows back into its initial position with a finger push, since a return force was not present. Otherwise the bellows would become compressed inside the confining tunnel, in which would not change the flow direction. This experiment could be compared to one exploiting a very weak spring.
- The third experiment was carried out as a result of the second experiment. The back part of the bellows was then fixed to the confining tunnel through two of the tunnels many holes with a steel tread (see Figure 4.12).

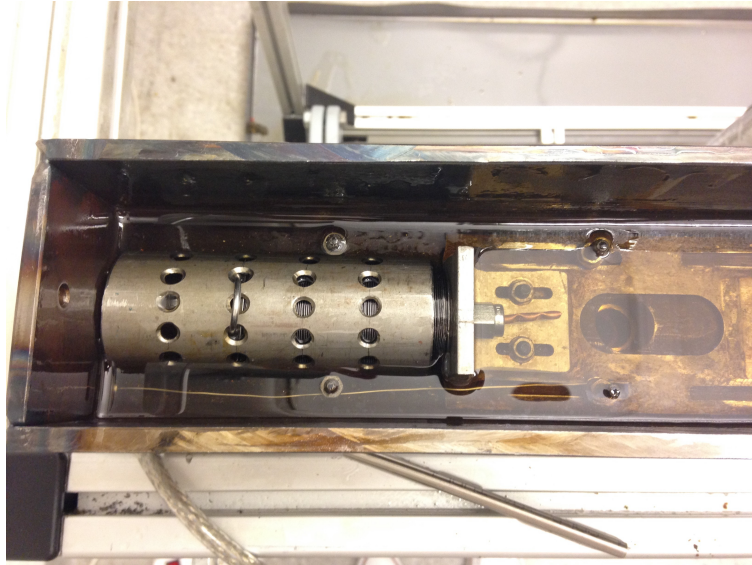


Figure 4.12: Illustration of the bellows and its position in the thermostat in the third experiment with ethanol. As can be observed in the picture the bellows has been attached to two of the holes in the confining tunnel by the use of a banded steel tread. This was done since a return spring was not present.

The results from the first experiment is presented in Table 4.8, and the second and third experiment are represented together in Table 4.9. All the results are illustrated graphically in Figure 4.13, Figure 4.14 and Figure 4.15.

Table 4.8: Test 4 - Temperatures Measured at the Surface of an Ethanol Filled Bellows in a Circulating Oil System

| Bellows filled with ethanol - 1 st experiment | | |
|--|--------------|--------------|
| | Heat cycle 1 | Heat cycle 2 |
| $T_1^{(a)}$ | 67.0 | - |
| T_2 - opening of port 3 is initiated | 86.0 | 82.0 |
| T_3 - port 3 fully open (port 2 fully closed) | 94.0 | 92.0 |
| T_4 - closing of port 3 is initiated | 82.0 | 83.0 |
| T_5 - port 2 fully open (port 3 fully closed) | 74.0 | 74.0 |

(a) T_1 represents the first bellows expansion. This expansion was believed to be a result of the characteristics of a vapor pressure curve.

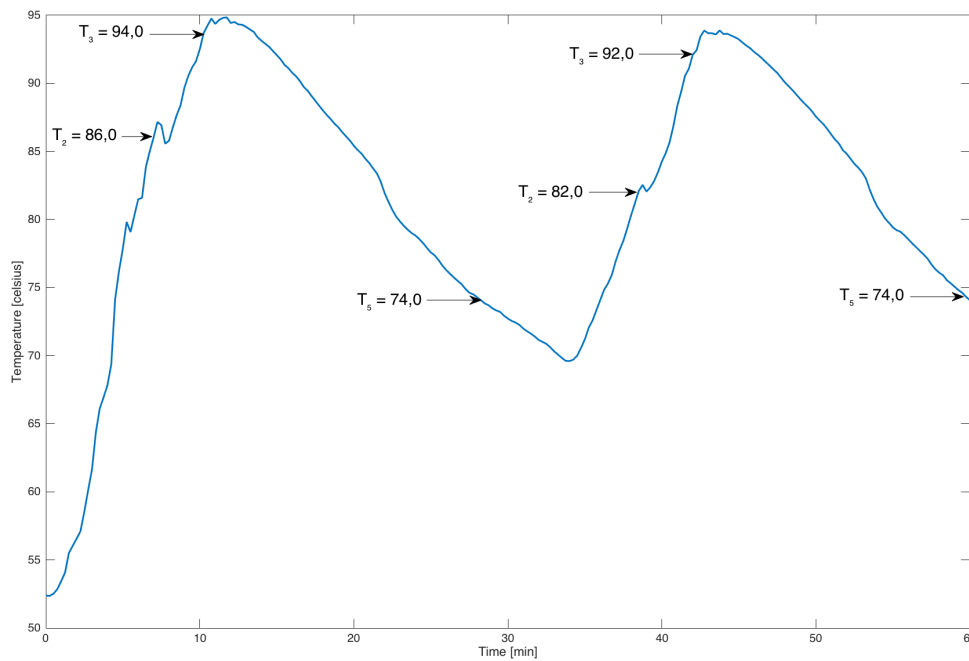


Figure 4.13: Plot of the circulating oil system with an ethanol filled bellows, and with the weak spring ($k = 0.237 \text{ N/mm}$) present in the thermostat. Highlighted temperatures represent bellows expansion and contraction. T_2 and T_3 indicates the beginning and the end of the bellows expansion, and T_5 represents the end of the bellows contraction. All the temperatures are measured at the surface of the bellows.

The results from the first experiment shows that the bellows still required a temperature interval of approximately 10°C in the expansion process. The temperature interval required for the contraction process was approximately 20°C , where half of this interval represented a stationary bellows.

Table 4.9: Test 5 and Test 6 - Temperatures measured at the surface of an ethanol filled bellows in a circulating oil system, without the presence of a return spring. In Test 6 the back part of the bellows was fixed to the confining tunnel

| Bellows filled with ethanol | | |
|---|---------------------------------|----------------------------|
| | 2 nd experi- ment | 3 rd experiment |
| $T_1^{(a)}$ | 67.0 | - |
| T_2 - opening of port 3 is initiated | 73.0 | 63.0 |
| T_3 - port 3 fully open (port 2 fully closed) | 78.0 | 75.0 |
| T_4 - closing of port 3 is initiated | 72.0 | 62.0 |
| T_5 - port 2 fully open (port 3 fully closed) | 67.0 | - |

(a) T_1 represents the first bellows expansion. This expansion was believed to be a result of the characteristics of a vapor pressure curve.

The results from the second experiment showed that without the return spring present, the bellows was expanding on a shorter temperature interval of about 5°C . However, the contraction process still required a longer temperature interval, of approximately 11°C . On that note, since there was not a spring present in

the thermostat, the bellows needed a finger push so that it would become compressed in the right direction (closing port 3 and opening port 2). The downward spike in the beginning of the plot, as illustrated in Figure 4.14, could be a result of an adjustment of the thermocouples. The oil was also continued heated a couple of minutes after the bellows expansion was over, which could have been a result of not immediately turning off the heating element.

The third experiment was conducted based on the results from the second experiment. As we did not have a return spring to ensure a resistance towards the bellows in the contraction process, we instead chose to conduct an experiment where we fixed the back part of the bellows to the confining tunnel (see Figure 4.12). Also in this experiment the oil was continued heated a couple of minutes after the bellows expansion process was over, again a result of not immediately turning off the heating element. As the bellows was fixed to the confining tunnel, the expansion of the bellows, from T_2 to T_3 , occurred on an earlier stage than in the previously conducted experiments. This was a result of the first expansion not taking place inside the confining tunnel, and instead directly in the direction causing a change in the oil flow. The expansion process occurred on a 12°C interval. For the contraction process, T_5 was not recorded, as the experiment was completed when the bellows was compressed halfway, thus at 55°C . At that point it was decided that it was not desirable to wait until the bellows was compressed completely back into its initial position. The temperature interval was already to inefficient halfway. As can be observed in Figure 4.15, T_5 is therefore not highlighted.

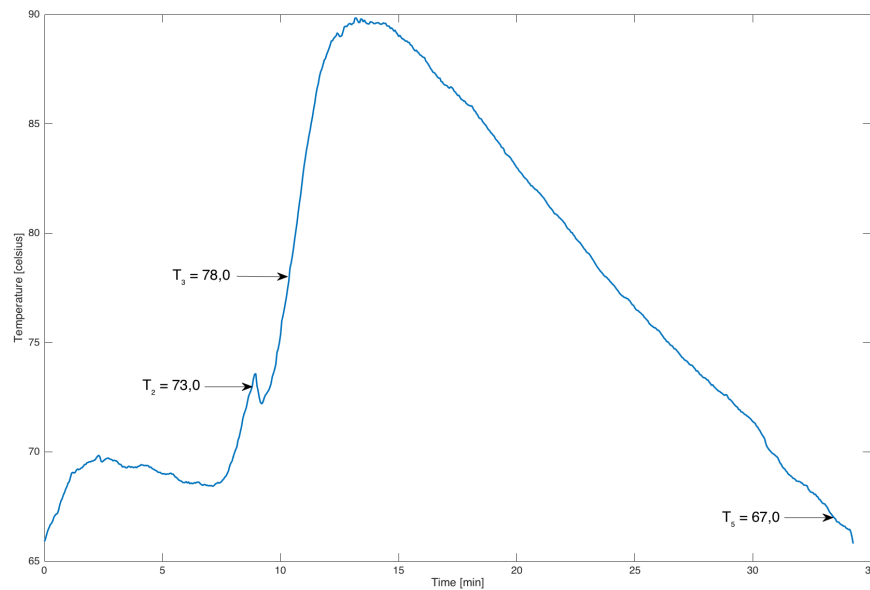


Figure 4.14: Plot of the circulating oil system with an ethanol filled bellows, without a spring present in the thermostat. Highlighted temperatures represent bellows expansion and contraction. T_2 and T_3 indicates the beginning and the end of the bellows expansion, and T_5 represents the end of the bellows contraction. All the temperatures are measured at the surface of the bellows.

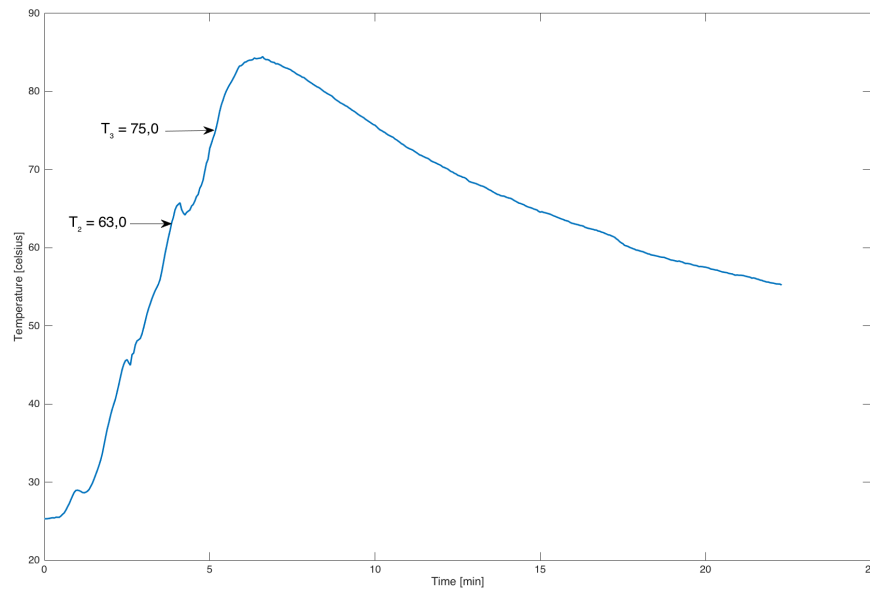


Figure 4.15: Plot of the circulating oil system with an ethanol filled bellows, without a spring present in the thermostat. The bellows was fixed to two of the holes in the confining tunnel, to ensure bellows expansion and contraction in the right direction (oil regulation direction). Highlighted temperatures represent bellows expansion and contraction. T_2 and T_3 indicates the beginning and the end of the bellows expansion. Bellows contraction was not completed.

Discussion

The first experiment showed similar results as the previously conducted experiments where the same spring ($k = 0.237 \text{ N/mm}$) was used, but with another fluid inside the bellows. The fact that T_2 in the first heat cycle was a couple of degrees higher than in the second heat cycle, could be a result of the heat conductivity of the stainless steel bellows. Thus, the temperature of the fluid inside could be at a slightly lower temperature than what was measured at the bellows surface during the first heating cycle. The condensation process was enhanced with a couple degrees, approximately 5°C , compared to the experiments with the antifreeze filled bellows. If this was due to the change of liquid, resistance that could exist in the bellows material at higher temperatures or other potential factors, is difficult to establish. Nevertheless, the results from this experiment is not satisfactory, as the temperature intervals, especially for the contraction process, is still not efficient enough. The bellows expands on a 10°C temperature interval, and becomes compressed on a 20°C interval. Still, as observed from the antifreeze experiments, the bellows is stationary in half of this process. Meaning that the initialization of the condensation process inside the bellows requires a 10°C temperature drop before the bellows contraction process is taking place. It seems likely that the bellows, in the expansion process, follows the vapor pressure curve of ethanol. However, this does not seem to be the case for the contraction process.

Even though there was no spring present in the second experiment, we believe that it is reasonable to compare it with an experiment where a spring with low spring rate could have been used. The bellows

expands on a short temperature interval when it does not face any resistance from a spring. Hence, it only experiences volume change and no change in the internal pressure (the pressure is constant). However, without a return force, the bellows needed a finger push so that it could become compressed in the right direction. Consequently, a weak spring will have to be present in the thermostat configuration to exert a return force onto the bellows. Regardless of this, the phase transition processes were still not symmetric.

The third experiment showed a longer temperature interval for the expansion process than what was observed in the other experiments. In addition, T_5 was not recorded as the experiment was completed before the bellows was back at its initial position. Not only did this experiment reveal that the expansion process was too long, but also that the contraction process halfway was too inefficient. Whereas the expansion process required a 12°C temperature interval, the contraction process required a 20°C interval halfway.

Even though some enhancements were observed when experiments without a spring (a spring with low spring rate) were conducted, the bellows valve-controlling behavior did not show efficient enough. Antifreeze and ethanol were chosen based on their easy accessibility and their inexpensiveness. However, these types of liquids could have their limitations, as they are not pure, and thus might contain substances that could have a disturbing impact on the phase transition processes. Some final experiments were therefore decided to conduct, to observe if the expansion and contraction of the bellows could be enhanced when filled with another type of liquid; a special ordered one-component liquid. These experiments will be carried out in the next section.

Test 7 and Test 8

The last experiments conducted was done with a 1,2-Propylene glycol diacetate filled bellows, a one-component liquid, boiling at $190\text{--}191^\circ\text{C}$ at atmospheric pressure. The experiments were not carried out on the same system setup as before. Rather, on a system setup including a storage, a system which will be presented in more detail in Chapter 5. For an illustration of this system, see Figure 5.1a. As can be observed in the figure, pipe 3 has been extended due to an application unit included in the system. Thus, the experiments with 1,2-Propylene glycol diacetate will experience a larger heat loss on this stretch.

The motivation for testing the bellows with this liquid was to observe whether it would have any enhancement effect on the expansion and contraction processes. A pure one-component liquid could have an advantage in terms of not containing any disturbing substances, in which presence could influence the phase transition processes. The vapor pressure curve was unavailable, as the producer, was not able to retrieve it. The only information given was that at 20°C the vapor pressure should be below 1 mbar. Thus, the results collected in these experiments have been interpreted based on the previous experiments.

Three experiments were conducted with a 1,2-Propylene glycol diacetate filled bellows. The first two experiments were similar, using the same spring ($k = 0.237\text{ N/mm}$), and in the third experiment the strong spring ($k = 0.7\text{ N/mm}$) was used. The third experiment was conducted based on the results from the two first experiments. They showed a bellows operating completely differently from what had been observed in

previously conducted experiments, where the strong spring was rejected for further testing.

All the experiments are presented together in Table 4.10 and illustrated in Figure 4.16, Figure 4.17 and Figure 4.18.

Table 4.10: Test 7 and Test 8 - Temperatures measured at the surface of a 1,2-Propylene glycol diacetate filled bellows in a circulating oil system. The two first experiments used the weak spring ($k = 0.237$ N/mm), and the third the strong spring ($k = 0.7$ N/mm)

| Bellows filled with 1,2-Propylene glycol diacetate | | | |
|--|----------------------------|----------------------------|----------------------------|
| | 1 st experiment | 2 nd experiment | 3 rd experiment |
| T ₁ | 87.0 | 87.0 | 85.0 |
| T ₂ - opening of port 3 is initiated | 109.0 | 109.0 | 110.0 |
| T ₃ - port 3 fully open (port 2 fully closed) | 113.0 | 110.0 | 125.0 |
| T ₄ - closing of port 3 is initiated | 103.0 | 103.0 | - |
| T ₅ - port 2 fully open (port 3 fully closed) | 89.0 | 89.0 | 94.0 |

(a) T₁ represents the first bellows expansion. This expansion was believed to be a result of the characteristics of a vapor pressure curve. However, the remaining temperature results did not occur when expected. It was difficult to interpret the results, as the vapor pressure curve was unavailable, as the producer, was not able to retrieve it.

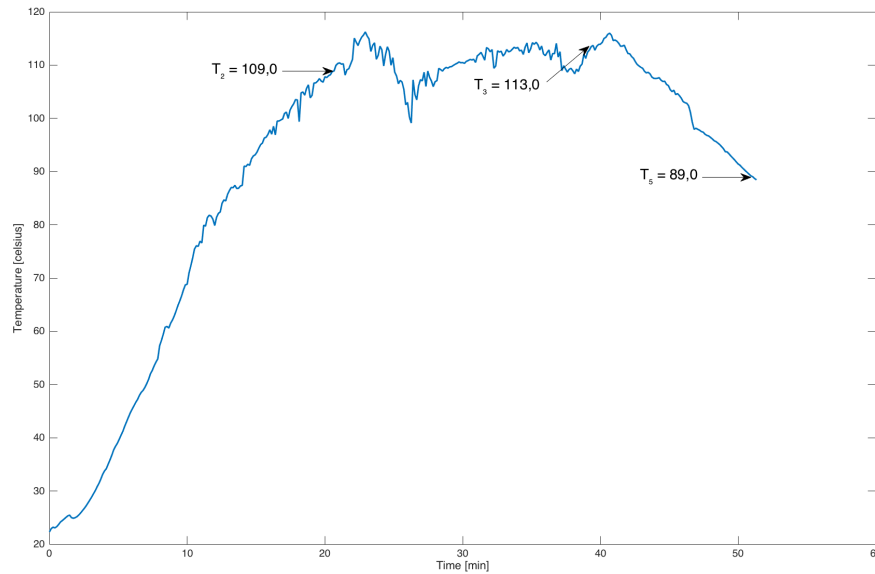


Figure 4.16: Plot of the circulating oil system with a 1,2-Propylene glycol diacetate filled bellows, with the weak spring in the thermostat ($k = 0.237$ N/mm). Highlighted temperatures represent bellows expansion and contraction. T₂ and T₃ indicates the beginning and the end of the bellows expansion. T₅ represents the end of the bellows contraction. All the temperatures are measured at the surface of the bellows.

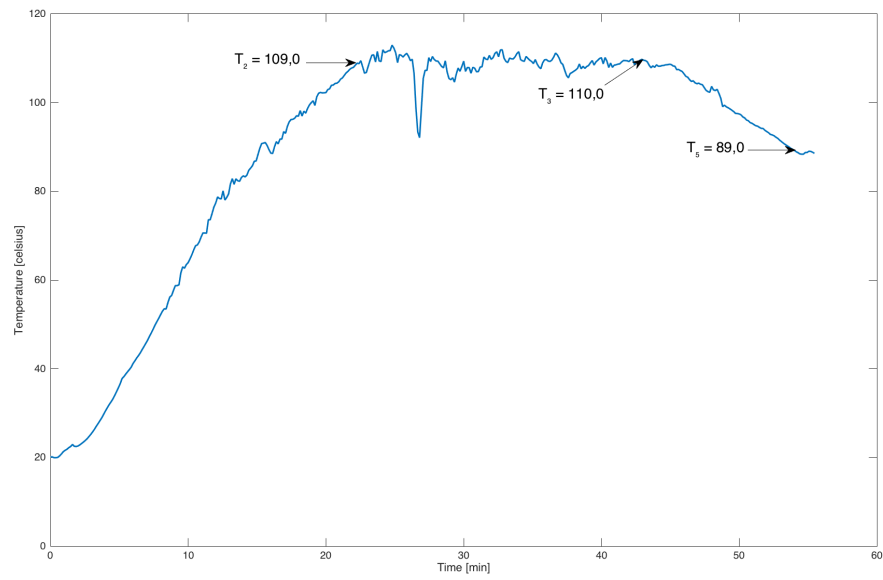


Figure 4.17: Plot of the second circulating oil system with a 1,2-Propylene glycol diacetate filled bellows, with the weak spring in the thermostat ($k = 0.237$ N/mm). Highlighted temperatures represent bellows expansion and contraction. T_2 and T_3 indicates the beginning and the end of the bellows expansion. T_5 represents the end of the bellows contraction. All the temperatures are measured at the surface of the bellows.

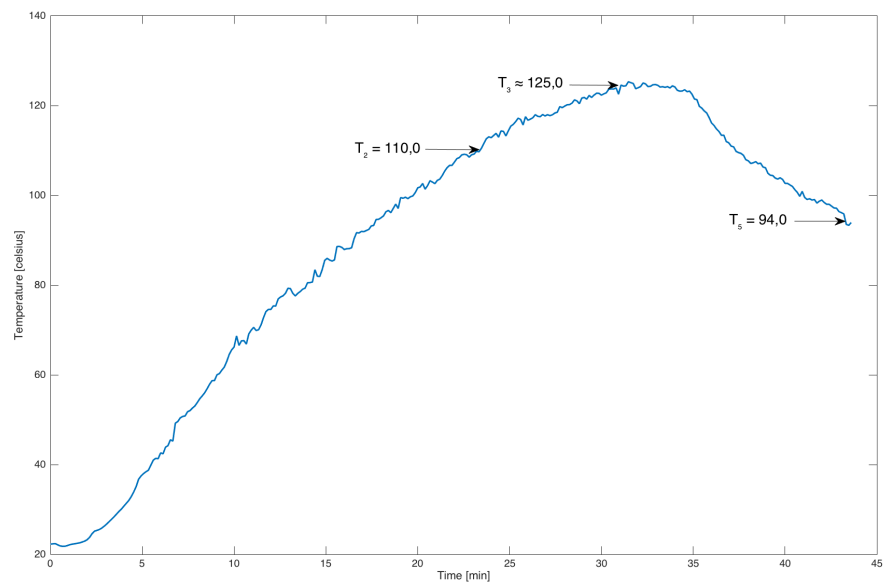


Figure 4.18: Plot of the first circulating oil system with a 1,2-Propylene glycol diacetate filled bellows, where the strong spring was present in the thermostat ($k = 0.7$ N/mm). Highlighted temperatures represent bellows expansion and contraction. T_2 and T_3 indicates the beginning and the end of the bellows expansion. T_3 was not reached completely due to leakage out of nozzle of the bellows. T_5 represents the end of the bellows contraction. All the temperatures are measured at the surface of the bellows.

Discussion

The first two experiments showed similar results. However, the results were not concentrated around the liquids boiling point at atmospheric pressure, 190-191°C. The bellows expansion from T_2 to T_3 occurred on a short temperature interval, 109°C to 110/113°C, but on a significantly longer time interval than in the previously conducted experiments. However, the longer time interval was most certainly a result of the extended length of pipe 3 (as the complete system setup was used during the experiments with this liquid). In the expansion process of the bellows, opening of port 3, there would therefore be a larger temperature drop in the oil. From Figure 4.16 and Figure 4.17 one can observe that the temperatures are oscillating considerably over a long time interval. Temperatures above 109°C caused the bellows to expand, whereas temperature dropping below 100°C initiated bellows contraction. Consequently, a result of the now more prominent heat losses. For the contraction process, T_3 to T_5 , a temperature interval of more than 20°C was required in both of the experiments.

The third experiment was carried out as it was desirable to observe the bellows motion with the stronger spring, when utilizing this type of liquid inside. Justified by the fact that this liquid was somehow acting differently compared to the other liquids tested. What was observed was however the similar situation as earlier, thus the bellows started to expand at approximately the same instance as with the weak spring. This was occurring even if the strong spring was having a stronger spring rate than that of the bellows, and the weaker spring was having less. Due to leakage in the nozzle of the bellows at 125°C, the expansion process was stopped before port 3 was completely open (2.00 mm before). The heating element was therefore switched off, and a 31°C temperature interval later the bellows had contracted back into its initial position. The instance, T_4 , in which the contraction of the bellows was initiated, was not recorded. The contraction process was however introduced almost immediately after the heating element was turned off. The leakage seemed to be a result of a high internal pressure inside the bellows, causing the fluid inside to penetrate through the nozzle. The stronger spring was therefore not working with this type of liquid either. The higher pressure did not cause the bellows to be more temperature sensitive. It seems like the pressure increase occurs at a very fast rate, causing the stronger spring to not have any visible effect on the temperature instance of expansion. However, the large pressure build-up required to overcome the force of the spring during the expansion process, makes the expansion process slower. The contraction process of the bellows is also still too inefficient, even though a stronger return force is present. The stronger spring did therefore not have any enhancement effect on either of the processes.

The experiments with the 1,2-Propylene glycol diacetate filled bellows did not show any enhancement of the bellows motion. The long time interval, which in itself is not a problem, illustrated that the bellows exhibited a too weak responsiveness. As a result of the extension of pipe 3, there was a large temperature drop in the oil (compared to the previous system setup). Hence, bellows expansion was initiated, but when the temperature dropped the bellows did not manage to contract fast enough. As observed in the previously conducted experiments, the bellows needed a decrease in temperature of approximately 10°C, before the

contraction process would be initiated. This offers an operational problem for our system, as only oil at an adequate high temperature should be sent into the storage or to the application unit.

Due to the fact that the vapor pressure curve for this liquid was unavailable, as the producer, was not able to retrieve it, it was difficult to understand the observations made. From the safety data sheets of antifreeze and ethanol, it is specified that the vapor pressure at 20°C is 0.013 mbar for antifreeze, and above 23 mbar for ethanol. That the vapor pressure for 1,2-Propylene glycol diacetate is less than 1 mbar, could possibly mean that the vapor pressure is much lower than that of antifreeze at the same temperature. However, this becomes a very vague presumption. Nevertheless, if this could be the case, it could as a consequence be the reasons for the early evaporation initialization at 85/87°C, inside the bellows. However, as the bellows second expansion occurred much earlier than expected, 109/100°C, instead of 190-191°C, this presumption will be inadequate. The reason why the second expansion occurred approximately 80°C before expected is difficult to interpret. As the vapor pressure curve is not readily available, there is a clear limitation in terms of using special ordered one-component liquids. Nevertheless, one-component liquids does not seem to offer any advantages when it comes to the phase transition processes.

When looking at the first two experiments, it seems like we are facing what could be a heat capacity problem for the expansion process from T_2 to T_3 . This observation, together with the observations of the bellows motions in general throughout the experiments, could thus be a result of the heat capacity of the stainless steel bellows. It was believed that this would be an issue after the preparatory work for this thesis was completed. Several experiments later, it clearly seems like it is on of the main problem in terms of being able to use the bellows as a control valve in the system. Stainless steel bellows requires a larger amount of heat to decrease/increase the temperature of the material, compared to what, for instance, a copper bellows would require (expensive). As the time interval is longer, heat is being absorbed by the bellows over a longer period of time, which could be the result of the short temperature interval for the expansion process. As the cooling process of the oil would be faster due to the extension of pipe 3 (more heat losses), the contraction process would not be more efficient. As was observed.

4.7 Discussion and Comparison of The Experiments

The results from the experiments are represented in Table 4.11. More experiments than the ones shown in the table were conducted, however, those having close to equal temperature intervals to open and close port 3, have been presented only ones. The first results collected were from the experiments with antifreeze. It seems like the overall heat transfer system was improved from the oil bath experiments to the circulating oil experiments. Thus, when it comes to the condensation process inside the bellows. The contraction process, however, showed different temperature intervals depending on the filling method used. The third filling method gave enhanced results, and removal of air inside the bellows could therefore seem to have had an effect. The responsiveness of the bellows was as good as constant during the evaporation process of antifreeze,

Table 4.11: Comparison of the Temperature Intervals Required to Open and Close Port 3 in the Experiments With the Liquid Filled Bellows

| Temperature intervals for closing and opening of port 3, based on the different fluids tested. | | | | | | |
|--|-----------------|------------------|-----------------|------------------|----------------------------|------------------|
| | Antifreeze | | Ethanol | | 1,2-Propylene glycol diac. | |
| | ΔT open | ΔT close | ΔT open | ΔT close | ΔT open | ΔT close |
| Oil bath | 10.0 | 40.0 | - | - | - | - |
| Circulating system, filling Method 2 | 12.0 | 30.0 | - | - | - | - |
| Circulating system, filling Method 3 | 10.0 | 25.0 | 10.0 | 20.0 | 1.0 - 4.0 | 25.0 |
| Filling Method 3, strong spring | 20.0 | 25.0 | - | - | 15.0 (not fully completed) | 30 |
| Filling Method 3, no spring | - | - | 5.0 | 10.0 | - | - |

until the strong compression spring was tested. The results with the strong spring was showing a less efficient bellows. The higher pressure did not cause the bellows to be more temperature sensitive. It seems like the pressure increase occurs at a very fast rate, causing the stronger spring to not have any visible effect on the temperature instance of expansion. However, the large pressure build-up required to overcome the force of the spring during the expansion process, makes the expansion process slower.

The experiments carried out with ethanol gave enhanced results when the weak spring was not present. However, the condensation process was still too inefficient. The most efficient operating bellows, filled with antifreeze or ethanol, showed that the condensation process required approximately twice the temperature interval of the evaporation process.

A final experiment was conducted with a one-component special ordered liquid, 1,2-Propylene glycol diacetate. If there could be any other factors than air limiting the condensation process, for example any disturbing substances (could be the case in multi-component liquids), this issue should be eliminated with a pure one-component liquid. However, as Table 4.11 shows, the motion of the bellows was not enhanced with this type of liquid. The observations were neither easy to interpret. 1,2-Propylene glycol diacetate boils at 190-191°C at atmospheric pressure. Compared to the two other liquids, the results with this liquid does therefore not seem to correspond to the characteristics of a given vapor pressure curve. As needed information regarding the liquid was not possible to acquire from the company producing it, it became difficult to understand what the bellows motions were representing.

Consequently, the final thoughts about the bellows experiments is that air, even though the percentage must be significantly small, could have a substantial limiting effect on the condensation process. Additionally, the high heat capacity/low thermal conductivity of the stainless steel material could also cause delayed reaction processes inside the bellows. However, this would not impact the different temperature intervals observed for the expansion and contraction processes. The concluding remarks is that non of the experiments

conducted resulted in the phase transition processes being symmetric. Therefore, this type of bellows does not appear to be efficient enough to be used as a heat controlling valve in the thermostat. Cold oil should not flow into a storage or to an application point. Cold oil will cause reduced system efficiency, and thus the system would not be functional. Other thermostat solutions should therefore be examined.

4.8 Procedure With The Gas Filled Bellows

The work with the gas bellows was a direct response to the results obtained with the liquid filled bellows. It was believed that in a system containing only gas there would not be issues with non-equilibrium effects, where the expansion and contraction processes does not occur at the same rate. At a desired temperature, a large air volume connected to a small diameter bellows, would be shut off from the surroundings with a valve. What would occur thereafter would be that a further increase in the oil temperature would result in a superheated condition of the air. Consequently, starting out at an atmospheric pressure condition, would result in a pressure increase per further increase in temperature. Expansion of the bellows would then be initiated.

Before constructing the system setup with the gas bellows, there were some preparatory work that had to be done. For instance, the type and the size of the unit containing the required amount of air, at which would result in a bellows expansion/contraction of 2.50 cm, had to be calculated. 2.50 cm was chosen based on the fact that the bellows (in the end) would be incorporated into a similar thermostat design as the one used in the experiments with the liquid filled bellows. The unit containing the required air volume was a copper coil, desired to have an as small diameter as possible. With a coil holding a small diameter one obtain a large surface area per amount of air inside, and as a consequence, one achieve sufficient heat transfer between the oil and the air. In addition, copper has a high thermal conductivity, and it is easy to make a coil of the material as it is very bendable. The size of the copper coil could be computed after calculating how much air the bellows would require in terms of expanding 2.50 cm. On that note, if a large diameter bellows would have been used, this volume would have been required to be significantly large, and therefore too large for a small diameter copper coil to be used (the heat transfer between the oil and the air would not have been as efficient). It was necessary to compute the appropriate diameter of the bellows, thus to know how much air the bellows would require to provide the required expansion. Since the bellows is welded, it has an inside diameter being less than the outside diameter, and therefore it would not be correct to use any of these two diameters. Archimedes principle was therefore exploited in terms of finding the more appropriate diameter. The principle concerns displacement volume, meaning that as a substance is being immersed in water, it will displace a water volume equal to its own volume. How this was done in our case as visualized in Figure 4.19.

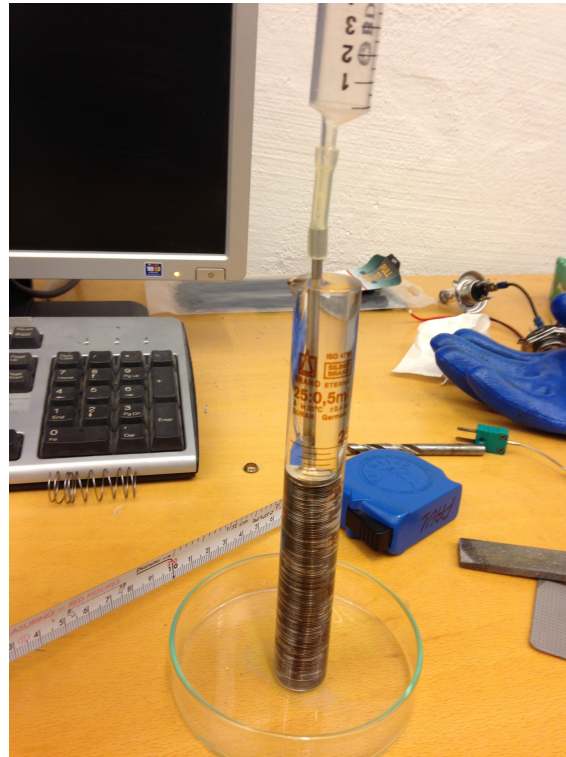


Figure 4.19: The picture illustrated the system setup used in terms of finding the displacement volume of the bellows, as it expands 2.50 cm. The bellows was fully immersed in a test tube filled with water, where a syringe had been connected to its nozzle. Air was injected through the nozzle until the bellows had expanded the required length. The displacement volume was collected in a small glass container located beneath the test tube. This volume could then be used in terms of finding the bellows diameter.

The bellows was fully immersed in a test tube filled with water to the brim, where a syringe was connected to its nozzle. Air was then injected through the nozzle until the bellows had expanded the required length of 2.50 cm. The injection of air into the bellows was done with a measuring tape next to the test tube, thus to know when to stop the injection. 8.23 cm (free length of bellows) plus 2.50 cm (expansion length) and 0.30 (test tube thickness), gives 11.03 cm, hence the point where injection should be stopped. As this distance was reached (read of the measuring tape) the filling was completed. The displacement volume was collected in a small glass container located beneath the test tube. The displacement volume of the water could then be used in terms of finding the diameter of bellows, calculated to be 10.10 mm. This property, together with the temperature instance of expansion, set to 190°C , the temperature interval at which the bellows was to expand on, set to 5°C , and its required expansion length, 2.50 cm, was together with the ideal gas law equations for the bellows and the copper coil, used to compute the size of the copper coil. The output of the calculations were as visualized graphically in Figure 4.20. The graph shows the required diameter of the coil when varying its length. As there were 15 mm pipes available in the lab, this diameter was chosen, in which corresponded to a 1.05 m coil length.

The experimental setup was then constructed, and the complete setup became as visualized in Figure 4.21. As can be observed in Figure 4.21b, a tee-tube-fitting was connected to the outlet of the coil, where

the bellows was connected to the one outlet and a valve to the other. From the tee-tube-fitting outlet to the valve there was a pipe in between to make it convenient to close the valve as the desired oil temperature was reached. Since this extra pipe connection was included in the setup, the coil length had to be reduced to some extent. After the length of the extra pipe connection was subtracted, the coil length required became 0.864 m (instead of 1.05 m). The coil had a center diameter of 19.00 cm, and thus the amount of coil rounds became $0.864/(\pi \times 0.19) \sim 1.45$. The spring force/mechanical resistance of the bellows was not taken into consideration when calculating the size of the system setup. It was assumed that due to its small size, and therefore small volume, the superheated air in the copper coil would cause an expansion of the bellows almost regardless of this property. The results of the experiments will be carried out in the next section. The results will be divided into two parts.

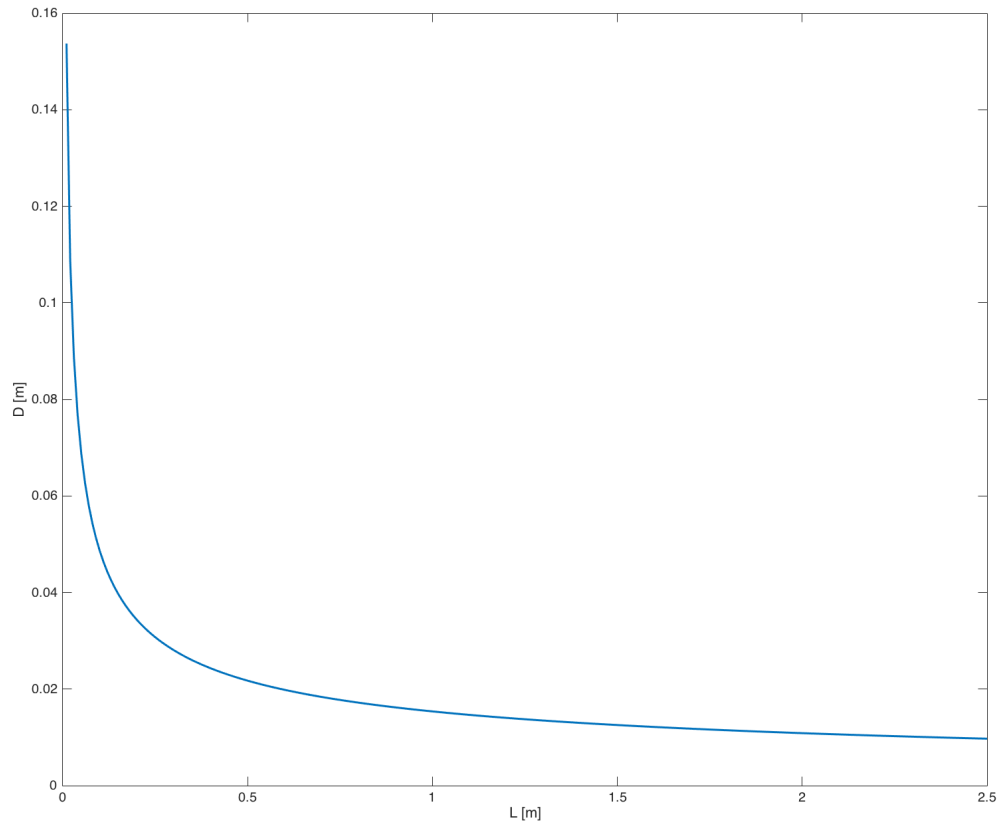


Figure 4.20: Plot of the copper coil dimensions for given gas bellows parameters. The plot shows the required diameter of the coil when varying its length.



(a) The setup used for the testing of the gas bellows. The oil bath contains a heating element immersed in the oil, together with a copper coil filled with air. The bellows was connected to the coil as visualized in Figure 4.21b. A short copper pipe, connected to the coil, holds the valve which was to be closed at a given oil temperature. The temperature was measured by the temperature reader, and the heat from the heating element was controlled by the regulator.



(b) A close-up picture of the gas bellows system. In the picture the heating element can be observed in the bottom section of the oil bath, where the copper coil has been located on top of it (without being in direct contact due to a copper pipe working as a separating unit). A tee-tube-fitting was connected to the outlet of the coil, where the bellows was connected to the one outlet and the valve to the other.



(c) The copper coil made out of 15 mm diameter pipes. The picture was taken right after the coil had been rotated around a cylinder, giving the coil a center diameter of 19.0 cm.



(d) After the coil was cut at the point giving the desired coil laps (approximately 1.5 rounds), the one outlet was closed and soldered completely, whereas the other outlet was soldered to a tube fitting. This tube fitting was then connected to the bellows.

Figure 4.21: The gas bellows system setup. Pictures showing some of the work that had to be conducted prior the experimental testing, together with pictures of the complete system setup.

4.8.1 Results

The results will be divided into two parts; Part 1 and Part 2. Part 1 will be based purely on performed calculations, whereas Part 2 will be based on observations made during the first part.

Part 1

The first two experiments with the gas bellows was carried out based on the results from the calculations. The experiments were very similar, and the results were compliant.

In the first experiment the valve was closed off at an oil temperature of 190°C , and the bellows was observed over a 5°C temperature interval. An experiment corresponding to the conducted calculations. However, the experiment did not illustrate a bellows expansion as expected. It did not seem like the bellows expanded at all on the 5°C interval. After assessing the observations, the oil was continued heated, thus to observe whether a longer temperature interval would affect the expansion. It was considered that the mechanical resistance of the bellows could have had an impact, making it capable of resisting the pressure change. However, as the temperature reached 210°C , a temperature interval of 20°C instead of 5°C , the expansion was still not even close to a length of 2.50 cm. Not more than a 4-5 mm expansion had taken place.

In the second experiment the oil was again heated up to 190°C . However, compared to the preceding experiment, the bellows was this time compressed completely together before the valve was shut off. This was done with an aim to try eliminate any mechanical resistance in the bellows (at a compressed condition the bellows will always want to go back to its free/equilibrium length). As the calculations did not account for the mechanical resistance in the bellows, this compression was worth a try. However, what happened after the bellows was compressed, and after having released it, was that it immediately jumped back into its free length. Thus, the results were the same as in the first experiment.

Discussion

After the two first experiments with the gas bellows was conducted, it was believed that there could have been a leaking point in the system. This became evident during the second experiment, as the compression of the bellows did not seem to work. Nevertheless, after doing multiple tests on the system by introducing compressed air inside, and by covering the system with soap, Zalo, which should bubble at a leaking point, leakage was not believed to be the issue. There were no visible bubbles, and after compressed air was introduced, the bellows sustained the expanded length it was given. It was then started to believe that either air in itself would not be the correct gas to use in this type of system, or the bellows was possibly holding too much mechanical resistance. Thus, the air molecules increase in kinetic energy (kinetic energy increase proportionally with the increase in temperature), would not manage to exert enough force/pressure to overcome the bellows embedded resistance. An additional limitation of this system could therefore be the compressibility of the air.

It was, however, motivation for conducting one last experiment. The experiment was carried out to observe how long the temperature interval would have to be, before it would be possible to identify a more substantial expansion of the bellows. A long temperature interval would not be favorable in the end, but in terms of understanding the bellows features in this type of system it was desirable to conduct such an experiment.

Part 2

In the third and last experiment it was decided to close the valve at an earlier instance, and make the temperature interval longer. The valve was therefore shut off at 130°C. A 40°C temperature interval later the experiment was stopped. At 170°C the bellows had expanded approximately 1.0 cm. At this moment it became apparent that the bellows would require a too long temperature interval to complete the 2.50 cm expansion process. It was rather decided to bend the tiny pipeline, connecting the bellows with the rest of the system (see Figure 4.21b), and immerse the bellows into the oil. This was done to observe whether any heat losses from the bellows surface could stand out as a system limitation. There was, however, not observed any evident changes in the bellows length after this immersion.

4.8.2 Discussion

The system constructed with the gas bellows did not show a system operating as anticipated. Clearly, using the ideal gas law will have its deviations when it comes to real life experiments. However, the deviations from the calculations these experiments show, seems to be based on other factors. After the first experiments was conducted, several tests were carried out aiming to understand the behavior of the system. First, the bellows was compressed completely together preliminary to the closing of the valve. This was done to reduce the bellows mechanical resistance. However, the bellows was not capable of holding a compressed position, and jumped straight back into its equilibrium length. On that note, compression might not work because of the large gas volume in the copper pipe. The results collected were not different from the first experiment. As leakage did not appear to be a system limitation after several leakage testes had been conducted, it clearly seemed like it would have to be the mechanical resistance of the bellows, together with the compressibility of air that would be the main issues.

One last experiment with a larger temperature interval was tested, to observe how large this interval would have to be to obtain any visible expansion. In addition to this the whole surface of the bellows was immersed into the oil to eliminate that any heat losses from its surface could appear to be a system limitation. The 1.0 cm movement occurring after a 40°C temperature interval was carried out, implies that the pressure required to cause expansion has to be significantly large. Therefore, we believe that if this system setup is to be functional, some major changes will have to be conducted. A bellows with less mechanical resistance, and/or another type of gas should be the follow up to these experiments. Before using another type of gas, the system should be evacuated, thus an internal vacuum should be introduced, to eliminate the presence

of air inside the system. The gas would have to be chosen based on its properties, so that the result would be a bellows expansion initiated at a temperature instance somewhere between 180-200°C. The temperature interval of expansion should not exceed 5°C, and the mechanical resistance of a given bellows should be taken into consideration in the search for an appropriate gas, with an appropriate compressibility.

Chapter 5

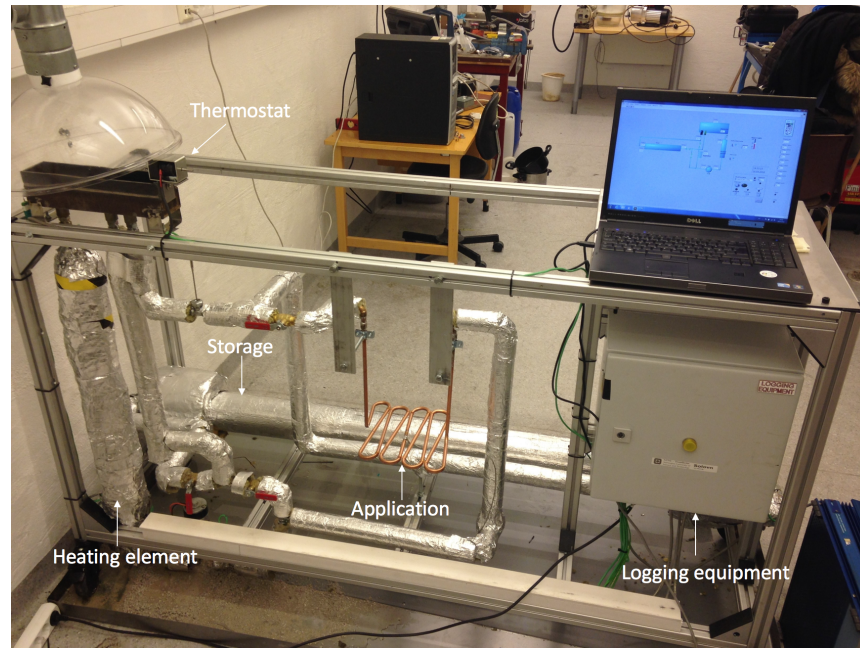
Experiments With The Solenoid & The Storage

The complete system setup was a direct extension of the circulating oil system setup. Hence, the system was extended to include an application unit and a storage, where the thermostat concept utilized was based on another approach than a bellows. A solenoid was used, requiring power supply, thus where temperature change alone could not be exploited. There will first be conducted a review of how the system setup was constructed, before the results from the experiments will be presented. The experiments will focus on demonstrating the principles of the system setup, and therefore not on constructing a complete system. Results will show whether a solenoid can work as a controlling valve in this type of system, and if it will be possible to obtain forced stratification inside the storage.

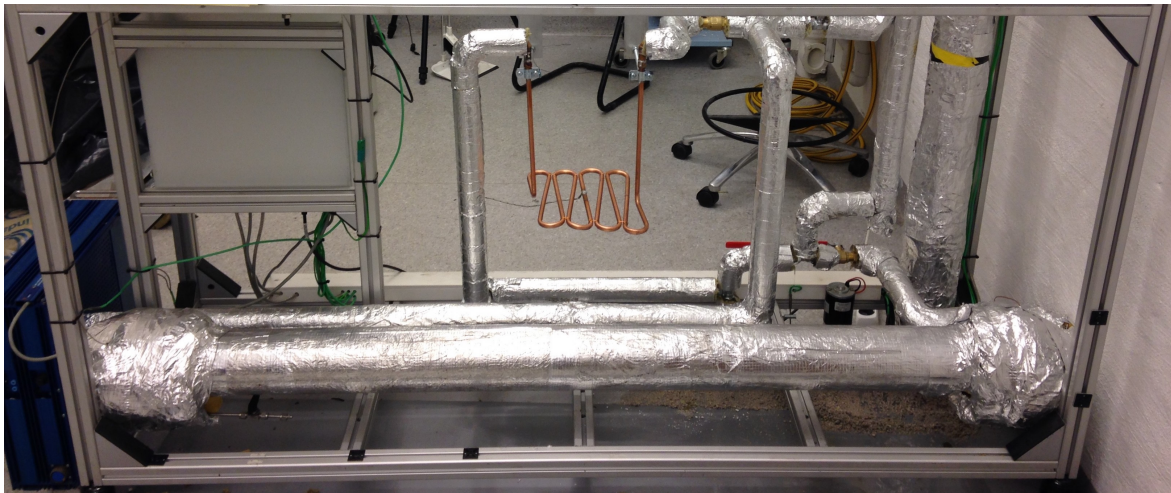
5.1 System Setup

The system contained the similar piping setup as before, however, with some rearrangement and extensions to include an application unit and a storage. Figure 5.1a shows how the complete system was arranged. At the highest point in the system the thermostat with the solenoid was located. As before, three pipes were connected with tube fittings directly into the bottom section of the thermostat configuration. Thus, one inlet pipe, pipe 1, surrounded by a heating element, and two outlet pipes, pipe 2 and pipe 3. While pipe 1 and pipe 2 had a similar arrangement as before, pipe 3 had been divided into two branches; one causing the oil to flow into the storage, and the other to the application. The total amount of pipes in the system were all copper pipes having an outside diameter of 15 mm. With an exception of the application unit, in which was constructed with 12 mm copper pipes. As can be observed in Figure 5.1, the application unit comprised one pipe length, bended to form the shape as illustrated (a shape in which was easier to achieve with 12 mm pipes instead of 15 mm). The application was reached via the one copper pipe branch in which emerged

from pipe 3. The storage, which principle and working function has already been described in Chapter 2, was connected to the other copper pipe branch emerging from pipe 3. A close-up picture of the storage and its location in the system was as visualized in Figure 5.1b.



(a) Picture of the circulating oil based system setup containing an application unit and a storage. Arrows are indicating where the main components in the system are located.



(b) Closeup of the storage when the system is seen from behind.

Figure 5.1: Picture of the circulating oil based system setup containing an application unit and a storage.

The temperature measuring devices arranged into different parts of the system were special ordered, mineral insulated thermocouples (type K). They were arranged with some sort of concealing caps into tee-tube fittings, causing them to be in direct contact with the oil. Figure 5.3 illustrates the arrangement of one of the thermocouples, Temp.2, located at the beginning of pipe 3. The temperatures measured in the

thermostat and at the application unit was not based on this tee-tube-fitting procedure. In one of the walls of the thermostat, a hole was drilled, where a thermocouple was injected. The hole was holding a small steel unit, which was the connection head between the thermocouple and its cable, welded onto the thermostat wall so that no leakages would be present. In the left corner of Figure 3.6b the arrangement of this thermocouple is visualized. When it comes to the application unit, the thermocouple was soldered onto its midpoint. Thus, this was the only thermocouple in the system at which was not in direct contact with the oil.

Thermocouples were also installed directly at the inlet and outlet of the storage. Even though it was already thermocouples in tee-tube-fitting nearby the inlet and the outlet, it was desirable to obtain temperatures even closer to the storage. In terms of being able to install these thermocouples, Teflon tape had to be added between the flanges. The tape was necessary in terms of supporting the cable connected to the thermocouples, so that no leakage would take place. The thermocouples also had to be thin enough, so that they could be suitable for this arrangement. Hence, more simple thermocouples had to be used, where the ones chosen were plastic insulated. As a consequence, in which will be observed in the experiments, these thermocouples were more temperature sensitive compared to the mineral insulated thermocouples.

The thermocouples measured the oil temperature at several different oil locations in the system; in the thermostat, at the beginning of pipe 3, at the inlet and outlet of the storage (two thermocouples each place), at the application unit, the inlet and outlet of the pump, and at the heating element. The amount of thermocouples present in the system varied during the experimental testing, at which will become apparent in the following sections. Figure 5.2 illustrate a simple sketch of the system setup, containing locations and specifications for pipes, thermocouples and valves. The numbering of the thermocouples, Temp.1 to Temp.5 represent the temperature measuring points of main interest. Respectively the temperature measured in the thermostat, at the beginning of pipe 3, at the inlet and outlet of the storage (two thermocouples each place) and the application unit. Further information regarding these temperatures will be presented later in the following sections.

As illustrated in Figure 5.1a and Figure 5.2, three valves were present in the system; Valve 1, Valve 2 and Valve 3. These valves would, for different system setting, have arrangements as illustrated in Table 5.1. As the table shows, these settings were divided into three cases; Case 1, Case 2 and Case 3. Close-ups of their arrangements in Case 1 is visualized in Figure 5.3. Case 1 and Case 2 indicates how the valves would be arranged during the day, thus between sunrise and sunset. Case 1 represents the setting where oil would be sent to the storage when it had reached a set temperature; hot oil would flow into the storage, and cold oil would flow out (due to the piston). Case 2 represented valve arrangements when hot oil from the thermostat would be used directly. Case 3 would be the setting used after sunset. The irradiation from the sun (heating element) will not be present anymore, and when hot oil is required, it would therefore have to be withdrawn from the storage. From the storage it would be sent directly to the application unit.

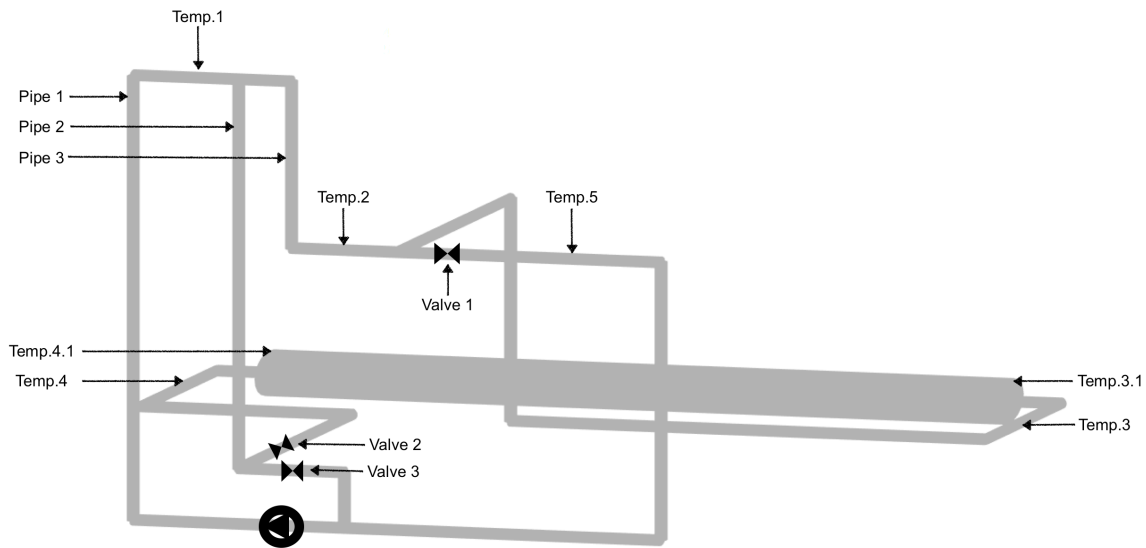


Figure 5.2: Simple sketch of the circulating oil system, including locations and specifications for pipes, thermocouples and valves.

Table 5.1: Valve Arrangements in the Complete System Setup

| Valve arrangements | | | | |
|--------------------|---------|---------|---------|--|
| | Valve 1 | Valve 2 | Valve 3 | Objective |
| Case 1 | Closed | Open | Open | Filling of storage with hot oil |
| Case 2 | Open | Closed | Open | Direct use of hot oil |
| Case 3 | Open | Open | Closed | Emptying of hot oil from storage for usage |

5.1.1 Data Acquisition With LabVIEW

The data acquisition setup used in the experiments with the solenoid, was also using the programmable software, LabVIEW, to control/simulate the heating of the oil. Thus, the setup was based on the same method as described in Chapter 3, in terms of recording the temperature results. However, the number of measuring points in the system had to be extended, and in addition, the output was decided to visualize based on another approach. The graphically output became as illustrated in Figure 5.4. As can be observed in the screen shot represented in the figure, temperatures were measured at nine different oil locations in the system; in the thermostat unit (Temp.1), at the heating element (Temp.2), at the inlet and outlet of the pump (Temp.3 and Temp.4), at the inlet and outlet of the storage (Temp.5, Temp 5.1 and Temp.6), at the application unit (Temp.7), and at the beginning of pipe 3 (Temp.8). That said, the naming of the measuring points will be different in the experimental method section, which will be presented in the next section.

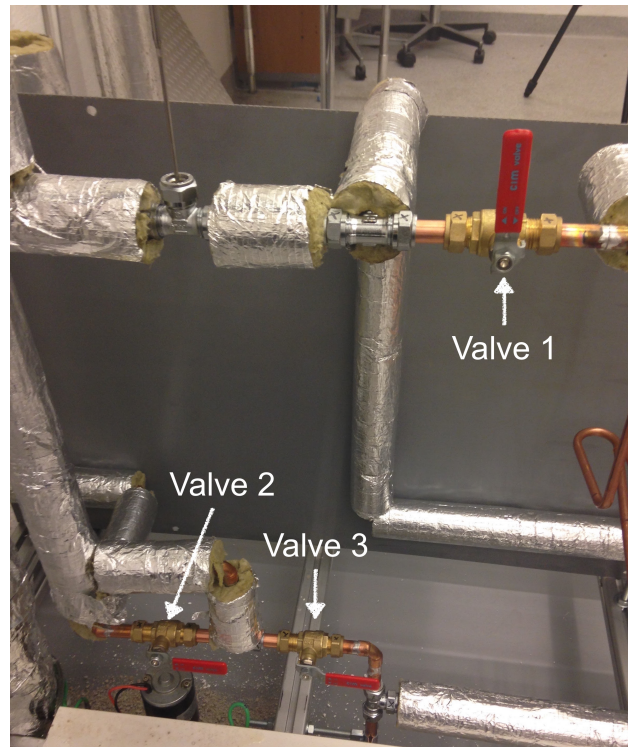


Figure 5.3: Picture showing the arrangement of the valves in Case 1; Valve 1 is closed whereas Valve 2 and 3 are open.

The program was constructed so that all the thermocouples (Type K)/temperature sensors were included, together with the pump and the heating element. The program was also constructed to include a manual switch for the pump to be turned on and off, where a running pump was represented with a green light. This same method applied to the heating element. A regulating device to control the effect of the heating element was also added in LabVIEW. The effect was constantly set to approximately 60 percent. For visualization reasons only, the three valves were given a constant green light. LabVIEW cannot understand whether they are on or off. The temperature value in the 'Thermostat' box, was interlinked with the 'Temp.1' box. When these temperatures became equal, the result would be a pulse signal (1 sec.) sent to the solenoid. The pulse signal would make the solenoid become energized, and as a consequence make it obtain a latched position. When Temp.1 would drop below the 'Thermostat' temperature again, the result would be a new pulse signal sent to the solenoid (1 sec), with reversed polarity. The solenoid would at this instance fall back into its unlatched position. Temp.1 was therefore, together with a given temperature value in the 'Thermostat' box, utilized to control the on and off switch of the solenoid. The 'Setpunk' box (set-point temperature), was added for safety measures only, and was also interlinked with the 'Temp.1' box. Thus, if Temp.1 became larger than the 'Setpunk' temperature, the heating element would be switched off. In the program there was also a box for the output current, together with an extra set of boxes for the temperature measuring points (as can be observed in the right hand side of Figure 5.4). These temperature boxes were included only to provide color changes in the system. As the picture shows, a given temperature value would decide the color

of a given system unit, blue (cold) or orange (hot). Color changes were possible since the whole system in LabVIEW was constructed with LED lights.

There were two measuring point at the inlet of the storage, and as can be observed in Figure 5.4 this was Temp.5 and Temp.5.1 respectively. The reason for having two measuring points was due to the fact that while Temp.5 measured the temperature at an oil location a small distance outside the inlet of the storage, Temp.5.1 was given a location directly at the storage inlet (between two flanges). Temp.5.1 was arranged into the system a couple of experiments after the other thermocouples had been installed. After it was installed, it was observed that Temp.5.1. gave a better approximation of the temperature inside the storage, when hot oil was stored over a longer period of time. To add on that note, there were also two thermocouples in the outlet region of the storage in the beginning. However, due to leakage from where the added thermocouple was installed (same procedure as at the inlet), and the issue with trying to reinstall it, it was decided to precede with the experiments without its presence. It was, regardless of this, important to have the two measuring points in the inlet area of the storage (due to the temperature change in the storage with time), which will become understandable when the results from the experiments will be reviewed.

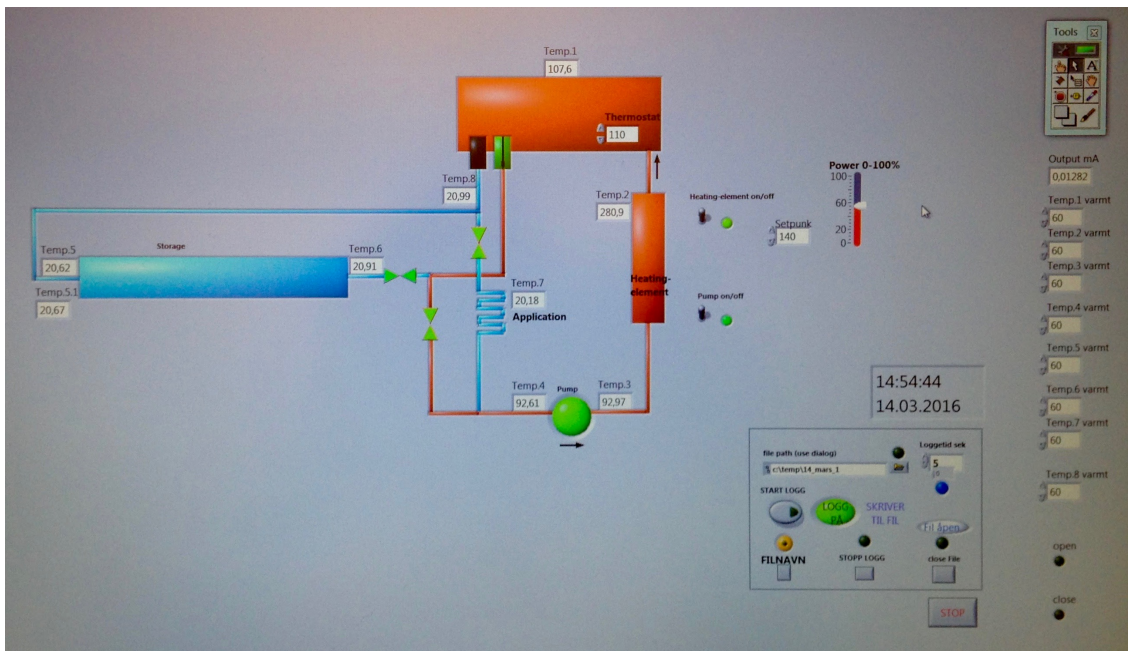


Figure 5.4: A screen shot visualizing the experimental data acquisition setup in LabVIEW.

5.2 Experimental Method

There were conducted several experiments with the system setup containing the solenoid and the storage. The intention with the experiment was to observe the features of the system as heated oil was being sent to its different parts. Hence, the experiments will be based on the following cases:

- Case 1 - Heated oil sent directly from the thermostat to the storage. Observe how long time it takes

to fill the storage with hot oil.

- Case 2 - Heated oil sent directly from the thermostat to the application unit. Observe the period of time required for the application unit to obtain maximum temperature.
- Case 3.1 - Stored oil sent to the application unit in one stage. Observe how long time it would take to drain the storage completely for hot oil, and the temperature at which would be possible to achieve in the application unit.
- Case 3.2 - Stored oil sent to the application unit in several stages, over a longer period of time. Observe how long time it would take to drain the storage completely for hot oil with this stepwise procedure.

Case 3.2 is of interest to test due to the fact that a given storage will surely not be drained completely in e.g. one cooking session. Parts of the oil volume inside should therefore be possible to use, without the rest of the hot oil being influenced by the cold oil side. This test will therefore show the separation ability of the piston at various locations inside the storage.

The results will be presented in terms of plots, where the different cases will be illustrated. Each experiment will include several case. There will be five to six graphs in each plot, depending on the measuring points included. Measuring points at the inlet and outlet of the pump, and at the heating element will not be included.

The different temperatures represented in a given plot will be the ones illustrated in Table 5.2.

Table 5.2: Temperatures of Interest - Complete System Setup

| Temperature measurements in the system | |
|--|--|
| Temp.1 | The temperature measured in the thermostat |
| Temp.2 | The temperature measured at the beginning of pipe 3 |
| Temp.3 | The temperature measured close to the inlet of the storage (thermocouple connected to a tee-tube-fitting) |
| Temp.3.1 | The temperature measured at the inlet of the storage (thermocouple connected between flanges) |
| Temp.4 | The temperature measured close to the outlet of the storage (thermocouple connected to a tee-tube-fitting) |
| Temp.4.1 | The temperature measured at the outlet of the storage (thermocouple connected between flanges) |
| Temp.5 | The temperature measured at the application unit |

The outlined temperatures can also be found illustrated in Figure 5.2. Before reviewing the experimental results, the observations made of the system during the experimental testing will be reviewed.

5.2.1 Observations of The System

Observations of the system during the experimental testing will be carried out in this section. The focus will be on the adjustments made consecutively, together with justifications for conducting them.

The Solenoid

The compression spring required some minor adjustments, as its force was slightly higher than the pulling force of the solenoid. Therefore, parts of its length was cut off, so that its initial length would be its equilibrium length, instead of being somewhat compressed. This was a necessary adjustment to do, so that the solenoid would become latched without any problems. See Figure 3.6b for an illustration of the arrangement of the solenoid and the compression spring. The adjustment of the spring did not affect the push/release mechanism of the solenoid.

The Piston

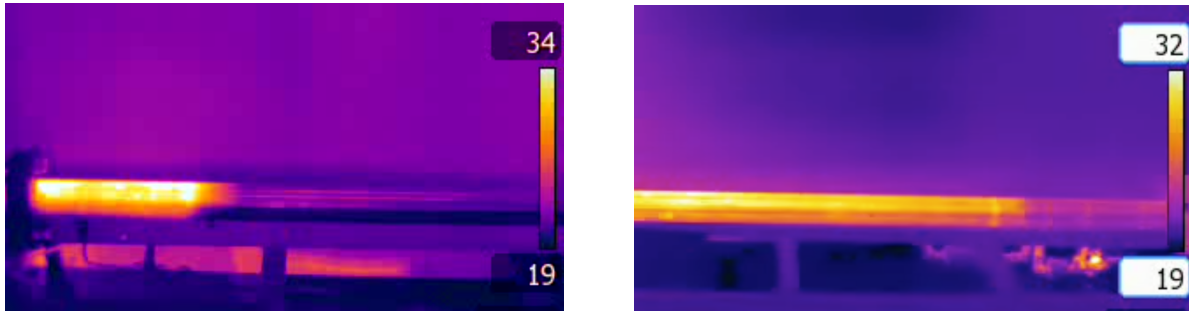
To track/control the motion of the piston inside the storage, a magnet was connected to its surface before insertion. A magnet ball was then placed at the surface of the storage, in which would give the exact position of the piston. Figure 5.5 gives an illustration of how this principle could be exploited. A thermal camera was also used to observe whether hot and cold oil separation was obtained with the piston, and whether it corresponded to the position of the magnet ball. See Figure 5.6. The thermal pictures were taken before the system was insulated.

The pistons tested in the experiments have already been introduced in Chapter 2. However, as the experiments were carried out, one acquired further understanding of their motion characteristics.



Figure 5.5: The magnet ball travelling on the outside of the storage. At the inside of the storage, at this position, the piston would be located.

The first piston tested, was the one made of stainless steel, described in Chapter 2. What was observed during the testing was that the magnet ball would stop running, even when the storage was still being filled with hot oil. Thus, there would have to be some issues with the configuration of the piston, as it did not



(a) Picture taken with a thermal camera when hot oil is entering the storage.

(b) Picture taken with a thermal camera when half of the storage contains hot oil.

Figure 5.6: Pictures of the storage taken by a thermal camera.

seem to move properly. For instance, its length of 30.4 mm could be a problem in terms of tilting. A problem which also could be amplified due to the attached metal bracket holding the magnet (attached to the one side of the piston). An added component in which would give the piston an uneven weight. A metal piston in a metal storage also has its limitation when it comes to friction, which in addition to the possible tilting, would be enough resistance to make the piston stop. Another observation made, when the piston was taken out of the storage, was that oil had been leaking into a cavity (due to the added metal bracket). The leakage was believed to happen because of oil penetration through edges of the bolt, fixing the metal bracket onto the piston. The weight of the piston would therefore increase, and the oil would meet even more resistance in terms of moving it towards the other side of the storage. On that note, the configuration of the stainless steel piston could most likely be improved so that it could become functional. With an extended length, more rounded edges, and without the metal bracket holding the magnet, it could be possible for this piston to work satisfactory. However, as friction also still could be too much of a limiting factor, it was desirable to make the piston with another material.

The new piston was therefore made in POM. POM is a thermoplastic product having good sliding properties, and with an even lower thermal conductivity compared to stainless steel. The length of this piston was 80.0 mm, and its outer diameter was extended to 55.4 mm, compared to the stainless steel piston which had an outer diameter of 55.3 mm. Thus, the diameter was not extended to have any specific impact, whereas the length was, aiming to reduce the possibility of tilting. Additionally, a longer piston could be favorable with regards to leakage. As the location of the magnet was positioned in the center of the piston, its weight would also be equally distributed. Some preliminary testing of the piston immersed in a heated oil bath was done to examine whether it would swell or not, prior inserting it into the storage. The test was conducted in a casserole on a stove. The temperature of the oil was increased to some extent, and the test revealed that the POM material was not swelling. If it would swell this could have been a problem for the motion of the piston inside the storage. Figure 5.7a shows an illustration of the simple test.

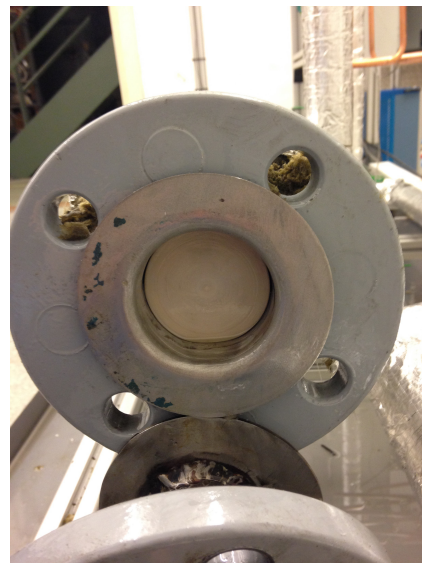
All the enhancements conducted, resulted in a piston moving satisfactory, where the magnet ball was running as long as the storage was being filled/emptied. The POM piston was therefore used throughout the

experiments. However, due to temperature limitations (melting point) of this material, the experiments were not carried out at substantially high oil temperatures (180-200°C), which will be required of the system in the end. Regardless of this, the objective of the experiments was to demonstrate the principles of the system setup, something which was possible with the POM piston.

The last piston inserted into the storage was the one made in PEEK, which also is a thermoplastic product. For the purpose of the experimental testing, it was not necessary to change the POM piston with the PEEK. However, it was desirable to observe the features of this piston inside the storage, as the continued work with this system should be at higher oil temperatures. The PEEK piston was designed to be almost identical to the POM piston, where the only difference was that the diameter was increased with 0.2 mm. This small increase was justified with the fact that the POM piston was working so efficiently, and designing the piston to be closer to the inner diameter of the storage (56 mm) was not believed to be of any issue. The reason why it was not increased further was because it was desirable to have a tiny gap between the storage and the piston. A thin oil layer could make the sliding effect more smooth. The features of the piston were observed by filling and draining the storage, without heating the oil. Its sliding effect was the same as the POM piston. Figure 5.7b illustrates how this piston was arranged inside the storage.



(a) The POM piston in an oil bath. Test to examine whether it would swell.



(b) Picture of the PEEK piston inside the storage.

Figure 5.7: Pictures of the POM piston in an oil bath and the PEEK piston inside the storage.

The Measuring Points

When the first experiments were carried out, oil started to leak from the one thermocouple added at the outlet of the storage (Temp.4.1). Due to this, the thermocouple was removed, and since there were some re-installation issues, it was decided to proceed without its presence. This thermocouple will therefore not be observed present in the last experiments conducted (thus, in Test 3 and Test 4). It was, however, important

that the measuring point at the inlet of the storage could be kept present, due to the temperature change in the storage as hot oil was being stored over a longer period of time. This will become understandable when carrying out the results from the experimental work. Thus, in the end, as illustrated in Figure 5.4, the system contained nine measuring points.

5.2.2 Results

The results will be divided into four parts; Test 1, Test 2, Test 3 and Test 4. Additionally, as mentioned earlier, the POM piston will be the one used throughout the experiments. The presentation of the results will be in terms of plots and tables, where the different cases will be illustrated. Each experiment will include several case. After each part has been presented, a discussion section will work as a follow up, in terms of evaluating the obtained results.

Test 1: Case 1, 2 & 3.1

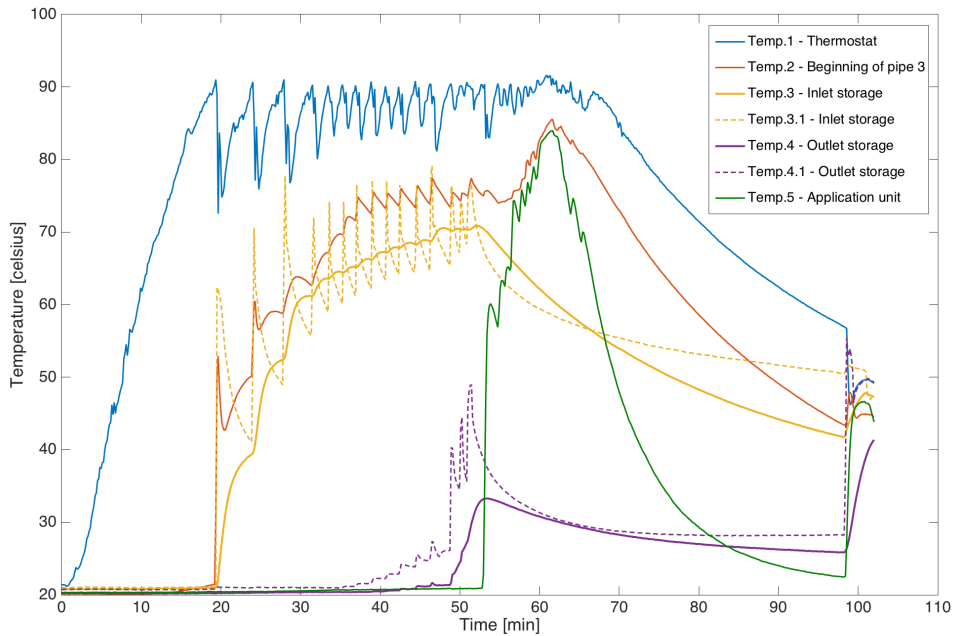
The first results collected were based on case 1, 2 and 3.1, where the temperature in the 'Thermostat' box in LabVIEW was set to 90°C. The cases were carried out one by one, thus in the order outlined. Two experiments based on these cases are illustrated graphically in Figure 5.8. Time intervals required for each case, and critical temperatures in the experiments are listed in the Table 5.3.

Table 5.3: Time Intervals and Critical Temperatures in Test 1 - Complete System Setup

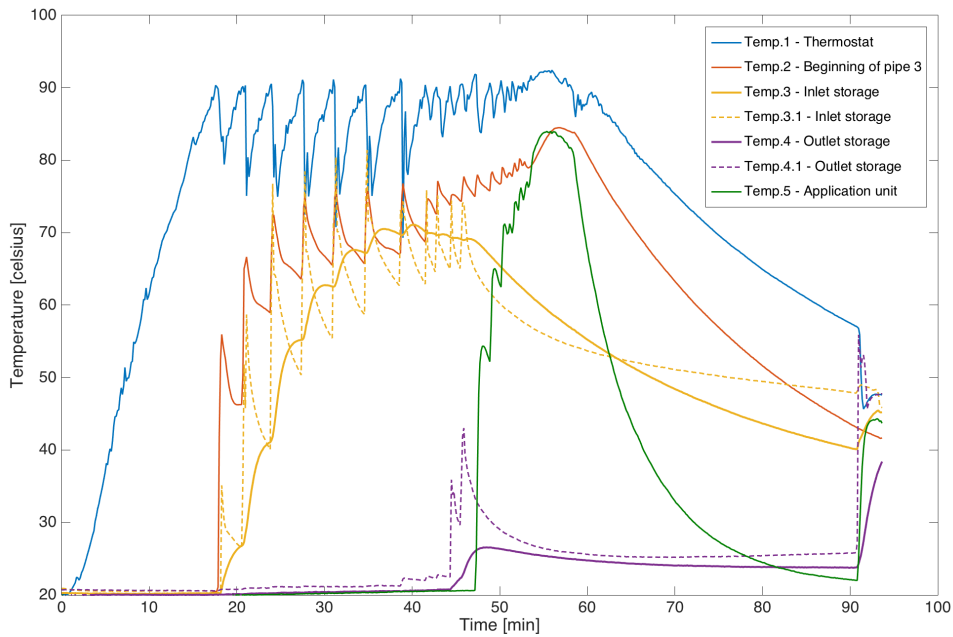
| System behavior - Test 1 | | |
|--|----------------------------|----------------------------|
| | 1 st experiment | 2 nd experiment |
| Time for Temp.1 to reach 90°C | 19.3 min. | 18.3 min. |
| Time to fill storage | 32.3 min. | 24.9 min. |
| Time to reach max. temperature at the application unit (time starts running when hot oil is entering) | 9 min. | 7.7 min. |
| Time at which the heating element was turned off | 59.9 min. | 54.0 min. |
| Time to empty storage | 153 sec. | 153 sec. |
| Maximum temperature at storage inlet (Temp.3) | 70°C | 70°C |
| Maximum temperature in the application unit | 84°C | 84°C |
| Temperature at the storage inlet 30 minutes after filled with hot oil (Temp.3.1) | 52.9°C | 50.5°C |
| Temperature at the storage inlet when the experiment was completed (50.4 minutes after the storage filling was completed) (Temp.3.1) | 47.5°C | 45.8°C |

Discussion

As can be observed in Table 5.3 there were significant heat losses in the system. A significant 20°C temperature drop was occurring on the distance from the thermostat to the storage, strongly believed to be due to the copper pipe lengths linking the two units together. Even though all the pipes were well insulated. 30 minutes



(a) Plot of the first experiment conducted.



(b) Plot of the second experiment conducted.

Figure 5.8: Plots of the first and second experiment conducted with the solenoid. The temperature of the thermostat was set to 90°C in LabVIEW. Experiment 1: Filling of hot oil to storage between 19.3 min. and 51.6 min. (Case 1). Direct use of hot oil between 52.8 min and 61.8 min. (Case 2). Emptying of hot oil from storage for usage between 99.5 min. and 102 min. (Case 3.1). Experiment 2: Filling of hot oil to storage between 18.3 min. and 43.2 min. (Case 1). Direct use of hot oil between 44.5 min and 52.2 min. (Case 2). Emptying of hot oil from storage for usage between 91.1 min. and 93.6 min. (Case 3.1). Notice: The inlet and outlet temperatures at the storage varies due to the use of different thermocouples. Temp.3.1 and Temp.4.1 were plastic insulated, whereas the others were mineral insulated thermocouples.

after the filling of the storage was completed, Temp.3.1 had dropped to approximately 50°C (52.9°C and 50.5°C depending of the experiment). The 30 minutes instance was randomly selected, however, the choice had to be at least 15 minutes after filling, as before this Temp.3.1 showed a steep decline in temperature. After 15 minutes a gradual decline was observed. Hence, one should expect a somewhat slow decrease in the storage temperature after a longer period of time.

As can be observed in the plots, all temperature profiles, except Temp.1, were stable until Temp.1 reached 90°C . At this instance, Temp.2, Temp.3 and Temp.3.1 would start to increase due to the solenoid becoming latched (pull action of the plunger). On that note, Temp. 2, even if located nearby the thermostat, would not manage to reach a temperature close to Temp.1, due to the short period the solenoid would maintain latched. As long as the solenoid would be held in the latched position, hot oil would flow into pipe 3, toward the storage (Case 1). The piston would start to move, pushing cold oil out, at which would be sent to the thermostat. Hence, causing Temp.1 to drop below 90°C almost immediately, causing the solenoid to become unlatched (push action of the plunger) again. As can be observed in the plots, a continuous pattern became the outcome. At the instance at which the storage was completely filled, one can observe a temperature rise in Temp.4 and Temp.4.1. The piston had reached the end/outlet of the storage. At this instance the oil was regulated to go from the thermostat towards the application unit (Case 2). As the solenoid would become latched, there would be an immediate temperature increase in Temp.5. Oil was sent to the application unit until the temperature reached a value where Temp.1 would not drop below 90°C anymore, and instead increase further above 90°C , due to the heating element. At this point the heating element was therefore switched off. The temperature profiles decrease more or less gradually after this, depending on heat losses at the thermocouples location. E.g. thermocouple Temp.5 was not measuring the temperature in the oil, but instead on the surface of the copper pipe configuration (application unit), which could be a result of the sharp temperature decline for the application unit. After the system was cooled down, thus Temp.1 and the temperature of the heating element were close to uniform (less than 5°C difference), oil was sent from the storage to the application unit (Case 3.1.). It took the piston approximately 153 seconds to empty the storage completely. The reason for waiting until the heating element was at a lower temperature (not present), was so that this test could reflect usage of hot oil after sunset (as this is the time of the day the storage is needed). Temp.5 increases, and the heat loss is about 5°C from what measured at Temp.3.1. However, Temp.3 and Temp.5 cannot be distinguished with more than a couple of degrees. Due to the temperature variations in the system at the instance of storage draining, $\text{Temp.1} > \text{Temp.3} > \text{Temp.2} > \text{Temp.3.1} > \text{Temp.4.1} > \text{Temp.4} > \text{Temp.5}$, the temperatures would increase/decrease depending on the given thermocouple. Temp.2 was not affected due to port 3 in the thermostat being closed. This was because the oil flowing from the storage to the application unit would not enter into the region, where Temp.2 was located.

The two experiments conducted were both based on a 90°C thermostat temperature, and where the same cases were carried out. As can be observed in the plots the system thus behaves approximately identically. However, there is a slightly difference in the temperature at the outlet of the storage. Whereas the temperature

at the outlet reached approximately 33°C in the first experiment, the temperature at the outlet was about 27°C in the second experiment. The reason for this difference was believed to be dependent on the instance at which the filling of the storage was completed. For instance, when comparing the time it took to fill the storage in the the two experiments, it clearly seems like filling has taken place after the storage was already full in the first experiment. Continuing filling, when already full, could then result in oil penetration over the surface of the piston. The pump was still running, and oil would therefore still be flowing. On that note, when we tested the piston inside the storage before the experiments were carried out, and thus before the oil was heated, the pump would make some distinct sound (of not receiving enough oil) at the instance at which the piston had arrived at the end. However, Duratherm 630 is a highly viscous oil, which viscosity decreases drastically with increase in temperature. Hence, when running the experiments with the heated oil, penetration over the surface of the piston should be less of a problem. Thus, the pump was being fed with oil, and the distinct sound was not being recognized. Due to the system being insulated, it was not possible to follow the motion of the piston with assistance from the magnet ball. Therefore, in the second experiment, the filling was stopped immediately when it was observed a sudden temperature increase at the outlet of the storage. Some insulation was removed at the end of the storage, and the magnet ball showed that the piston had arrived at the end. The insulation was inserted back again after this. There can be observed an insignificant increase in the temperature at the outlet, after the storage had been filled for some time. This could be a result of heat conduction in the material of the storage, stainless steel, and if possible, an insignificant oil portion escaping over the surface of the piston.

The temperature measurements Temp.3.1 and Temp.4.1 are significantly more fluctuating compared to the remaining temperature measurements. This was believed to be because these thermocouples, between the flanges at the inlet and outlet of the storage, were different from the other thermocouples in the system (plastic insulated instead of mineral insulated). However, it was desirable to have them present, especially Temp.3.1, to better understand the temperature gradient inside the storage over a longer period of time. After the heating element was switched off, Temp.3 would decrease with a rather high rate, whereas Temp.3.1 would flatten out gradually. However, it took Temp.3.1 approximately 15 minutes to stabilize. After the system had cooled down, to an instance where the temperature of the heating element would be close to Temp.1, hot oil was being sent from the storage to the application unit. At this instance one can observe a distinct difference between Temp.3 and Temp.3.1. While the temperature measured at Temp.3 increased with approximately 5°C, Temp.3.1 only increase with about 1°C. Thus, Temp.3.1 gives more accurate information of how the temperature inside the storage varies with time. However, as visualized in the plots, the end of the filling was showing a small temperature drop in Temp.3.1. The reason for this could have been some oil penetration over the surface of the piston, possibly during the period the storage was kept stationary after filling. Hence, occurring due to a density/pressure difference between the two edges of the piston. Otherwise it could be a result of trying to drain the storage for hot oil when already filled completely with cold oil. Thus, oil penetration over the piston surface. However, the density of the cold oil is higher than that of the hot oil,

and as can be observed in Figure 5.8, the temperature drop in Temp.3.1 was less than the corresponding temperature increase in Temp.4 in the opposite process (filling the storage with hot oil).

The system did show a tendency of having prominent heat losses. For instance, in the region of the Temp.3 measurement, as it can be compared to Temp.3.1 when stabilisation has been achieved. The Temp.3 measurement was located in a tee-tube-fitting linked to two copper pipes, a small distance (approximately 15 cm) outside the inlet of the storage. Insulation was applied in best possible manner, however, it was not insulated as substantially as the storage. Due to the tee-tube-fitting, and the bend where this thermocouple was located, there were some difficulties when trying to apply the insulation. In addition, copper has a significantly higher thermal heat conductivity compared to stainless steel. Hence, local heat losses would therefore be a possible implication of the temperature difference illustrated between Temp.3 and Temp.3.1. All thermocouples were calibrated before use, and thus this was not assumed to have any impact on the results.

Test 2: Case 1, 2 & 3.1

After the two first experiments had been conducted, the temperature in the 'Thermostat' box in LabVIEW was raised to 110°C. The experiment was similar to those illustrated in Test 1, hence, the results were still based on case 1, 2 and 3.1. It was desirable to compare this experiment with the two carried out in Test 1, thus to observe whether the operation of the system would be reflected. The graphical illustration of the experiment conducted is shown in Figure 5.9. Important time intervals for the different cases are presented in Table 5.4.

The reason for the somewhat higher starting temperature of the system in this experiment (compared to Test 1), was due to the experiment being carried out before the system had cooled down completely from the previous conducted experiment. Thus, the time it took for Temp.1 to reach 110°C would therefore have been slightly higher, than the tabulated value.

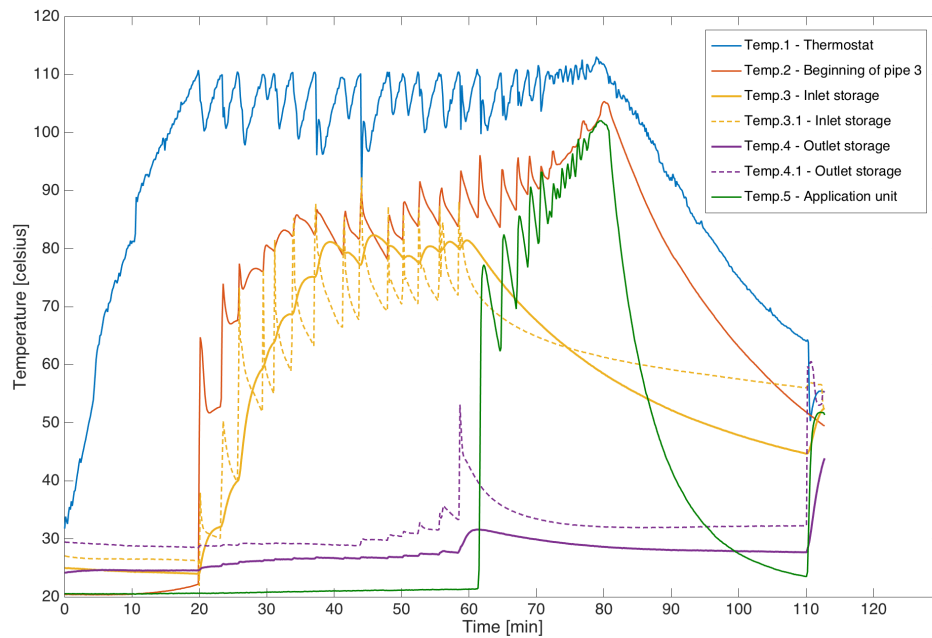


Figure 5.9: Plots of the third experiment conducted with the solenoid. The temperature of the thermostat was set to 110°C in LabVIEW. Filling of hot oil to storage between 19.8 min. and 38.7 min. (Case 1). Direct use of hot oil between 59.8 min and 78.2 min. (Case 2). Emptying hot oil from storage for usage between 110.3 min. and 112.8 min. (Case 3.1). Notice: The inlet and outlet temperatures at the storage varies due to the use of different thermocouples. Temp.3.1 and Temp.4.1 were plastic insulated, whereas the others were mineral insulated thermocouples.

Table 5.4: Time Intervals and Critical Temperatures in Test 2 - Complete System Setup

| System behavior - Test 2 | |
|--|-----------|
| Time for Temp.1 reach 110°C | 19.8 min. |
| Time to fill storage | 38.7 min. |
| Time to reach maximum temperature at the application unit (time starts running when hot oil is entering) | 18.4 min. |
| Time at which the heating element was turned off | 78.4 min. |
| Time to empty storage | 153 sec. |
| Maximum temperature at storage inlet (Temp.3) | 81°C |
| Maximum temperature in the application unit | 102°C |
| Temperature inside storage 30 minutes after filled with hot oil (Temp.3.1) | 59.5°C |
| Temperature at the storage inlet when the experiment was completed (54.3 minutes after the storage filling was completed) (Temp.3.1) | 52.2°C |

Discussion

The reason for conducting this experiment was to observe how the system would work at a higher temperature. The result imply that the system was operating in the same manner as the ones carried out in Test 1. Thus, there would only be differences due to the temperature set in the thermostat. An additional remark, Temp.4

did not increase to the same extent as in Test 1. Consequently, valves were rearranged from Case 1 to Case 2 even faster than in the experiments conducted in Test 1.

Test 3: Case 1 & Case 3.2

The following experiment mainly focuses on the storage and its heat capacity over a longer period of time. It was also desirable to get a further understanding of the separation ability of the piston. Thus, Case 1 and Case 3.2 were the ones carried out. The temperature in the 'Thermostat' box in LabVIEW was raised to 130°C. Figure 5.10 visualizes the experiment graphically. Important time intervals for the different cases are presented in Table 5.5.

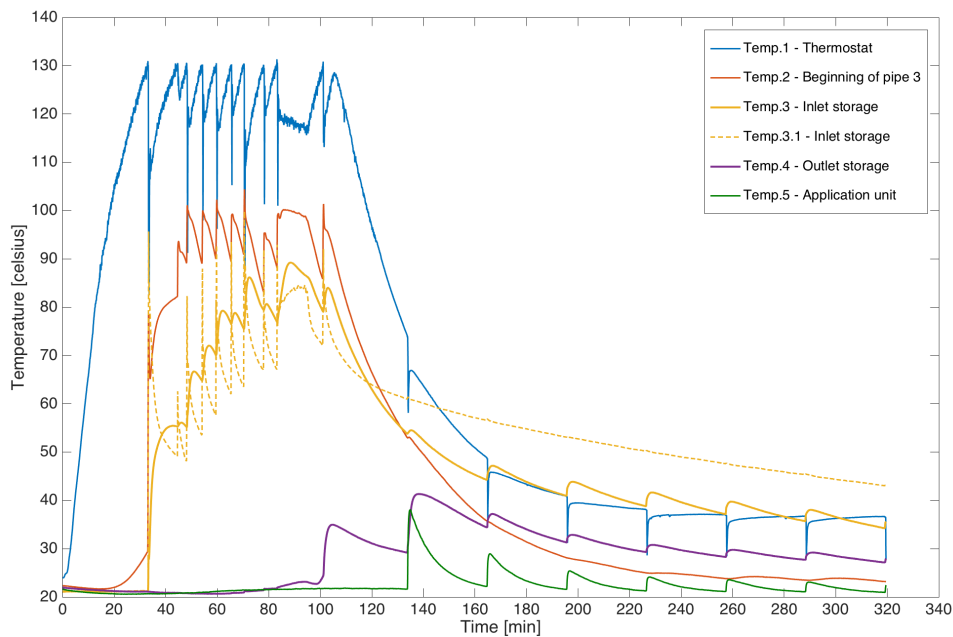


Figure 5.10: Plots of the fourth experiment conducted with the solenoid. The temperature of the thermostat was set to 130°C in LabVIEW. Filling of hot oil to storage between 33.0 min. and 68.1 min. (Case 1). Emptying 1/3 of hot oil from storage for usage in stages between 131.1 min. and 319.1 min. - ten stages, 30 min. between each (Case 3.2). Notice: The inlet temperatures at the storage varies due to the use of different thermocouples. Temp.3.1 was plastic insulated, whereas the others were mineral insulated thermocouples.

The results from Case 1 are based on the same information as carried out in the previous experiments. Where the only difference would be the set temperature in the 'Thermostat' box in LabVIEW. After the storage was filled with hot oil, the heating element was switched off. 30 minutes later, oil was being sent to the application unit in a period of 10 seconds. These stages were repeated seven times; we waited 30 minutes each time, before we sent oil to the application unit in a time period of 10 seconds. The experiment was completed when the piston had pushed out approximately 1/3 of the hot oil. The location of the piston was observed by removing some insulation (inserted back after), and then by using the magnet ball.

Table 5.5: Time Intervals and Critical Temperatures in Test 3 - Complete System Setup

| System behavior - Test 3 | |
|--|------------|
| Time for Temp.1 reach 130°C | 33 min. |
| Time to fill the storage | 68.1 min. |
| Time at which the heating element was turned off | 101.1 min. |
| Time to empty the storage | - |
| Maximum temperature at the storage inlet (Temp.3) | 89°C |
| Temperature at the storage inlet 30 minutes after filled completely (Temp.3.1) | 61.5°C |
| Temperature at the storage inlet when the experiment was completed (3 hours and 38 minutes after the storage filling was completed) (Temp.3.1) | 43.1°C |

Discussion

From the storage was completely filled with hot oil, until the experiment was completed, the temperature at the inlet of the storage, Temp.3.1, had dropped with approximately 46°C. Temp.3.1 had a steep decline the first 15 minutes, until a gradually decrease was taking place. As the plot illustrates, Temp.3.1 was not observed to be affected by the stages of oil flow out of the storage (towards the application unit). Therefore, we believe that it is possible to assume that the temperature gradient at Temp.3.1 would be more or less the same, starting 15 minutes after stabilization was achieved. It was observed a 1°C increase in this temperature as the storage was emptied completely in Test 1 and Test 2, however, we believe that this difference is of insignificance. Based on the information acquired regarding the temperature gradient, it was decided to end the experiment, even though the piston had not yet arrived at the other end. It was believed that the 7 intervals would cause the piston to be located closer to the middle section of the storage, based on the observations from Test 1 and Test 2. Tests showing that 153 seconds were required for the piston to arrive at the end. Thus, after approximately 70 seconds the piston location should have been more than only one third of the storage. However, static friction forces are reasonable to assume being present, where the magnitude would have an implication on the travel length of the piston in a given time interval. Additionally, density differences of the oil on the piston edges, could cause back pull of the piston while being stationary between the stages. The pressure would be higher on the side containing cold oil, and would due to nature of physics, want to escape to the low pressure side.

What was also observed in this experiment was that it seemed like oil was still being filled into the storage when it was already full. Temp.4 increased drastically after approximately 100 minutes, and thus it seems like oil has been forced over the piston surface at this instance. This was believed to be based on the same observations made in the first experiment in Test 1. A higher oil temperature will also result in an even lower oil viscosity. Therefore, this experiment could be more exposed to oil penetration over the surface of the piston, compared to the ones carried out in Test 1/Test 2. One last 130°C experiment was therefore desirable to conduct, were some insulation from the end part of the storage should be removed approximately

100 minutes into the experiment. Consequently, by using the magnet ball to indicate the arrival time of the piston.

The separation ability of the piston was not observed in this experiment either, as it was completed before the piston had arrived at the other end. Stages of only 10 seconds are most definitely also too short for the hot oil in the storage to arrive at the application unit, based on how this system has been constructed. Figure 5.10 shows that Temp.5 was almost not increasing at all when hot oil was being sent from the storage towards the application unit. The slightly temperature increase seems to be due to the oil in which has been present inside the insulated pipe lengths, prior the uninsulated pipes forming the application unit. However, a couple of longer stages could have been carried out to make the oil from the storage arrive at the application unit, and additionally the separation ability of the piston to be observed. Nevertheless, it was already decided to conduct one last experiment. Therefore, as will be observed in the next experiment, Test 4, longer and fewer stages were carried out. It was desirable to observe whether all the portions of oil leaving would have a temperature gradient similar to that illustrated in this experiment. Additionally, it was also of interest to compare the last experiment with Test 1 and Test 2. Hence, a comparison based on the time it would take for the piston to arrive at the other end with this stepwise procedure.

Test 4: Case 1 & Case 3.2

The last experiment conducted was similar to the one carried out in Test 3. However, with some changes done with the procedure of Case 3.2. Whereas Test 3 manage to give a comprehensive understanding of the temperature gradient of the hot oil inside the storage over a longer period of time, Test 4 was conducted purely to observe the separation ability of the piston. In addition, the magnet ball was utilized towards the end of the filling to obtain a clear understanding of the outlet temperature of the storage when completely filled. Figure 5.11 shows a graphical illustration of the experiment. Important time intervals for the different cases are presented in Table 5.6.

Table 5.6: Time Intervals and Critical Temperatures in Test 4 - Complete System Setup

| System behavior - Test 4 | |
|---|-----------|
| Time for Temp.1 reach 130°C | 31.3 min. |
| Time to fill storage | 52.9 min. |
| Time at which the heating element was turned off | 84.2 min. |
| Time to empty storage | 165 sec. |
| Maximum temperature at storage inlet (Temp.3) | 90°C |
| Temperature at storage inlet 30 minutes after filled with hot oil (Temp.3.1) | 59.9°C |
| Temperature at the storage inlet when the experiment was completed (2 hours and 7 minutes after the storage filling was completed) (Temp.3.1) | 44.5°C |

The results from Case 1 are based on the same information as carried out in the previous experiments.

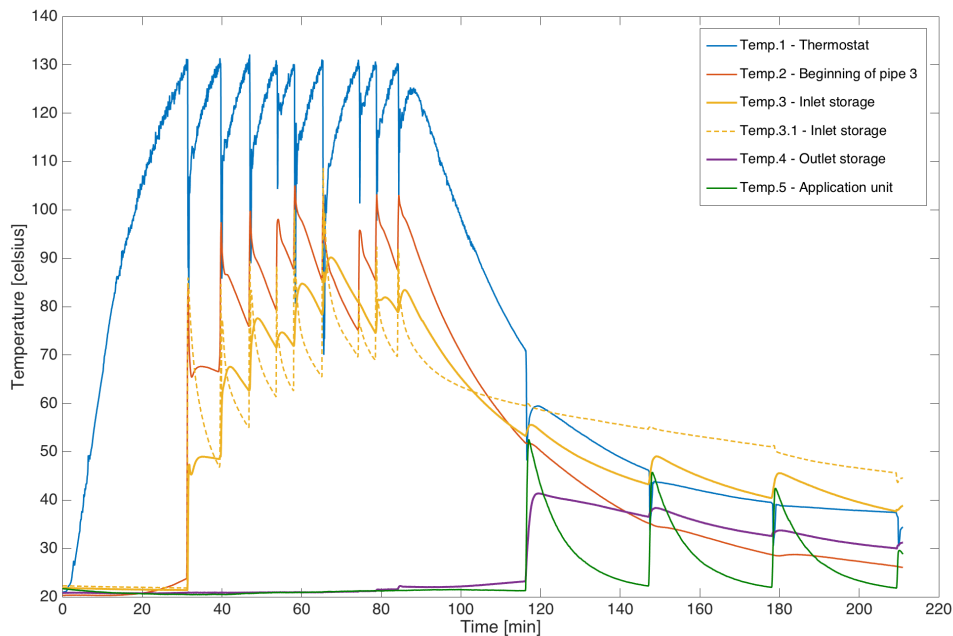


Figure 5.11: Plots of the fifth experiment conducted with the solenoid. The temperature of the thermostat was set to 130°C in LabVIEW. Filling of hot oil to storage between 31.3 min. and 84.2 min. (Case 1). Emptying hot oil from storage for usage between 145.5 min. and 211.2 min. - four stages, 30 min. between each (Case 3.2). Notice: The inlet temperatures at the storage varies due to the use of different thermocouples. Temp.3.1 was plastic insulated, whereas the others were mineral insulated thermocouples.

After the storage was filled with hot oil, the heating element was switched off. 30 minutes later, oil was being sent to the application unit in a period of 47 seconds. These stages were repeated three times. A fourth stage, requiring 24 seconds, completed the experiment. The piston required approximately 165 seconds to arrive at the other end.

Discussion

As can be observed in the plot, Temp.3.1 was virtually unchanged when emptying was taking place in several stages. However, 165 seconds was required to empty the storage for hot oil in this experiment. Thus, 12 seconds longer than when emptying the storage completely in one stage. However, due to fewer and longer stages, compared to Test 3, the time difference was not as prominent. In each stage, it could therefore be possible to assume a 3 seconds loss per movement, due to the implications already outlined in the discussing part of Test 3. What can also be observed in this experiment, was that the first three stages were long enough for the hot oil to reach the application unit. There were some heat losses, and as Figure 5.11 shows, the oil leaving the storage at a temperature corresponding to Temp.3.1, decreased with approximately 10°C before entering the application unit. In the last stage the increase in Temp.5 was so small that it seems to only have received oil from the pipe length connecting the application unit with the storage inlet.

5.3 Discussion and Comparison of The Experiments

The temperature results from the four tests are listed in Table 5.7. As can be observed, every 20°C increase in the set temperature of the thermostat, accordingly increased the maximum temperature in the storage with no more than 10°C. Thus, a higher thermostat temperature caused a corresponding higher heat loss in the system. For the application unit, in both Test 1 and Test 2, the difference between the temperature in the thermostat and the maximum temperature in the application unit was approximately 10°C.

The temperature inside the storage after filling was completed, was in all the tests showing a steep decline during the first 15 minutes. The decline was most prominent in Test 3 and Test 4. However, after this period, the decline became more gradual, and the gradients became virtually identical in all of the tests.

Table 5.7: Comparison of the Experiments Conducted on the Complete System Setup

| Temperatures obtained in the storage and in the application unit. | | | | | |
|--|---------------|-------------|----------------|----------------|----------------|
| | Test 1 (90°C) | | Test 2 (110°C) | Test 3 (130°C) | Test 4 (130°C) |
| Maximum temperature at storage inlet (Temp.3) | 70°C | 70°C | 81°C | 89°C | 90°C |
| Maximum temperature at the application unit | 84°C | 84°C | 102°C | - | - |
| Temperature at the storage inlet 30 min. after filling was completed (Temp.3.1) | 52.9°C | 50.5°C | 59.5°C | 61.5°C | 59.9°C |
| Temperature gradient in storage, based on the 15 first min. after filling | -0.90°C/min | -1.04°C/min | -1.18°C/min | -1.58°C/min | -1.75°C/min |
| Temperature gradient in storage, from 15 min. to 30 min. after filling | -0.24°C/min | -0.26°C/min | -0.25°C/min | -0.25°C/min | -0.25°C/min |
| Temperature gradient in storage, from 15 min. to 2 hours and 7 min. after filling | - | - | - | - | -0.17°C/min |
| Temperature gradient in storage, from 15 min. to 3 hours and 38 min. after filling | - | - | - | -0.11°C/min | - |
| Temperature drop in the oil sent from storage to application unit | 5°C | 5°C | 5°C | - | 7.5-9°C |

(a) The temperature gradients are based on Temp.3.1, as this temperature illustrates the temperature of the stored hot oil most precisely.

The system setup comprised long pipe lengths, and therefore substantial heat losses would be prominent in the system. For instance, the location of the inlet of the storage was linked with a rather long pipe length in terms of being connected to the thermostat. Building the system with copper pipes, even when well insulated, did seem to have a significant impact on the overall heat losses in the system. Thus, pipes made of another type of material, e.g. stainless steel (less thermal conductivity), could be used instead. Additionally,

the storage was long with a small diameter. Large amounts of the oil would therefore be in direct contact with the surface area of the storage at all times. As the storage material was having an initial temperature of approximately 20°C, when the hot oil was entering, heat conduction could strongly affect the temperature of the oil inside. Especially during the first period after filling (first 15 minutes), as results have suggested. At which would occur even though the thermal conductivity of stainless steel is weak. When feeling the insulation, it was warm at locations containing hot oil. For the further work with this type of storage, the diameter should be increased, thus to the right extent, for the stored oil to stay sufficiently warm over a longer period of time. The arrangement of the system components should also be looked at, so that it would be possible to shorten the lengths of the pipes connecting the system together.

Even though Temp.3.1 and Temp.4.1 were significantly fluctuating, they did give a better understanding of the temperature change inside the storage over a longer period of time. Since they were located directly at the inlet and outlet of the storage, they were also required to be plastic insulated, instead of mineral insulated (as the remaining others), to fit between the flanges. As they were calibrated before use they should give appropriated results, which they also did as the hot oil filling of the storage was completed.

The main objective of these experiment was to observe whether it could be possible to demonstrate a good thermostat solution, and additionally, if it would be possible to obtain forced stratification in the storage. As the tests reveal, and as can be observed in the graphical illustrations and tables, this was achieved. The solenoid became latched and unlatched based on a given temperature, and the settings constructed in LabVIEW. However, it was observed that the solenoid, a couple of times during an experiment, was having some problems in terms of moving the bracket in which the plunger was connected to. This problem was not believed to be due to the compression spring, because it had been adjusted and tested to be compliant with the pull and push forces of the solenoid. However, what was believed to be the reason, was the position of the solenoid in the thermostat design, embedded in the connection point of the plunger. Thus, since the plunger was connected at the top part of the bracket, the force exerted would be at this location, and not onto its center of mass point. The force would then propagate in a way causing the top part of the bracket to accelerate with a faster rate, compared to the bulk of the bracket. Hence, in the moment force is being exerted, some kind of twisting effect could be initiated. Consequently, this could have some limitations when it comes to the motion of the thin sliding plate; more prominent friction resistance between the bottom part of the thermostat and the plate, and resistance from the bolts connected to the sliding plate (can become somewhat stuck in their sliding arrangement). Some minor adjustments should therefore be done with the arrangement of the solenoid in this thermostat design, to avoid any sliding issues with the thin plate.

To observe whether forced stratification was obtained, one would have to look at the temperatures at the inlet and outlet of the storage. As the tests showed, this was also obtained. The main difference from test to test would be the understanding of when the storage was completely filled with hot oil. Thus, Temp.4/Temp.4.1 showed to increasing rapidly if filling was continued after the piston had already arrived at the end. Hence, causing hot oil to penetrate over the surface of the piston. Increasing the temperature

of this oil would decrease its viscosity drastically, and thus it would be easier for it to escape through the small cavities between the piston and the storage. It is not a problem that oil flows over the surface of the piston as it arrives at the other end of the storage during filling. However, if the cavities would not be small enough to prevent leakage occurring the opposite way, when the storage should be held stationary, this could be a problem. This was nevertheless not observed to be an issue. The temperature of the hot oil leaving the storage was more or less constant. The only observation made was a slightly increase in Temp.3.1 in the beginning, before a small drop was recognized in the final oil portion, a 1 °increase in the beginning against a 1°decrease in the end. This applied to both Case 3.1; hot oil drained from the storage in one stage, and Case 3.2; hot oil drained from the storage in several stages. In Case 3.2, the small temperature drop was observed in the two final stages. Hence, the separation ability of the piston was satisfactory.

Chapter 6

Dynamic Simulation

The objective was to develop a computational simulation model, based on the oil system constructed in the laboratory. The model was intended to be an useful tool for visualization and for investigation of the oil system. It could also be helpful in further work for an up-scaled system.

The system required high flexibility and user defined components. The assumptions of a 1D system was believed to give negligible errors. For a 1D system, an implementation in a three-dimensional simulation software is redundant. The MATLAB environment was therefore used as the platform for implementation of a simple, dynamic 1D model. This provided a flexible model with accurate solutions.

The model predicts temperature evolution in the oil system from the given initial and boundary conditions. A comparison between the experimental work and the computational model will be presented.

6.1 Equations for Fluid Flow and Heat Transfer

Computational fluid dynamics involve solutions of fluid flow with heat transfer. The governing equations and the mathematical model that has been used will be presented in the next paragraph.

Conservation Equations for Energy and Mass

The governing equations of fluid motion are based on the three fundamental principles of mass, momentum and energy conservation. The model used in the simulation is based on the x-directional 1D energy conservation equation (Chow [1979])

$$\rho \frac{De}{Dt} + p \frac{\partial u}{\partial x} = Q_v + \frac{\partial}{\partial x} \left(\frac{k\partial T}{\partial x} \right) + \phi$$

where

$$\frac{D}{Dt} = \frac{\partial}{\partial t} + u \frac{\partial}{\partial x}$$
(6.1)

and the x-directional 1D mass conservation equation

$$\frac{\partial \rho}{\partial t} + \frac{\partial(\rho u)}{\partial x} = 0 \quad (6.2)$$

where ρ is density, u represent the fluid velocity in x-direction, p is pressure, e is the specific internal energy, Q_v is the heat source term, t is the time, Φ is the dissipation term and k is the thermal conductivity.

Heat Transfer in Pipes

The heat source term, from the energy equation, contains heat source and sinks, and can be represented by three heat transfer principles: conduction, convection and radiation. Radiation has not been presented due to the assumed insignificant contribution it has at temperatures treated in this project.

$$\begin{aligned} q'' &= q''_{source} - q''_{out} \\ \text{where} \\ q''_{out} &= q''_{cond} + q''_{conv} + q''_{rad} \end{aligned} \quad (6.3)$$

where q'' represent the total heat flux.

Steady conductive heat transfer through the pipe wall yields:

$$q''_{cond} = \frac{A_s k}{\ln\left(\frac{r_o}{r_i}\right)} (T_o - T_i) \quad (6.4)$$

where r_o and r_i represent the outer and inner radius of the pipe. A_s is the surface area and k represent the thermal conductivity of the pipe wall. T_o represent the temperature at r_o and T_i represent the temperature at r_i .

Convective heat transfer across the surface is written with a heat transfer coefficient h . This gives:

$$q''_{conv} = h(T_o - T_{air}) \quad (6.5)$$

T_{air} is the temperature of the ambient air.

6.1.1 Simplifications

There were done assumptions and simplifications to the physical problem before it was implementing into the system model in MATLAB.

The energy equation for the pipe wall was neglected, and a steady heat transfer through the wall was assumed. The total heat transfer in the system, from the core of the oil to the surroundings, was implemented with an overall heat transfer coefficient, U . U refers to how effectively heat is conducted over a series of

mediums. In this model, U refers to the convective heat transfer from the oil to the pipe wall, the conduction through the pipe wall and the insulation, and the convective heat transfer from the insulation to the ambient air. The equation for the overall heat transfer to the surrounding is represented by:

$$q''_{out} = U(T_i - T_{air}) \quad (6.6)$$

where T_i represent the temperature of the oil and T_{air} the temperature of the ambient air.

The flow was assumed laminar and one-dimensional, in the longitudinal direction.

Continuity Equation

The flow was assumed incompressible, and the continuity equation consequently provides a constant flow rate.

$$\frac{\partial u}{\partial x} = 0 \quad (6.7)$$

For an incompressible fluid, the internal energy is expressed by $e = c_p T$. Where c_p represent the heat capacity.

Energy Equation

The heat capacity, c_p , was considered time and space independent. Appendix B shows the variation of c_p at different temperatures. Assuming an average constant heat capacity gave a relatively small deviation from the exact values presented in the appendix.

The axial conduction, $\frac{\partial}{\partial x}(k\frac{\partial T}{\partial x})$, was neglected. The thermal conductivity, k , from Appendix B shows small values for all temperatures. Whereas the corresponding values for the heat transfer coefficient, h , for oil flow in tubes, are typically in the range between 300-1700 [$\frac{W}{m^2K}$] (Kurganov). This results in a large Nusselt number, in which represents the relationship between the convective and the conductive heat transfer (AUW). Therefore, it was assumed that the heat convection in the system dominated compared to the conduction.

To simplify the system further, the viscous dissipation, Φ , was neglected. The heat source and convection was considered as dominating in the system.

6.1.2 The Mathematical Model

Implementing the assumptions carried out in the previous section: incompressible flow, neglected dissipation and axial conduction and by assuming constant ρ and C_p , equation 6.1 yields:

$$(\rho C_p) \frac{\partial}{\partial t}(T) + (\rho C_p) u \frac{\partial}{\partial x}(T) = Q_v \quad (6.8)$$

which is the mathematical model used in the 1D model.

Boundary- and Initial Conditions

The boundary conditions associated with the mathematical model were: ambient air temperature outside the pipe system, the heat source term, q''_{source} and the heat sink term, q''_{out} . Specified connections between the pipes required an energy- and mass balance between the pipes.

The initial fluid temperature in the model was set to a uniform temperature distribution, equal to the ambient air temperature. An initial flow rate is also required.

6.2 1D Dynamic Model

The mathematical model, from the last section, was implemented as a numerical model in MATLAB. It was structured as a pipe network, where the pipes were connected together building a complete system. The model was implemented with a thermostat and a storage. This will be presented in the next paragraph.

6.2.1 Discretized Energy Equation

Finite Difference Method, FDM, was used to solve the energy conservation equation numerically. Equation 6.8 was discretized in an upstream first order scheme and integrated explicit in time. The discretized equation thus became:

$$T_i^{t+1} = T_i^t + \left(\frac{\Delta t}{\Delta x}\right) \frac{A_s}{A_r} \frac{1}{\rho C_p} (q''_{source} - q''_{out}) - \left(\frac{\Delta t}{\Delta x}\right) u (T_{upstream}^t - T_i^t) \quad (6.9)$$

where q''_{out} is represented by the overall heat transfer coefficient:

$$q''_{out} = U(T_i^t - T_{air}) \quad (6.10)$$

and q''_{source} is the incoming heat flux towards the system and A_r represent the cross-section area. $T_{upstream}$ can either be T_{i+1} or T_{i-1} it depends on the direction of the flow.

Mesh

The geometry of the pipes was uniformly meshed, dx_{normal} , dividing each pipe into equally sized sections. The storage was implemented with a varying grid size. To imitate the movement of the piston, the mesh before and after the piston modified their grid sizes. The piston position is displayed in Figure 6.1.

When the storage was filled with hot oil, the grid size before and after the piston varied like this:

$$\begin{aligned} dx_{j-1} &= dx_{j-1} + u_s * dt \\ dx_{j+1} &= dx_{j+1} - u_s * dt \end{aligned} \quad (6.11)$$

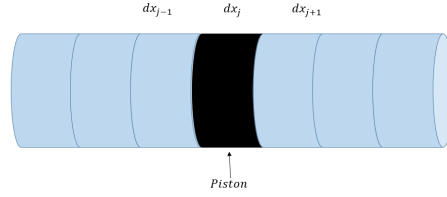


Figure 6.1: Discretization of the storage. The piston occupy one grid. The grid before and after the piston have varying grid size.

And when discharging the storage with hot oil, the grid size varied like this:

$$\begin{aligned} dx_{j-1} &= dx_{j-1} - u_s * dt \\ dx_{j+1} &= dx_{j+1} + u_s * dt \end{aligned} \quad (6.12)$$

Where u_s represent the velocity in the storage, dt represent the time-step and dx represent the grid size. When the grid on the decreasing side of the piston was less than a set minimum value, dx_{min} , the piston would move one grid in the direction of the flow.

Numerical Stability

A large time step is favorable to increase the simulation speed; however, a too large time step could also induce instability. The Courant-Friedrichs-Lewy Condition (CFL) is an important stability criterion, and a necessary condition for convergence when solving partial differential equations numerically (Anderson and Wendt [1995]). In explicit time integration schemes, CFL can be used to find the maximum allowable time-step. The CFL criteria is presented as:

$$C = \frac{u \cdot \Delta t}{\Delta x} \leq C_{max} \quad (6.13)$$

where Δt is the time step, u is the velocity through the cell and Δx is the cell size in the x-direction. For explicit schemes $C_{max} = 1$. To assure convergence:

$$\Delta t \leq \frac{C_{max} \cdot \Delta x}{u}$$

The time-step sizes for explicit stability and accuracy are usually equivalent.

6.2.2 Pipe Network Analysis

The model was designed as a network of pipes connected to each other. The pipe network contained several interconnected pipes, represented as branches. Each branch was given a number to identify the branch, indicated with an ID. The branches were divided into sections. The sections were numbered from 1 to a number representing the length of the branch. The mass and energy balance was conserved trough every

section and branch of the network, and through each split and merge.

Flow Direction

The flow direction in each pipe of the network could be in two directions. This was necessary because the circulation of the flow in the network varied. The direction was regulated by the temperature in the thermostat, and by the valve settings. The valve controlled heat output to the application, and the thermostat regulated the flow to the hot outlet or the cold outlet.

In the model the direction of the flow was defined by an indicator, I . $I = 1$ indicates a flow direction from low to higher section numbers, while $I = 0$ provides the opposite direction. The model used I to determine if it was the higher or lower section number who represented the upstream temperature to the section in question. $I = 1$ dictates $T_{upstream} = T_{i-1}$, while $I = 0$ dictates $T_{upstream} = T_{i+1}$.

Connections

The boundaries of each branch contained connections to other branches. Each section had four possible connections, two at the first section and two at the last section. In the setup, the model was provided with information about the connected branches at the first section, LPipe1 and LPipe2, and what section in the connected branches it was connected to, LSec1 and LSec2. This information was also provided to the last section, represented as RPipe1 and RPipe2 with the associated section connections RSec1 and RSec2. This is displayed in Figure 6.2.

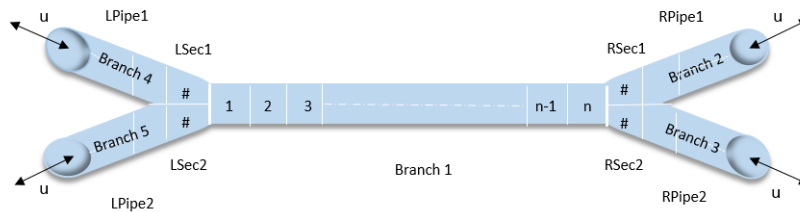


Figure 6.2: Illustration of one branch in a network of branches. Each branch has two inlets and two outlets. The oil flow can travel through the branch in both directions.

The branches could be connected in various ways. Consequently, the model can display different setups of the oil system.

Thermostat With Solenoid

The Solenoid, from the experiments, was represented as a switch between the flow rate in the two connected outlet branches of the thermostat in the model. The thermostat was activated when the temperature in Branch A reached a desired temperature. If the temperature was below the desired temperature, the flow was directed to Branch B, and if the temperature was higher, the flow was directed to Branch C. Together with the manual controlled valves, the thermostat controlled the flow pattern in the system.

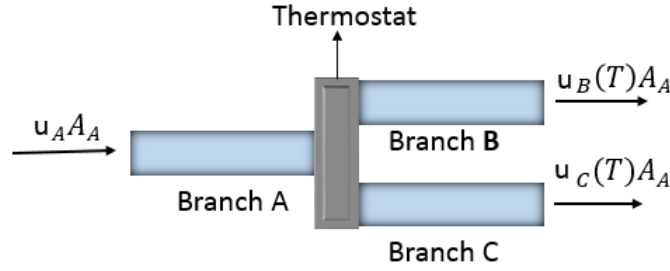


Figure 6.3: Flow conservation through the thermostat

Storage

The storage was implemented as a branch in the network, with a dividing section between the hot and the cold oil representing the piston from the experiment. The temperature in the piston was set to Not a Number, NaN, and there where no energy- or mass transfer through the piston.

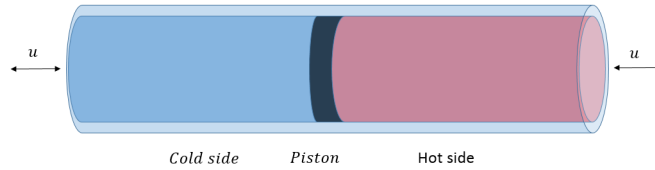


Figure 6.4: Storage with a dividing piston

As the storage was charged or discharged, the piston moved in the same direction as the flow. The branch representing the storage, had a bigger radius than the rest of the branches. To maintain mass balance, the velocity in the storage was represented by:

$$u_s = u_b * \frac{r_b^2}{r_s^2} \quad (6.14)$$

Where u_s and r_s represent the velocity and radius in the storage. And u_b and r_b represent the velocity and radius of the connected branch.

6.2.3 Implementation

Equation 6.9 was implemented to the MATLAB model like this:

$$T_i^{t+1} = T_i^t + \left(\frac{\Delta t}{\Delta x}\right) \frac{A_s}{A_r} \frac{1}{\rho C_p} (q''_{source} S - U(T_i^t - T_{air})) - \left(\frac{\Delta t}{\Delta x}\right) (inflow - outflow) \quad (6.15)$$

where $(outflow) = uT_i^t$, $(inflow) = uT_{i-1}^t$ when $I=1$ and $(inflow) = uT_{i+1}^t$ when $I=0$. S represent the susceptibility the branch had to the heat source.

The network was implemented in MATLAB as a structure; a collection of data representing one object. Each branch was represented in the structure as a field containing fifteen sub-pieces of data. The procedure

in the model can be represented as:

First, network setup:

- implementing all the branches in the system with: an ID, an initial temperature vector, an initial grid size vector, susceptibility from heat source, an index I for the initial flow direction, an initial flow rate, overall heat transfer coefficient U and connections to the other branches. Providing information about the boundary condition; air temperature, q''_{source} and fluid properties.

Then, running the program:

- looping over every section in every branch.
- if the piston is moving, calculate the grid size around the piston.
- if the program is at the first section in the branch: identify the flow direction in the branch, identify the branch and sections connections and calculate the inflow and outflow of the section.
- if the program is at the last section in the branch: identify the flow direction in the branch, identify the branch and sections connections and calculate the inflow and outflow of the section.
- if the program is at an intermediate section in the branch: identify the flow direction in the branch and calculate the inflow and outflow of the section.
- solve the energy equation for temperature (Equation 6.15)
- thermostat evaluation. Regulate the velocity and the flow direction index.
- next time step.

The simulation executive is shown in Figure 6.5.

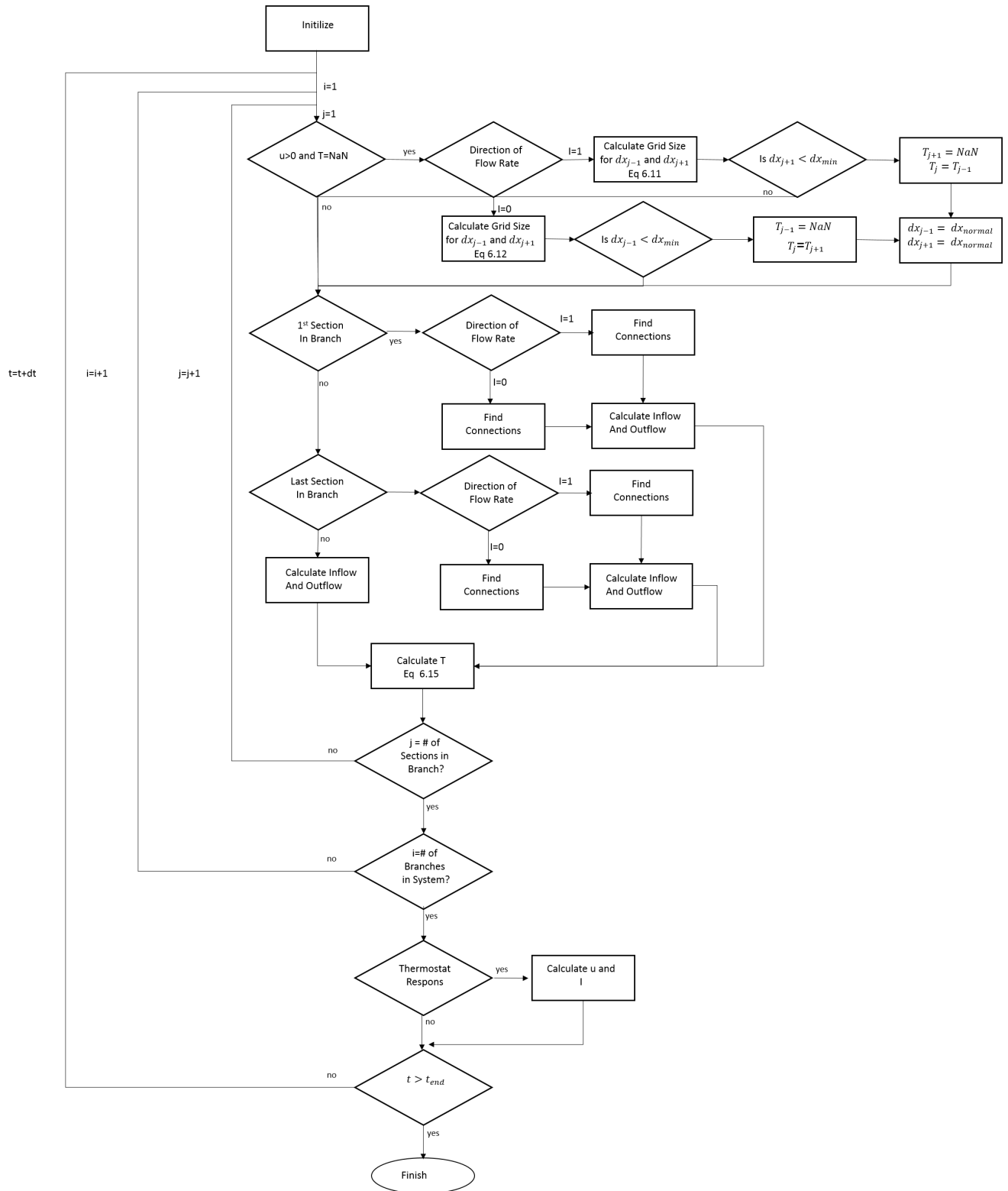


Figure 6.5: Figure show the flowchart diagram for the program executive.

6.3 Simulation of The Experimental Work With The Complete System

Two simulation were conducted. They were performed to imitate the experimental work conducted in the laboratory at NTNU. The first simulation corresponds to Test 1 2nd experiment and the second simulation corresponds to Test 4.

First, the initial setup and simulation procedure will be given. Then the simulations results will be presented and compared with the experimental measurements.

6.3.1 Network Setup

The model was designed to have the same geometry as the complete setup constructed at NTNU, with a solenoid, a storage (with a piston), an application and three valves. The simulation of the experiment was implemented as a network of ten pipes (branches). Figure 6.6 display the branches and how they were connected together.

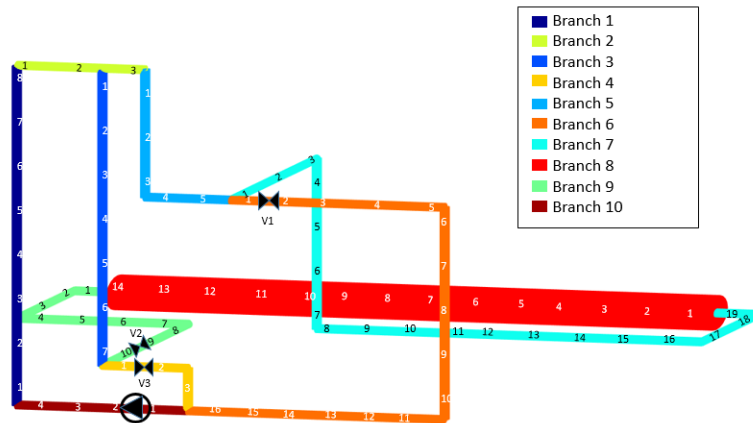


Figure 6.6: Figure display the system setup in the model. The model was designed to have the same geometry as the experimental setup. The valves and the pump is also displayed.

System Properties

Density and specific heat capacity was found in Appendix B. While the storage- and pipe dimensions was measured from the system in the laboratory. u_s , representing the velocity in Branch 8, was obtained from the experimental results by calculating the velocity of the magnetic ball running outside the storage. Equation 6.14 gave $u_b = 0.1m/s$, representing the velocity in the branches.

The heat element from the experiment provided 2kW and was used at 60 % effect, which gives a heat flux of $q''_{source} = 25464W/m^2$. The heating element was not in direct contact with the oil, and the heat flux to the oil was therefore presumed to be significant lower. By investigation of the experimental temperature increase, from before and after the heating element, it was found that the heating element used approximately

12 minutes to reach the maximum effect. The maximum effect provided an average of 12°C increase through the heating element. It was also found that approximately 30 minutes after the heat element was turned off, it provided a 2°C increase through the heating element, which stayed stable through the rest of the experiment. The heat flux growth was approximately linear, while the decay was better represented by an inverse exponential curve. By tuning it was found that a heat flux of $q''_{source} = 5500\text{W}/\text{m}^2$ provides a 12°C increase through the heating element in the model, and a $q''_{source} = 700\text{W}/\text{m}^2$ provides an increase of 2°C . A heat flux of $5500\text{W}/\text{m}^2$ correspond to a heat element of 259 W. The heat flux was therefore implemented with a linear growth from zeros to $q''_{source} = 5500\text{W}/\text{m}^2$, during the first 12 minutes after the heat element was turned on. While an exponential decay was implemented from $q''_{source} = 5500\text{W}/\text{m}^2$ to $q''_{source} = 700\text{W}/\text{m}^2$, after the heat element was turned off.

Losses through the system was difficult to obtain. The overall heat transfer coefficient U , was therefore tuned to match the experimental result.

Properties that applied to the entire system are displayed in Table 6.1.

Table 6.1: Boundary Conditions and Parameters Applied to the Entire System.

| Parameters and Boundary Conditions | |
|---------------------------------------|--|
| Parameter | Value |
| Ambient air temperature (T_{air}) | 20°C |
| Heat source (q''_{source}) | maximum $8000\text{ W}/\text{m}^2$ (259 W) |
| Density(ρ) | $700\text{ kg}/\text{m}^3$ |
| Specific Heat Capacity (C_p) | $1700\text{ J}/\text{kgK}$ |
| Radius of pipe (R) | 0.0075 m |
| Radius of storage (Rs) | 0.028 m |
| Velocity in branches (u_b) | $0.100\text{ m}/\text{s}$ |

Initial Setup

The initial setup was equal in both of the simulation, and is presented in Table 6.2. The information provided to each branch was: temperature vector (T), grid size vector (dx), susceptibility from heat source (S), flow rate (u), flow direction index (I), overall heat transfer coefficient (U), connected branches and section on the low numbered side (LP1, LP2, LS1, LS2) and connected branches and sections on the high numbered side (RP1, RP2, RS1, RS2).

The initial temperature was set to 20°C in each section of the temperature vector. The first section in the temperature vector in Branch 8 was set to $T=\text{NaN}$, representing the piston position. The initial grid size

Table 6.2: The table display the initial network setup of the model. S indicates the branches susceptibility from the heat source and U represent the overall heat transfer coefficient.

* link to connected branch in the system. ** link to connected section in the branch.

| Initial Network Setup | | | | | | | | | | | | |
|-----------------------|-------------|-------------------|---|------------------------|------|------|-------|-------|------|------|-------|-------|
| ID | Nr of grids | Branch length [m] | S | U [$\frac{W}{m^2K}$] | LP1* | LP2* | LS1** | LS2** | RP1* | RP2* | RS1** | RS2** |
| Branch 1 | 8 | 1 | 1 | 0 | 10 | 0 | 2 | 0 | 4 | 0 | 1 | 0 |
| Branch 2 | 3 | 0.375 | 0 | 65 | 1 | 0 | 3 | 5 | 8 | 0 | 1 | 1 |
| Branch 3 | 7 | 0.875 | 0 | 4 | 2 | 0 | 9 | 4 | 3 | 0 | 10 | 1 |
| Branch 4 | 3 | 0.375 | 0 | 4 | 3 | 9 | 10 | 6 | 7 | 10 | 1 | 16 |
| Branch 5 | 5 | 0.625 | 0 | 4 | 2 | 0 | 7 | 6 | 3 | 0 | 1 | 1 |
| Branch 6 | 16 | 2 | 0 | 10 | 5 | 7 | 4 | 10 | 5 | 1 | 3 | 1 |
| Branch 7 | 19 | 2.375 | 0 | 4 | 5 | 6 | 8 | 0 | 5 | 1 | 1 | 0 |
| Branch 8 | 14 | 1.75 | 0 | 2 | 7 | 0 | 9 | 0 | 19 | 0 | 1 | 0 |
| Branch 9 | 10 | 1.25 | 0 | 4 | 8 | 0 | 3 | 4 | 14 | 0 | 7 | 1 |
| Branch 10 | 4 | 0.5 | 0 | 7 | 4 | 6 | 1 | 0 | 3 | 16 | 1 | 0 |

was set to $dx=0.125$ at each section in the grid vector. A heat source susceptibility was applied to Branch 1. Valve 1 was initially set closed, while valve 2 and valve 3 were open.

The piston was initially set in Section 1 in Branch 8. When the grid at the decreasing side of the piston was less than $dx_{min} = 0.00125$ (1% of dx_{normal}), the piston moved one section in the same direction as the flow.

The thermostat was implemented at the end of Branch 2, regulating the flow rate to Branch 3 or Branch 5. When the temperature exceeded the set temperature (90°C in Test 1 and 130°C in Test 4) at the last section of Branch 2 the thermostat directed the flow to Branch 5. When the temperature was less than the set temperature, the thermostat directed the flow to Branch 3.

Space step was set to $dx = 0.125$. The CFL condition gave an upper restriction $\Delta t \leq \frac{1 \cdot 0.125m}{1m/s} \leq 0.125s$. The time step was therefore set to $dt = 0.1$.

6.3.2 Simulation Results

Simulation of Test 1, 2nd experiment

The model simulated 103 minutes model time. Corresponding to the experiment procedure for Test 1, 2nd experiment:

- the heated oil was first sent into the storage. When the storage was full, the heated oil was sent into the application.
- when there was a stable 90°C in the thermostat, the heat source was switched off.
- 45 minutes after the heat source was switched off, the storage was discharged.
- reacting temperature for the thermostat was set to 90°C.

Figure 6.7 display the temperature evolution in the system during the simulation. The temperature was plotted in the thermostat, the inlet and outlet of the storage and in the application, which correspond to the last section in Branch 2, the first and last section in Branch 8 and the 4th section in Branch 6 respectively.

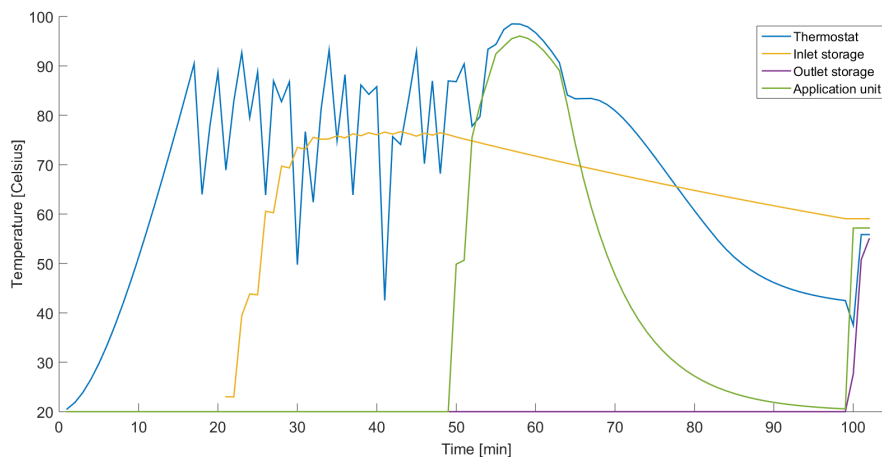


Figure 6.7: Plots display the simulation results from Test 1.

Table 6.3 present a comparison of the experimental and numerical system behavior of Test 1, 2nd experiment. It can be observed from the comparison that the numerical model used a longer time period to fill and discharging the storage than the experiment did. The model also presented higher temperatures in the storage and application unit.

Table 6.3: Time intervals and critical temperatures in Test 1 2nd experiment. Comparison of experimental and simulated data

| System behavior - Test 1 | | |
|---|----------------------|---------------|
| | Experimental results | Model results |
| Time for Thermostat to reach 90°C | 18.3 min. | 17 min. |
| Time to fill storage | 24.9 min. | 33 min. |
| Time to reach max. temperature at the application unit (time starts running when hot oil is entering) | 7.7 min. | 10 min. |
| Time at which the heating element was turned off | 54.0 min. | 50.0 min. |
| Time to empty storage | 153 sec. | 160 sec. |
| Maximum temperature at storage inlet of the storage | 70°C | 76.6 °C |
| Maximum temperature in the application unit | 84°C | 96 °C |
| Temperature at the storage inlet 30 minutes after filled with hot oil | 50.5°C | 75.9 °C |

Simulation of Test 4

The model simulated 211 minutes model time. Corresponding to the experiment procedure in Test 4:

- the heated oil was first sent into the storage. The heat source was switched off when the storage was full.
- Valve 1 was opened and Valve 2 was closed 30 minutes after the storage was full. This dictates the heated oil from the storage to the application.
- 47 seconds after the heated oil was sent from the storage to the application, Valve 1 was closed and Valve 2 was opened. This was repeated 4 times, until the storage was empty.
- reacting temperature for the thermostat was set to 130°C.

Figure 6.8 display the temperature evolution in the system during the simulation. The temperature was plotted in the thermostat, the inlet and outlet of the storage and the application which correspond to the last section in Branch 2, the first and last section in Branch 8 and the 4th section in Branch 6 respectively.

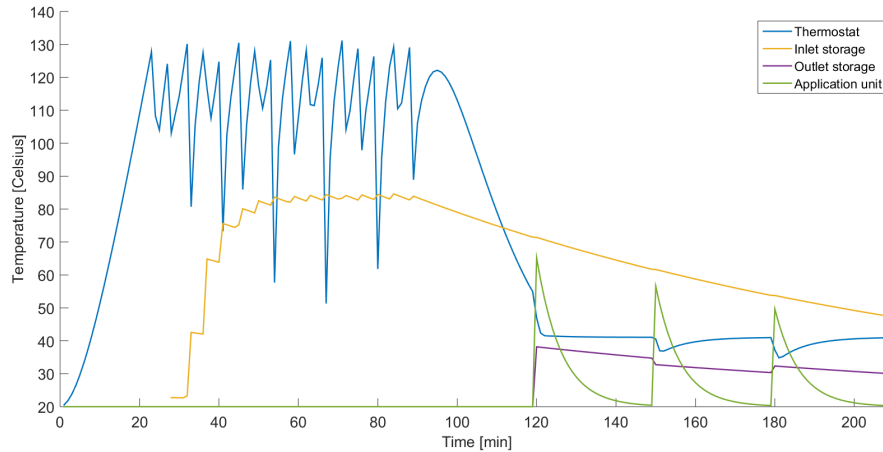


Figure 6.8: Plots display the simulation results from test 4.

Table 6.4 present a comparison of the experimental and numerical system behavior of Test 4. These results points out longer time periods for filling the storage, but a more rapid discharging process in the numerical model compared to the experimental results. During the first time period after the storage was filled, the experimental measurements indicates a steeper temperature decline than the simulations.

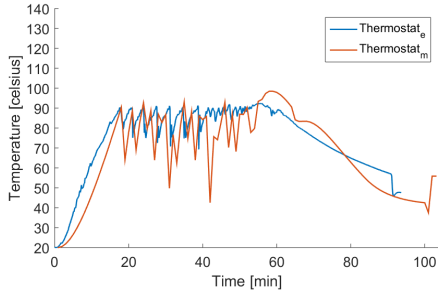
Table 6.4: Time intervals and critical temperatures in Test 4. Comparison of experimental and simulated data.

* 2 hours and 7 minutes after the storage filling was completed. ** 2 hours and 1 minutes after the storage filling was completed.

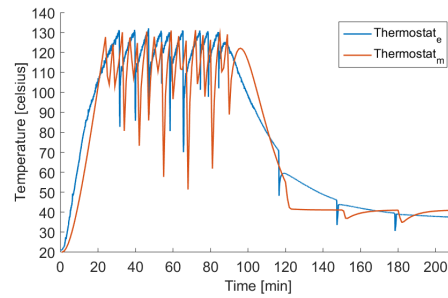
| System behavior - Test 4 | | |
|--|----------------------|---------------|
| | Experimental results | Model results |
| Time for thermostat reach 130°C | 31.3 min. | 28 min. |
| Time to fill storage | 52.9 min. | 58 min. |
| Time at which the heating element was turned off | 84.2 min. | 89 min. |
| Time to empty storage | 165 sec. | 160 sec. |
| Maximum temperature at storage inlet | 90°C | 84.6°C |
| Temperature at storage inlet 30 minutes after filled with hot oil | 59.9°C | 71.5°C |
| Temperature at the storage inlet when the experiment was completed | 44.5°C * | 47°C** |

Validation

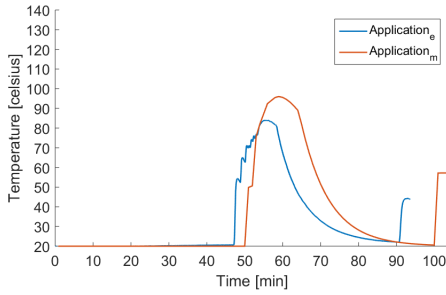
Validation of the the numerical model was done by comparing the simulated results with the experimental results, this is displayed in Figure 6.9.



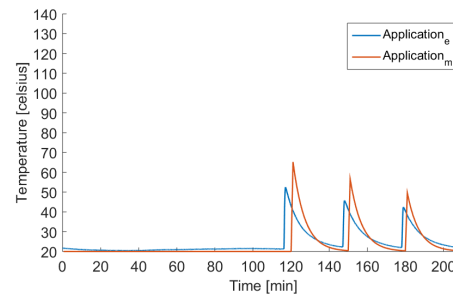
(a) Plot of the temperatures in the thermostat from Test 1, 2nd experiment.



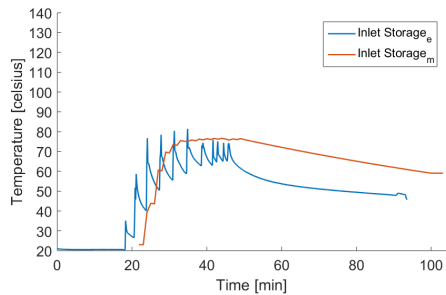
(b) Plot of the temperatures in the thermostat from Test 4.



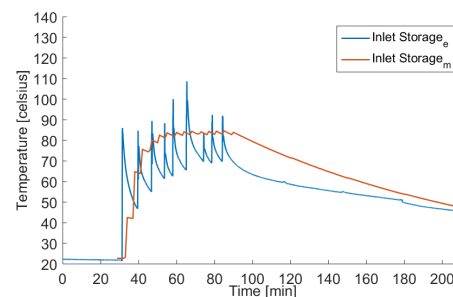
(c) Plot of the temperatures in the application unit from Test 1, 2nd experiment.



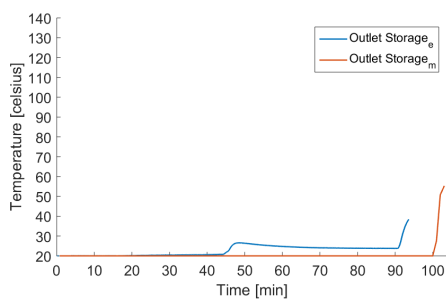
(d) Plot of the temperatures in the application unit from Test 4.



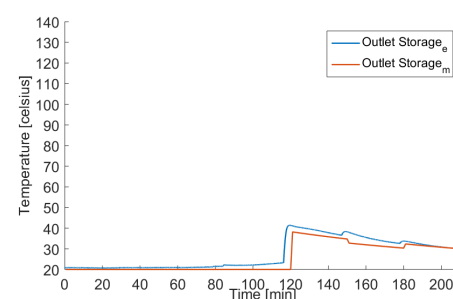
(e) Plot of the temperatures in the inlet of the storage from Test 1, 2nd experiment.



(f) Plot of the temperatures in the inlet of the storage from Test 4.



(g) Plot of the temperatures in the outlet of the storage from Test 1, 2nd experiment.



(h) Plot of the temperatures in the outlet of the storage from Test 4.

Figure 6.9: Comparison of the numerical and experimental results. Subscript e indicates results from the experiment, and subscript m indicated results from the numerical model.

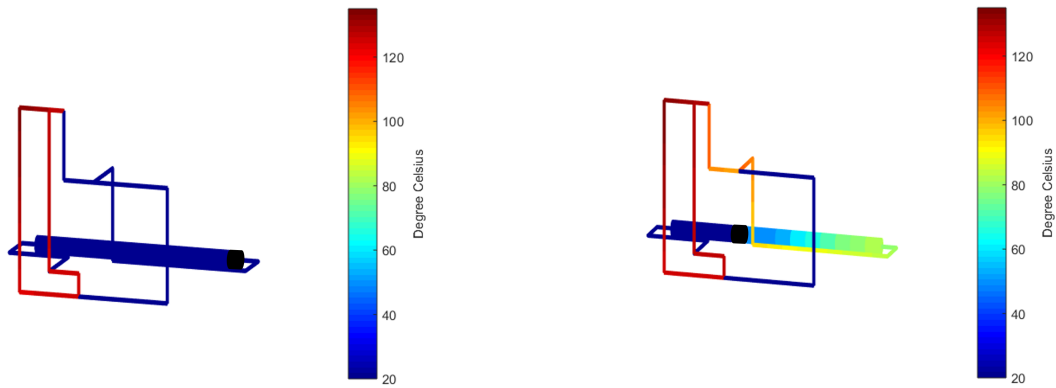
It can be observed that during the heating period, the variations in the simulated thermostat temperatures was larger than the measured temperatures from the experiments. This is shown in Figures 6.9a and 6.9b. After the heat source was turned off, the simulated temperatures provided a steeper decline than the corresponding measured temperatures. Figure 6.9a indicates that the temperature in the thermostat, from the model, continues to increase in a longer time period after the the heating element was turned off, compared to the experimental results.

The simulated temperatures in the inlet of the storage had a smoother temperature increase, with less oscillations, than the measured temperatures from the experiments. During the discharging process of the storage, the experimental measurements provided a steeper decline in the first period compared to the simulated temperatures. From Figure 6.9f, it can be observed that temperatures in the inlet of the storage tend towards the same temperature over time. Due to higher temperature in the simulated inlet storage, the simulated temperatures in the application also presents higher temperatures compared to the corresponding experimental temperatures, displayed in Figures 6.9c and 6.9d. This temperature difference decreases when the inlet storage temperatures in the simulations- and experimental results approaches each other.

The temperature in the outlet of the storage, displayed in Figures 6.9g and 6.9h, presents minor differences between the simulated and experimental temperatures. The experimental temperatures present a modest increase when the storage is fully charged. While the simulated temperature do not experience any increase before the storage discharges.

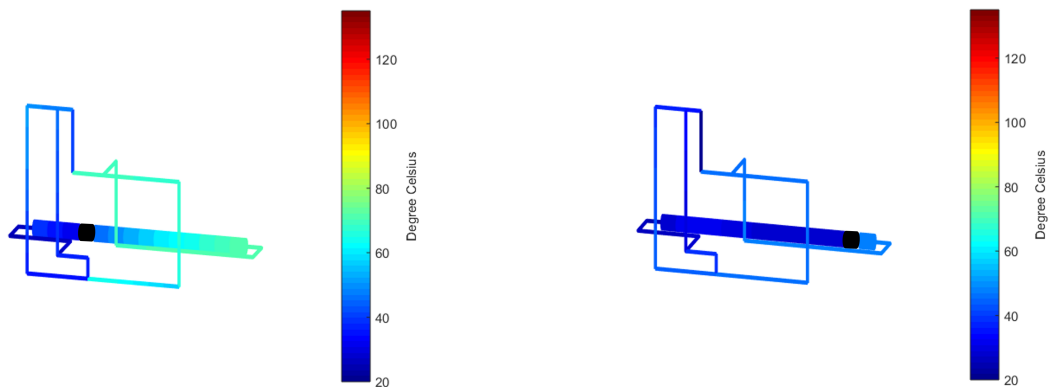
Graphical Visualization

Graphical visualization of the simulation results was made to visualize the concept of the oil system. Frames from the video made of the simulation results, from Test 4, are displayed in Figure 6.10.



(a) Picture displaying the oil system after 27 minutes model time, one minute before the thermostat reacts and sends the heated oil into the storage.

(b) Picture displaying the oil system after 75 minutes model time. The storage is charging with heated oil.



(c) Picture displaying the oil system after 120 minutes model time. The storage is discharging, sending the heated oil to the application.

(d) Picture displaying the oil system after 210 minutes model time. The storage is fully discharged.

Figure 6.10: Graphical Visualization of the Simulation Results. The piston is represented by black color.

6.3.3 Discussion

The model predictions were mostly in good agreements with the measured data from the experiments. Although there were some deviation between the numerical and experimental results, the model gave the same tendency and overall behavior as the experiments. The pipe network operated as desired. The inlet and the outlet of connected branches behave coupled, and the entire system as one closed loop. The charging and discharging of the storage behaved satisfactory.

Losses through the system was difficult to obtain, and the overall heat coefficient was therefore tuned to match the experimental results. The precision of the model predictions is affected by the uncertainties associated with the obtained parameters from the experiments. Inaccurate parameters from the experiment can affect the quality of the model predictions.

Some of the deviations between the numerical and experimental results, could have been a consequent of the neglected energy equation of the pipe wall. Images taken of the storage with the thermal camera, displayed in Figure 5.6, indicates a fairly homogeneous temperature distribution on the hot side of the storage. The images visualize the temperature distribution on the surface of the storage, and thus not the actual temperature distribution of the oil. From this, it can be assumed that axial conduction through the pipe wall might affect the oil temperature in the system. As a consequent of ignoring the axial conduction through the pipe wall, higher temperature gradients may occur in the system. As visualized in Figure 6.10b, the model presents distinct temperature variations in the heated oil inside the storage. Consequently, the temperatures in the outlet of the storage presents a steeper decline when discharging the storage, than the corresponding experimental results.

The thermostat showed similar behavior in the simulation as in the experience. However, the simulations required more time to fill the storage with hot oil than the experiments. The thermostat in the model had an immediate response to changes in temperature, while the solenoid in the experiments had a one second response time. This could have caused the observed time differences.

The model assumed that the hot and cold storage compartments were completely separated by the piston. No leakage was implemented between the cold and the hot oil, and it was assumed negligible heat conduction through the piston. As displayed in Figures 6.9g and 6.9h, some leakage or heat transfer were present through the piston in the experiments. This provided some deviation between the simulated and the experimental results.

As a tool for visualization and investigation, the model provided good indications of the temperature evolution in the oil system and the graphical display can be used to demonstrate the concept of the system.

Chapter 7

Field Work at Mekelle University, Ethiopia

A field study was conducted at Mekelle University, at The Ethiopian Institute of Technology. The intention of the field study was to construct and test an oil based solar heat collection system, with an integrated storage based on forced thermal stratification. The setup was similar to the complete system constructed at NTNU. The experiments conducted at Mekelle University utilized a solenoid in the thermostat solution and the oil was heated by concentrated solar energy. Electrical power was supplied to the pump from a battery, charged by a PV panel. As the solenoid requires current signals with different polarities (a device in which was not readily available at the university), it was connected to an electronic board; requiring normal power supply (AC).

First, the motivation behind the field study will be introduced. Then the material and equipment utilized will be discussed, before the system setup will be reviewed. Finally, the experimental method will be presented followed by the results and a discussion part.

7.1 The Motivation

The motivation behind constructing the system in Ethiopia was to evaluate important features of the system:

- A feasible system has to be robust, low-cost and easy to build and use
- The system has to work efficiently with concentrated solar energy heating

Building the system in Ethiopia gave an indication on whether the system could meet these requirements. For the system to be a suitable alternative for cooking with firewood, it was important that it could be built locally and at low cost. Accordingly, it was critical that the components were easily accessible. Accessibility can often be a problem in remote areas, and therefore it was an advantage if only basic components were

needed to construct the system. High-technology equipment is expensive and often not readily available. A system that only requires basic tools for production was therefore vital. It was desirable to test the system with concentrated solar energy heating, and additionally it was desirable to exploit PV panels for electricity supply to critical components. Ethiopia has an average of twelve hours of daylight, and except for in the rainy season (summer), there is about 8 hours of sunshine every day (Redwoods [2016]). Ethiopia was therefore a good location to conduct the experiments. The experiments were performed in April, which is a sunny period.

7.2 System Components, Material And Equipment

Components necessary to construct the system were:

- A pump to circulate the oil in the system
- Thermostat concept utilizing a push-pull solenoid together with a capillary thermostat
- Pipes with a small diameter
- A pipe working as the storage, with a piston
- An application unit
- A receiver
- A parabolic dish to concentrate the sun radiation
- PV panels and a battery

The pump, solenoid and capillary thermostat was brought from NTNU. The pump was a cheap drain pump with a capacity of 5.5 liter/min, and with operating temperatures from $-10^{\circ}C$ to $60^{\circ}C$ (Oljeskiftpumpe). Due to the temperature restriction, it was only used as a temporary solution. If the oil were to reach higher temperatures during the experiment, cooling of the pump would be necessary. The thermostat concept tested at Mekelle University was the same as the thermostat concept with the solenoid tested at NTNU. The thermostat had one port at the side plate, representing the inlet to the thermostat. It had two port in the bottom plate, representing the hot and the cold outlet. The ports were placed approximately 2.5 cm apart, and the sliding plate had an oval opening that was 3 cm long and 2 cm wide.

The storage had the same principles as the storage tested at NTNU. It was made of a steel pipe with an outer diameter of 19 cm, an inner diameter of 15 cm and a length of 1 m. The piston was designed as a hollow cylinder, with a length of 8 cm and a diameter of 14.5 cm. The application unit was designed as a circular container, illustrated in Figure 7.1a. The receiver was built based on the similar configuration. See Figure 7.1a. The application unit was 5 cm deep and the receiver was 20 cm deep, where both had a

diameter of 20 cm. The piston, application unit, thermostat and receiver was made of steel plates, where the required number of plated were welded together to form a desirable design.

An offset parabolic dish together with a receiver was applied to the system. The dish concentrated solar radiation towards a receiver, where the oil was heated. The offset parabolic dish was designed and constructed, together with a support frame, by Ashenafi Kebedom (et al.) at Mekelle University in 2014 (Asmelash et al. [2014]). The support frame included the receiver, parabolic dish and a cooking stand. The dish had a diameter of 90 cm and was 7 cm deep. It was designed for direct cooking, and could achieve boiling water within 30 minutes. A joint and handle mechanism was used to effectively maneuver the dish along the vertical and horizontal planes, in order to track the sun (Asmelash et al. [2014]). The dish should be adjusted every 10 minutes to gain a perfect focal point. A ready-made parabolic TV antenna, could also have been used as a dish concentrator. They are often easily accessible and will decrease the complexity of the design (Asmelash et al. [2014]).

A normal cooking oil, displayed in Figure 7.1b, was utilized as the heat transfer and storing medium. Tube fitting such as bends, tees, unions, sockets and valves were necessary to assemble the system. This, together with the pipes, were bought in Mekelle. These components were all fairly easy and cheap to obtain. However, it was a limited choice of pipe diameters at the local market. Consequently, steel pipes with a diameter of 20 mm was applied instead of the previously used copper pipes of 15 mm. Mekelle University supplied the remaining components; steel plates, insulation material, the pipe for oil storage, the parabolic reflector, the PV panel and the battery.



(a) Picture of the application unit to the right and receiver to the left. Connections are welded on to enable attachment to the pipes in the system.



(b) Picture of the oil used as heat transfer and heat storing medium.

Figure 7.1: Pictures of the application unit, receiver, heat transfer and storing medium, utilized in the system constructed at Mekelle University.

Equipment available for construction was: welding machine, drilling machine, grinder, bending machine, metal cutter machine and a thread machine. Pictures of the machines are displayed in Figure 7.2.

During construction of the system it was crucial that all of the components and connections were leak-proof. The pipe threads was made with a threading machine. To prevent leakage a sealing material was wrapped around the threads and a red paint was applied upon it. A picture of the painted sealing material is



(a) Picture of the welding machine.



(b) Picture of the cutting machine.



(c) Picture of thread machine.



(d) Picture of the bending machine.



(e) Picture of the grinder.



(f) Picture of the grinder attached to the drilling machine.

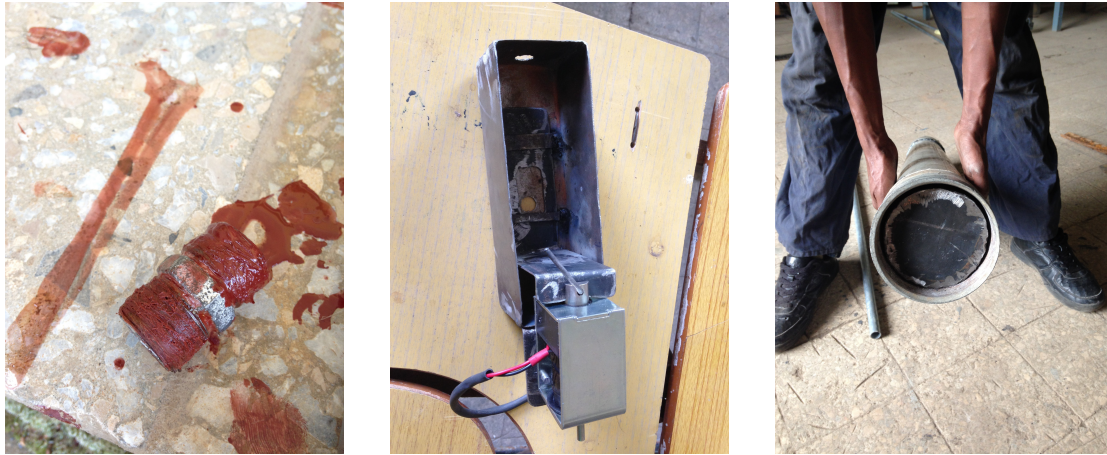
Figure 7.2: Picture of the machines utilized during construction of the system at Mekelle University.

displayed in Figure 7.3a. A vital challenge was to construct the sliding and bottom plate in the thermostat solution flat and smooth. The friction between the sliding plate and the bottom plate should be as small as possible to achieve an operational solenoid. It was also important that they were in close contact, to prevent leakage into the blocked port. The sliding plate was thin, and it easily buckled and bent during welding of the thermostat configuration. Thus, making the construction of the thermostat solution challenging. A picture of the solenoid attached to the thermostat is visualized in Figure 7.3b.

To ensure that the piston could slide smoothly through the storage, the inside of the storage required grinding. This required a drill that could handle large diameters, in which was not readily available. A creative solution was made, by attaching the grinder blades to the drill. See Figure 7.2f. The storage also required a well fitted piston. Understanding that the inside of the storage was not perfectly round or smooth, this was difficult to achieve. A picture of the piston inside the storage is shown in Figure 7.3c.

7.3 System Setup

The experiments carried out at Mekelle University utilized a solenoid as the thermostat concept and had an integrated storage based on forced thermal stratification. The heat transfer medium was heated by



(a) Picture of a union with sealing material and painting.

(b) Picture of the thermostat with the slider.

(c) Picture of piston inside the storage.

Figure 7.3: Picture of the critical components which will affect the quality of the system

concentrated solar energy and the pump obtained electrical power from a battery which was charged by a PV panel.

Figure 7.4 shows the complete system arrangement.



Figure 7.4: Picture of the circulating oil based system setup at Mekelle University. Arrows indicates where the main components in the system are located.

The system setup was similar to the complete system setup constructed at NTNU. A frame with an offset parabolic reflector was already constructed at Mekelle University, and the system was integrated into this frame. The heated pipe from the setup at NTNU, was replaced by a receiver. It was positioned at the parabolic reflectors focal point. Other components, such as the pipe connections and the manual valves, were

arranged similarly as the system setup constructed at NTNU. The thermostat was located at the highest level of the system, as illustrated in Figure 7.4. The application unit was located at a comfortable height for cooking, and the storage was arranged conveniently inside the frame. The pump was placed at the lowest level of the system setup.

The steel pipes, all with a diameter of 20 mm, were threaded and sealed as shown in Figure 7.3a. Pipe connection points were welded onto the application unit, the thermostat and the receiver, so that they could be attached to the pipes in the system. Figure 7.1a shows a picture of this. The receiver was insulated at the top and at the sides, while the application unit was insulated at the bottom and at the sides. Glass wool with insulation tape was used as insulation material.

To control the temperature of the oil in the system, a solenoid was used. What a solenoid is, and how it works, has already been described in Chapters 3. In short, its functionality is that it becomes energized, latched/unlatched, when a distinct/preset temperature has been reached. To control the temperature of the oil a capillary thermostat was used in the system constructed in Ethiopia. Appendix G contains an illustration, together with a description of the chosen capillary thermostat. The function of this type of thermostat is that it operates from a remote bulb, where a knob is present so that a desired temperature can be tuned (temperature at which the solenoid should become energized). A temperature sensor is directly linked to the bulb with a 1 m capillary, at which is connected to a changeover electric switch. The thermostat came with a SPDT (single pole, double throw) switch. This type of switch has three terminals; one common, one that is normally closed and another that is normally open. The latter two were directly connected to the conductors included in the configuration of the solenoid (one positive and one negative). In terms of connecting the SPDT switch to power, three additional cables were required. One of the cables were joined with the positively charged conductor from the solenoid to the open terminal, while another was joined with the negatively charged conductor from the solenoid to the closed terminal. The last cable was connected to the common terminal. The three cables were then linked to connection points at an electronic board, to respectively +15 V, -15 V and ground. Before the cables were connected, a voltmeter was used to ensure that the voltage from the electronic board was maintained at 12 V, due to the tolerance of the solenoid. As the electronic board required AC 220 supply, it was directly connected to a normal power source. PV panels (DC) could therefore not be used during this testing. The electronic board would then convert the AC supply to DC, at which the solenoid required. Figure 7.5 shows a picture of the electronic board and the voltmeter used.

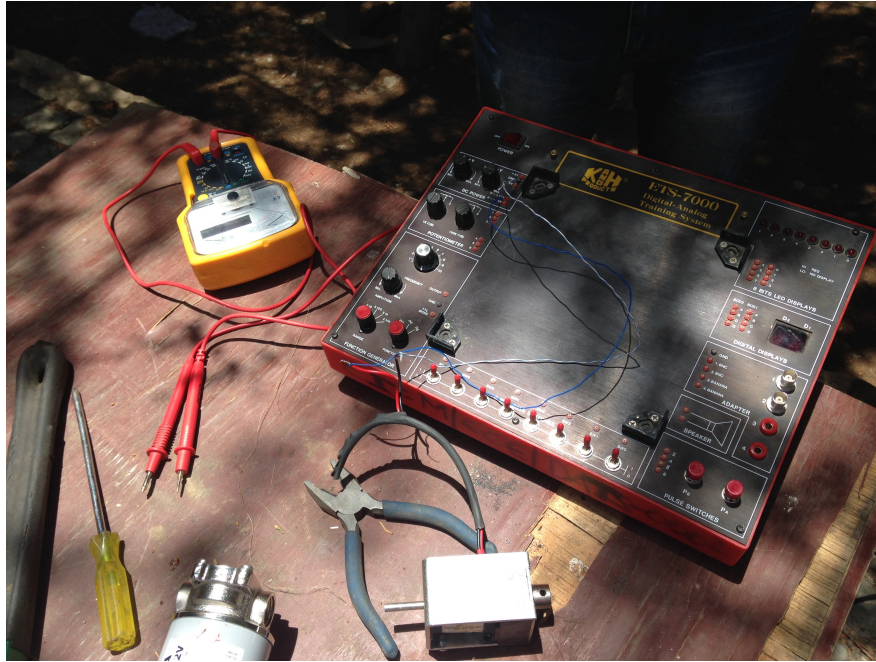


Figure 7.5: The electronic board connected to the solenoid. The voltmeter is located to the left side of the board, at which was used to ensure that the voltage to the solenoid would not exceed 12 V.

The system would work in the manner that when the tuned temperature would be reached, a pulse signal would be sent directly to the solenoid, making it become energized. However, what was realized during the testing of the system, was that it was not possible to obtain reversed polarity from the switch. For that to be obtained a DPDT (double pole, double throw) switch or two SPDT switches would have been required. However, as this was not readily available in Mekelle, we only manage to test the solenoid in one direction (pull action).

Ideally, the solenoid would be powered directly by 12 PV panels (DC) during the day, and by a charged battery (DC) after sunset. The voltage of the PV panels and battery should not exceed 12 V, due to the tolerance of the solenoid. However, due to the solenoid becoming latched/unlatched based on opposite polarities, we would have needed a similar controlling device as the electronic board between the PV panels/battery. However, this was not available at the University. Additionally, since we did not have a DPDT switch, it was adequate to test with the electronic board connected to a normal power supply (AC).

The pump was connected to a battery of 12 V, charged by a PV panel. The PV panel was delivering a maximum voltage of 17.4 V, and due to a 12 V limitation of the pump, it was therefore not connected directly to the PV panel. Figure 7.6 shows the battery used, and the specifications of the PV panel utilized to charge it.

An offset parabolic dish constructed together with a support frame was already built at the site. An arm supporting the receiver was constructed (fixed onto the frame), holding the receiver over the dish. The inlet and outlet pipes to the receiver were positioned in a way that did not reduce the reflectors rotational maneuverability around the offset horizontal axis. A picture of the receiver and the dish is visualized in



(a) Picture of the battery used to supply power to the pump.



(b) Picture of the PV panel specifications. This was the PV panel utilized to charge the pump.

Figure 7.6: Pictures of the pump and the specifications of the PV panel used.

Figure 7.7b.

Thermocouples measured the temperature at eighth different locations in the system. The thermocouples applied was the same as the ones used at NTNU, mineral insulated thermocouples (type K). The thermocouples were attached with tape on the surface of the pipes. The tape prevented direct exposure of sunlight onto the thermocouples.



(a) Picture of the thermostat solution with the solenoid and the capillary thermostat.



(b) Picture of the offset parabolic dish with the focal point at the receiver.

Figure 7.7: Picture of the thermostat solution and the offset parabolic dish with the receiver utilized at Mekelle University.

7.3.1 Data Acquisition With Pico Data Logger

The data in the experiments were collected by using a thermocouple data logger from Pico Technology, illustrated in Figure 7.8b (PicoTech). The data logger measured the temperature from eight thermocouples located at different locations in the setup. This was done by plugging the thermocouples into the data logger, and where the data logger was connected with an USB port to a computer. The computer was installed with a PicoLog data acquisition software, which recorded the measurements. An illustration of this setup is shown in Figure 7.8a.

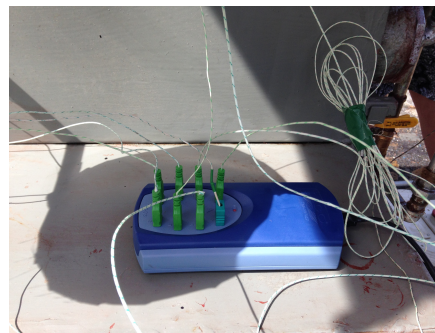
The measuring points were labeled from Temp1 to Temp8. Thus, the different temperatures represented in a given plot will be the ones listed in Table 7.1.

Table 7.1: Measured Temperatures - Sytem Setup in Mekelle

| Temperature measurements in the system | |
|--|---|
| Temp1 | The temperature measured at the outlet of the receiver |
| Temp2 | The temperature measured at the hot pipe outlet of the thermostat |
| Temp3 | The temperature measured at the outlet of the storage |
| Temp4 | The temperature measured at the inlet of the application unit |
| Temp5 | The temperature measured at the inlet of the receiver |



(a) Picture of the computer connected to the data logger, plugged with thermocouples.



(b) Picture of the 8 channeled thermocouple data logger with 8 thermocouples inserted.

Figure 7.8: Picture of the Data Acquisition With Pico Data Logger.

7.4 Experimental Method

Three experiments were carried out at Mekelle University. The first experiment was executed from 14 pm to 17 pm, the second experiment from 08:45 am to 13 pm and the third experiment from 8:45 am to 11:35 am. The experimental procedure was identically in all the experiments.

Problems related to the focal point on the receiver, the accuracy of the thermocouples, and clouds (interrupting direct sunlight), were sources of inaccuracy in the experiments. The third experiment gave the most reliable results and will therefore be reviewed in detail. Sufficiently high temperatures were not achieved during the experiments. Consequently, the storage was tried tested at an oil temperature of 70°C. Unfortunately, the temperature measurements from Temp5 gave indication of poor quality in this experiment. Therefore, to present the effect of the receiver and the parabolic dish, the first part of the second experiment will also be included in the result.

Observations made during the experiments will be discussed before the results will be presented.

7.4.1 Observations of The System

There were issues regarding filling the system with oil. The system would not fill completely, consequently air was present in the system during the experiments. Changing flow patterns in the system led to an increase or decrease of the oil volume in the thermostat, which required manually refill or draining of oil to the system. Leakages was present in the system, both in the components and in the connections. It was not severe, but it would not been feasible in continuous operation.

Problems with the piston emerged during the experiments when trying to charge the storage with hot oil. The piston was positioned at the hot side of the storage, and did not move when the storage was attempted charged. Accordingly, the storage could not be tested during the experiments. The sliding plate in the thermostat did not move as smooth as desired. Occasionally it got stuck and needed a stronger force than the solenoid could provide for movement. A gap between the sliding plate and the bottom plate was also observed, allowing cold oil to leak into the hot outlet pipe. This was solved by closing the valve controlling the storage (Valve 2). As only the pull function was operative from the solenoid, the push movement had to be manually performed during the experiments.

During the experiments there were difficulties adjusting the parabolic dish to achieve a focal point onto the receiver. The parabolic reflector was rotated around an offset horizontal axis, and the entire system was physically rotated. But a focused focal point on the receiver was only obtained from from 8 am to 10 am. This caused difficulties in the experiments after 10 am.

Temperature readings from the thermocouples varied in quality. The thermocouples that obtained distinct incorrect measurements were shifted during the experiments, but still some of the results were unreliable. Some of the measuring points were exposed to the sun, while some were in the shadow. This might have affected the measured results. The thermocouples were attached to the pipe and did not have direct contact

with the oil.

7.4.2 Results

The second experiment is presented to demonstrate the temperature increase through the receiver. Only the first 77 minutes of the experiment is plotted, visualized in Figure 7.9. This due to inconclusive results in the measurements from Temp5 after this. The plot presents the temperature evolutions in Temp1 and Temp5 from 8:45 am to 10:02 am. There was a stable temperature increase in the system with approximately $0.4^{\circ}\text{C}/\text{minutes}$. The sudden temperature drop in Temp5 after 38 minutes was caused by thermocouple adjustments.

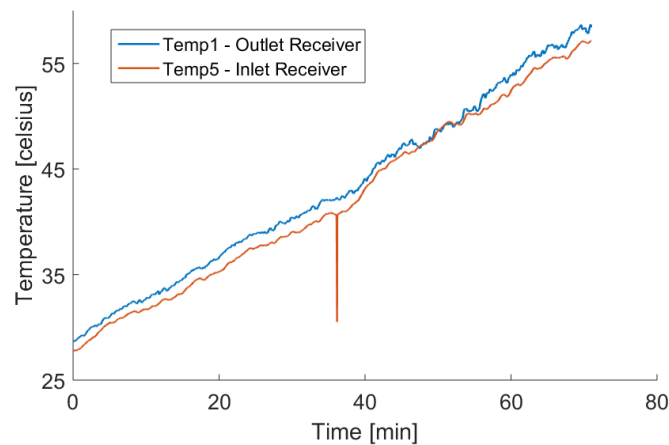


Figure 7.9: Plot of the second experiment conducted at Mekelle University. The graphs illustrate the results from the experiment conducted between 9 am and 10:07 am.

The third experiment was conducted from 8:45 am to 11:45 am. The thermocouple in Temp5 gave highly irregular measurements and has therefore been excluded from the results. The temperature in the system was already at a high temperature when the logging started. As visualized in Figure 7.10, the dish and receiver did not work efficiently together after the first 90 minutes, around 10:15 am. The temperature at the outlet of the receiver stagnated at a temperature around 70°C . After 2 hours and 33 minutes, hot oil was sent from the thermostat into the storage for about one minute. This was repeated after 2 hours and 43 minutes. A rapid increase in Temp2 can be observed at this instance. The results in Figure 7.10 also indicates a temperature increase in Temp3, likely to be caused by leakage around the piston. Thus, as outlined in the section above, the piston did not seem to move inside the storage.

7.5 Discussion

The heating process did not give satisfying results. In the second experiment, the temperature increased with about $0.4^{\circ}\text{C}/\text{minute}$ from 08:45 am to 10:02 am (see Figure 7.9. At this rate, the oil would have reached

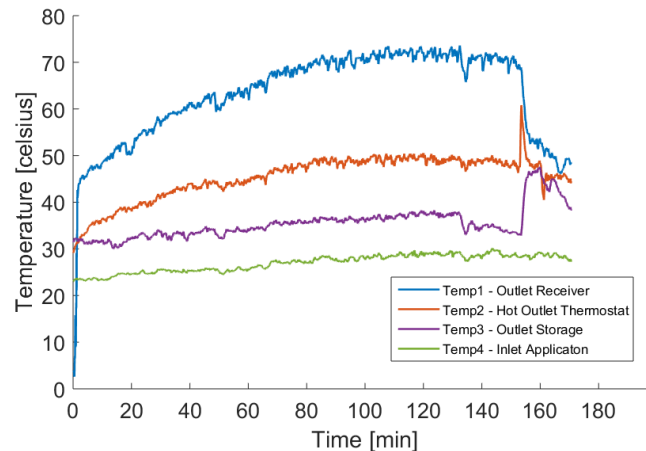


Figure 7.10: Plot of the results of the third experiment conducted at Mekelle University. The experiment was conducted between 8:45 am and 11:45 am. After 2 hours and 33 minutes, and after 2 hours and 43 minutes, hot oil was sent into the storage.

180°C within 6 and a half hours. This indicates that a bigger dish or a smaller receiver would be advantageous to achieve an effective heating process.

Obtaining a focal point on the receiver was difficult after 10 am. As displayed in Figure 7.10, the temperature evolution stagnated. The receiver was held stationary, and would therefore require a parabolic reflector with a fixed focal point. The axis of rotation did not coincide with a focal point focused on the receiver. This axis would have to be adjusted to obtain a fixed focal point on the receiver.

Measurements from the experiments provide limited information about the characteristics of the storage, as the piston was stuck. Temp3 increased when hot oil was sent into the storage which suggests leakage around the piston, visualized in Figure 7.10. The storage solution requires smooth surfaces and high accuracy to obtain a perfect fit between the piston and the inside walls of the storage. Despite much effort and skilled technicians, this was difficult to obtain with the material and tools available.

Several problems associated with the thermostat solution emerged through the experiments. As mentioned, the solenoid required a DPDT or two SPDTs to achieve both a pull and a push function, and the sliding plate occasionally fastened and required a greater push/pull than the solenoid could provide. This was caused by irregularities in the thermostat construction. Welds on the pipe connections and buckles on the bottom plate made the surface uneven. As with the storage, the thermostat solution required smooth surfaces with small friction forces to operate satisfactory. This was difficult to achieve with the equipment and materials available.

Problems associated with air in the system can be fixed by inserting air release valves in the system. It was suspected that the problem arose in the application unit, since air bubbles gather at high points. Incorporating an air valve after the application unit could solve the problem. A thinner application unit could also reduce the amount of air in the system. Leakage points in the system could have been fixed if more time was available.

The test system was constructed during a short time period. Given a higher accuracy in the manufacturing

of the components, and a solar reflector arrangement which could provide a fixed focal point onto the receiver, this system should be expected to be feasible to build and operate.

Chapter 8

Conclusions and Recommendations for Further Work

8.1 Conclusions

The objective of the experimental work, was to design a thermostat capable of regulating the heat in an oil based system. The first thermostat concept tested was based on a liquid filled bellows, utilizing the phenomenon of phase transition. Thus, where thermal energy would be converted into mechanical work in terms of expansion and contraction of the bellows. A thermostat concept at which would be fully independent of external power supply. However, it is important that the expansion and contraction processes (the phase transition processes) are in equilibrium, as the bellows would hold the same features as a control valve in the system. Thus, oil flowing through the inlet of a given thermostat configuration, would leave through one out of two outlets, depending on the temperature of the oil. The regulation between the outlet ports was obtained with a sliding plate placed in the bottom section of the thermostat, ensuring that while one outlet was covered/closed, the other was open. A compression spring was used to assist the bellows in the contraction process.

Several experiments were conducted with the liquid filled bellows, in a stationary oil bath as well as in a circulating oil system. Additionally, fluids with different boiling points were tested, based on different filling procedures, in terms of understanding the features of the bellows. The first observation made was that the overall heat transfer rate between the oil and the bellows was enhanced from a stationary oil bath to a circulating oil system. Thus, the expansion occurred at an earlier temperature instance in the circulating oil experiments. However, the temperature interval required for the expansion to be completed was unchanged from the one system setup to the other. For the multi-component liquids tested, antifreeze and ethanol, the bellows expansion occurred at a temperature interval of approximately 10°C in all of the experiments. The expansion was independent of the filling method utilized, as long as the same compression

spring was used. When a stronger return spring was tested ($k = 0.7$ N/mm instead of $k = 0.237$ N/mm) the temperature interval was doubled, and when no spring was being used the temperature interval was halved. The contraction of the bellows was, however, not in equilibrium with the expansion process. This process was dependent on the filling procedure used, and thus showed different temperature intervals in all of the experiments. The oil bath experiments required a temperature interval of about 40°C , whereas the circulating oil experiments required a temperature interval of approximately 30°C . When an internal vacuum was introduced in the bellows before filling the temperature interval was reduced to 25°C . Thus, it could seem like removal of air inside the bellows was having an effect on the condensation phenomenon. The stronger compression spring gave the same temperature interval, whereas when no spring was being used, the temperature interval was reduced to 10°C . Even if air had been removed from the inside of the bellows, the two phase transition processes were still not symmetric.

After some tests had been conducted with the multi-component liquids, a one-component liquid, 1,2-Propylene glycol diacetate, was tested. It was desirable to observe whether there could be any disturbing substances present in the multi-component liquids, in which could affect the condensation process. The results were not enhanced. The expansion of the bellows occurred significantly earlier than expected. As the provider of the liquid could not supply information regarding its features, it was difficult to understand the observations made during the experiments. The concluding remarks therefore became that presence of air inside the bellows seemed to be a limiting factor, even though the percentage would be significantly small. Consequently, evaporation and condensation seems to be limited by non-equilibrium effects, as the processes does not occur at the same rate. Additionally, the high heat capacity of the stainless steel material, could also be a limiting factor causing delayed reactions inside the bellows.

The second thermostat concept was based on a gas filled bellows. It was believed that in a system containing only gas, in which was going to be superheated, one would not experience issues with non-equilibrium effects. The selected gas was air. The volume required to obtain a desired bellows expansion, 2.50 cm on a 5°C temperature interval, was calculated, where a copper coil was constructed based on the required amount. Since the gas bellows had a small diameter, the volume needed was at a magnitude where a small diameter copper pipe could be used, and thus where efficient heat transfer between the oil and the air could be obtained. However, this was not achieved. A 20°C temperature interval showed an expansion of between 4-5 mm. Hence, it seems like the mechanical resistance of the bellows, in addition to the compressibility of air, limits the functionality of this concept.

The final thermostat concept tested was based on another approach than a bellows. The concept utilized a linear solenoid actuator. The solenoid actuator is based on a coil with a plunger running through the center of it. By applying a current to the coil, electromagnetic flux will move the plunger depending on the direction of the current. The solenoid actuator was therefore, via its positive and negative conductors, connected to a system programmed in LabVIEW. The programme contained multiple thermocouples measuring the temperatures in the system. The thermocouple measuring the temperature in the thermostat was interlinked

with a preset temperature in the program, which was controlling when the solenoid actuator would become energized. Observations and results indicated that the functionality of the solenoid actuator was satisfactory. Its responsiveness managed to change the course of the oil flow in less than one second.

However, occasionally during an experiment, the solenoid actuator was having issues moving the bracket, and thus the sliding plate, in which the plunger was connected to. The problem was not believed to be due to the compression spring, as it had been adjusted and tested to be compliant with the pull and push forces of the solenoid actuator. However, what was believed to be the reason, was its position in the thermostat design. The plunger was connected at the top part of the bracket, and the force exerted would therefore not be onto its center of mass point. The propagation of the force could therefore occur in a manner where the bulk of the bracket would accelerate at a slower rate compared to the top part. Hence, in the moment force would be exerted, a twisting effect could be initiated, which could affect the motion of the sliding plate. A more prominent friction resistance between the bottom part of the thermostat and the sliding plate, and resistance from the bolts connecting the two together, could be a factor limiting the force exerted by the solenoid actuator.

The solenoid actuator was tested on the complete system setup, containing an integrated storage. The aim was to observe whether forced stratification could be achieved with the utilization of a piston. The piston was functioning as a physical barrier between the hot and cold side inside the cylindrical storage configuration. The results from the experiments showed that stratification was achieved. Hot oil was entering through the storage inlet, and was leaving through the storage outlet, due to the motion of the piston. As a result of the responsiveness of the solenoid actuator, oil at the same high temperature was being stored. In addition to the solenoid actuator, the system included manual valves. Their arrangement ensured that the hot oil could be used directly in the application unit or directed towards the storage. However, due to the material of the piston, POM (thermoplastic), the temperature in the system had to be adjusted based on its physical properties. Hence, the material could only handle temperatures up to 100°C. Therefore, the temperature of the thermostat in LabVIEW was not set higher than 130°C, at which resulted in a maximum temperature at the storage inlet of 90°C. Observations of the system indicated that it was having significant heat losses, believed to be embedded in the wide use of copper pipes. Copper has a high thermal conductivity, and even though the material was being well insulated, heat losses seemed to be prominent. Additionally, the oil inside the storage was experiencing substantial heat losses, believed to be due to the storage design; long length and small diameter. Even though the material of the storage, stainless steel, offers low thermal conductivity, heat losses in the oil would be substantial (especially in the beginning due to the initial temperature of the material) as large amounts of the oil would be in direct contact with the walls of the storage. Nevertheless, in the experiments focus was on demonstrating the principles of the system setup. This was obtained.

A piston made of PEEK, a material handling temperatures up to 260°C, was tested inside the storage at the end of the experimental work. It was designed to be virtually identical to the POM piston. The diameter of the new piston was, however, slightly increased (0.2 mm), to make it as uniform as possible with the inside

diameter of the storage. Its sliding effect was the same as the POM piston. High oil temperatures were not tested.

The computational model was designed as a simplified dynamic 1D model, based on numerical integration of the conservative equations of mass and energy for a fluid. An upstream first order explicit scheme, with a finite different approach, were used. The simulation result predicts the temperature evolution in the fluid. The model was designed as a network of branches connected to each other. The flow pattern in the network was controlled by user-controlled valves, and by a thermostat. The thermostat was implemented in the model as a switch between the flow rate in the two connected outlet branches. The storage was modeled as a branch in the network, with a dynamic separating section that represents the position of the moving piston. The model was simplified by assuming a laminar and incompressible flow, with constant flow rate and c_p . Axial heat conduction and viscous dissipation was neglected, and a stationary overall heat transfer coefficient, between the oil and the surroundings, was assumed. Losses through the system was difficult to obtain, and the overall heat coefficient was therefore tuned to match simulation results.

Two simulations were performed, and comparisons between the experimental- and simulated results were carried out. The simulation results were consistent with the measured data from the experiments, although simplifications made in the model caused some deviations. Neglected axial conduction through the pipe wall could have caused higher temperature gradients in the system, than observed in the experimental results. The model did not assume leakage or heat transfer through the piston, this also caused minor deviation between the simulation- and the experimental temperatures in the storage.

However, the model were in good agreement with the measured data from the experiments and the pipe network operated as desired. It was easy to change the connections, properties and flow pattern in the branches. This makes the model flexible and suitable as a design tool. The model provided indications of the temperature evolution in the oil system, and can therefore be used as a tool for visualization and investigation. The graphical display can be used to demonstrate the concept of the system.

A similar system to the oil circulating system constructed at NTNU, with a storage and a solenoid actuator, was built and tested during a field study at Mekelle University in Ethiopia. The system was heated with concentrated solar energy, utilizing a parabolic dish. The pump was supplied with electrical power from a battery, charged by a PV panel. As the solenoid actuator requires current signals with different polarities (a device in which was not readily available at the university), it was connected to an electronic board; requiring normal power supply (AC). The solenoid actuator, a capillary thermostat and the pump was brought from NTNU, while the remaining components were bought at the local market if not already available at the university. The construction of the system was challenging with the equipment and material available. The result became that the thermostat did not operate smoothly, the piston fastened in the storage and there were leaking points in the system.

A focal point was not achieved on the receiver after 10 am, because the axis of rotation did not coincide with a focal point on the receiver. This axis would have to be adjusted to obtain a fixed focal point. A bigger dish or a smaller receiver would be advantageous to achieve an effective heating process. Hence, it would have taken approximately 6 and a half hours for the oil to reach 180°C if the heating process would have continued with the same temperature increase, as observed between 8 am and 10 am.

The test system was constructed during a short time period. Given a higher accuracy in the manufacturing of the components, and a solar reflector arrangement - which always provides a focal point on the receiver, the system is expected to be feasible to build and operate in Mekelle.

8.2 Recommendations for Further Work

Based on the findings in this study, the following recommendations have been made:

The Bellows

The liquid filled bellows did show clear limitations in terms of functioning as a control valve in the system. Nevertheless, if the thermostat could be modified to handle a smaller bellows expansion it would be possible to use it. However, one should be aware of the limitation with the contraction process. If, for instance, a small diameter bellows could be used (like the gas bellows), the overall heat transfer between the liquid inside and the bellows material could be enhanced. Additionally, by demanding a small expansion, one would be able to reduce the temperature interval required for the expansion and contraction processes. Even if the processes would be unsymmetrical, the difference could be considered to be small enough for the bellows to be accepted as a control valve in the system.

It should also be done some research with regards to pre-filling of bellows. After being in contact with the company behind the bellows used in this research, Metal Flex, they could inform that they had vendors that could assist them with sealing a gas inside a bellows. However, they could not pre-fill the bellows with a liquid. Further research on the gas filled bellows should therefore be conducted as pre-filling is an option. If a gas with desirable compressibility could be sealed inside, and a bellows having less mechanical resistance could be used, it would be possible for this thermostat concept to have substantial potential.

Linear Solenoid Actuator

In the further work with the solenoid actuator, when it is to be tested in a system in which would not include LabVIEW, a DPDT switch will be required. Together with, for instance a capillary thermostat. The solenoid actuator requires current signals with different polarities for the plunger to become latched/unlatched, in which could be obtained with this type of switch. The SPDT switch tested during the field study at the University of Mekelle was only having a single pole, and therefore the plunger was becoming latched, but not unlatched. Additionally, it will be important to have some kind of device/switch which can turn off the

power supply after the solenoid actuator has received a pulse signal. This is not incorporated into any of the switches mentioned above, but should be present in a thermostat concept based on a solenoid actuator. Due to the system comprising a solenoid actuator and a pump, a given battery (required after sunset) would be discharge at a slower rate if this type of switch could be found or developed.

What is also important to notice, is that this solenoid actuator has a voltage limitation of 12 V, and to function it requires a power supply of 80 W. For the further work, where PV panels should be used, this limitation would have to be taken into consideration. What we observed at the University in Mekelle, was that the 12 V PV panels available only could supply 20 W. Therefore, to obtain the required 80 W, four of these panels would need to be connected together, in parallel. As the amount of power supplied by a given PV panel will vary, the number of PV panels required will also have to be adjusted accordingly.

When it comes to the design of the thermostat this would also have to be adjusted to some extent, to avoid any sliding issues with the thin plate. Hence, the arrangement of the solenoid actuator should be in a manner causing the force exerted to be onto the center of mass point of a given unit. An arrangement which could cause a sufficient axial movement of the sliding plate.

Other Thermostat Options

There are multiple thermostat solutions available on the market, where some have been reviewed in Chapter 2. However, whereas some are too expensive, others does not meet the requirements of the oil based system. For instance, it was motivation to test a copper bellows. Copper is a material with low heat capacity/high thermal conductivity, and thus the responsiveness of a bellows could be enhanced. Unfortunately, a bellows constructed in this material will be too expensive (information provided by a company named Duraflex). A further effort should be to continue the search for an appropriate thermostat solution where temperature change alone could be used to operate a given device.

The Application Unit

The application unit was made of 12 mm copper pipes, bended to form a distinct design. Due to its configuration, it would not represent a final hot plate design. However, focus was not on constructing it based on a final design, as the focus of the experimental work was to demonstrate the principles of the system setup. For the further work with the application unit, focus on design and insulation will therefore be of importance.

The Storage

The cylindrical storage in the system setup was suggesting large heat losses. This was believed to be due to its design; long length and small diameter. For the further work with this type of storage, the diameter should be increased, thus to the right extent, so that the stored oil would stay sufficiently warm over a longer

period of time. The size of the storage will also have to be adequate, allowing for a required volume amount of hot oil to be stored during a day.

The Piston

The piston exploited in the experimental work was made of POM, a material at which should not be exposed to high oil temperatures due to its physical properties. For the further work with the system, higher temperatures should be tested, based on the application purpose of the oil system. A piston made of PEEK was tested inside the storage during the final work with this thesis. However, it was not tested at high oil temperatures. In the further efforts with the system this would have to be conducted. Additionally, since the design of the storage should comprise a larger diameter, the diameter of the piston will need to be adjusted accordingly.

Pipe Connections

The system comprised several copper pipes, in which was connecting the system components together. Even if well insulated, heat losses were prominent. In the further work with the system, the copper pipes lengths should be reduced, where it is possible. In addition, it could be necessary to replace copper with another material, for instance stainless steel having low thermal conductivity.

Solar Concentrator

The system should be tested with a solar concentrator with fixed focal point. This is a simple way to track the sun and achieve a focal point on the receiver. With a moving focal point, the receiver must be attached to the concentrator and moved with it. Hence, pipes to and from the receiver requires a more complicated design.

Numerical Enhancement

Including axial conduction through the pipe wall, would provide a more accurate analysis of the system. Especially since copper has a high thermal conductivity, and thus it is reasonable to assume that it will affect the oil temperature in the system. An implicit scheme would allow greater time-steps without facing stability issues. An implicit scheme could make the simulation faster than the explicit scheme, which could be desirable.

There should be performed a more detailed representation of the sensible heat storage. A parametric study investigating the effect of the gap size between the piston and the inner radius of the storage could provide valuable information for further design of the storage. It should also be performed a study to investigate the material properties of the piston. By including conduction through the piston, and friction forces between the surfaces, knowledge about sliding properties and heat transfer for the different material options would be obtained.

Bibliography

- John David Anderson and J Wendt. *Computational Fluid Dynamics*, volume 206. Springer, 1995.
- Haftom Asmelash, Ashenafi Kebedom, Mulu Bayray, and Anwar Mustofa. Performance Investigation of Offset Parabolic Solar Cooker for Rural Applications. In *International Journal of Engineering Research and Technology*, volume 3. ESRSA Publications, 2014.
- Autodesk University Workshop AUW. Nusselt Number Relationship. URL <http://www.thermopedia.com/content/841/>. [Online; accessed 09-December-2015].
- Devrim Aydin, Sean P Casey, and Saffa Riffat. The Latest Advancements on Thermochemical Heat Storage Systems. *Renewable and Sustainable Energy Reviews*, 41:356–367, 2015.
- Materials AZO. Stainless Steel. URL <http://www.azom.com/properties.aspx?ArticleID=965>. [Online; accessed 16-May-2016].
- Bagges. Produktkatalog Teknisk Plast. 2016.
- William P Bahnfleth and Amy Musser. Thermal Performance of a Full-Scale Stratified Chilled-Water Thermal Storage Tank. *ASHRAE Transactions*, 104:377, 1998.
- Jo Barrett and C Clement. Kinetic Evaporation and Condensation Rates and Their Coefficients. *Colloid and Interface Science*, 150(2):352–355, 1991.
- A Belward, B Bisselink, et al. Renewable Energies in Africa. 2011.
- Robert P Benedict. *Fundamentals of Temperature, Pressure and Flow Measurements*. John Wiley & Sons, 1984.
- Bruno Cárdenas and Noel León. High Temperature Latent Heat Thermal Energy Storage: Phase Change Materials, Design Considerations and Performance Enhancement Techniques. *Renewable and Sustainable energy reviews*, 27:724–737, 2013.
- Chuen-Yen Chow. An Introduction to Computational Fluid Mechanics. 1979.

- Clorius-Controls. Self-Acting Temperature Controls, n.d. URL <http://www.cloriuscontrols.com/data-GB/3.4.01-GB.pdf>. [Online; accessed 07-June-2016].
- E. Cuce and P. M. Cuce. A Comprehensive Review on Solar Cookers. *Applied Energy*, 102:1399–1421, 2013.
- Ibrahim Dincer and Marc Rosen. *Thermal Energy Storage: Systems and Applications*. John Wiley & Sons, 2002.
- Matthew J Duffy, Marion Hiller, David E Bradley, Werner Keilholz, and Jeff W Thornton. Trnsys-features and functionality for building simulation 2009 conference. 2009.
- Basic Electronics. Basic Electronics, 2016. URL <http://www.electronics-tutorials.ws/electromagnetism/electromagnetism.html>. [Online; accessed 03-June-2016].
- A Fernández. Stratification in Oil-Based Heat Storage. 2014.
- J. Halpern. Vapor Pressure, n.d. URL [http://chemwiki.ucdavis.edu/Textbook_Maps/General_Chemistry_Textbook_Maps/Map%3A_Chemistry%3A_The_Central_Science_\(Brown_et_al.\)/11._Liquids_and_Intermolecular_Forces/11.5%3A_Vapor_Pressure](http://chemwiki.ucdavis.edu/Textbook_Maps/General_Chemistry_Textbook_Maps/Map%3A_Chemistry%3A_The_Central_Science_(Brown_et_al.)/11._Liquids_and_Intermolecular_Forces/11.5%3A_Vapor_Pressure). [Online; accessed 27-April-2016].
- SM Hasnain. Review on Sustainable Thermal Energy Storage Technologies, Part I: Heat Storage Materials and Techniques. *Energy Conversion and Management*, 39(11):1127–1138, 1998.
- HVAC-Specialist. Hvac Bimetallic-Type Thermostat, 2011. URL <http://www.hvacspecialists.info/control-devices/hvac-bimetallic-type-thermostat.html>. [Online; accessed 16-December-2015].
- International Energy Agency IEA. Energy access database, 2015. URL <http://www.worldenergyoutlook.org/resources/energydevelopment/energyaccessdatabase/>. [Online; accessed 12-December-2015].
- Anton DJ Kaasjager and GPG Moeys. A Hot Plate Solar Cooker With Electricity Generation-Combining a Parabolic Trough Mirror with a Sidney Tube and Heat Pipe. In *Global Humanitarian Technology Conference (GHTC), 2012 IEEE*, pages 6–11. IEEE, 2012.
- Hans-Joachim Kilger. Heat Transfer Media. URL <http://www.thermopedia.com/content/842/>. [Online; accessed 19-Mars-2016].
- V.A. Kurganov. Heat Transfer Coefficient. URL <http://www.thermopedia.com/content/841/>. Online; accessed 09-Desember-2015.
- Doerte Laing, Thomas Bauer, Wolf-Dieter Steinmann, and Dorothea Lehmann. Advanced High Temperature Latent Heat Storage System-Design and Test Results. *Effstock 2009, Abstract Book and Proceedings*, 2009.
- WJ Minkowycz and EM Sparrow. Condensation Heat Transfer in the Presence of Noncondensables, Interfacial Resistance, Superheating, Variable Properties, and Diffusion. *International Journal of Heat and Mass Transfer*, 9(10):1125–1144, 1966.

- M Mussard. A Solar Concentrator with Heat Storage and Self-Circulating Liquid. 2013.
- O.J Nydal. Small Scale Concentrating Solar Energy Systems With Heat Storage. *Final Report, Network Projects*, pages 4–11, 2014.
- K. Nyeinga. Dynamic Model for Small Scale Concentrating Solar Energy System with Heat Storage. 2012.
- Biltema Oljeskiftpumpe. Oljeskiftpumpe. URL <http://www.biltema.no/no/Bat/Motor/Motortilbehor/Verktoy-og-tilbehor/Oljeskiftpumpe-2000034861/>. [Online; accessed 23-May-2016].
- Schrock V.E. Peterson, P.F and T. Kageyama. Diffusion Layer Theory for Turbulent Vapor Condensation With Noncondensable Gases. *Heat Transfer*, 115(4):998–1003, 1993.
- thermocouple PicoTech. Thermocouple Data Logger. URL <https://www.picotech.com/data-logger/tc-08/thermocouple-data-logger>. [Online; accessed 23-May-2016].
- Likhendra Prasad, Hakeem Niyas, and P Muthukumar. Performance Analysis of High Temperature Sensible Heat Storage System During Charging and Discharging Cycles. 278:1240–1247, 2013.
- Jason Rapp. Construction and Improvement of a Scheffler Reflector and Thermal Storage Device. 2010.
- Amstelveen Redwoods. Sunrise and Sunset Times, 2016. URL <http://sunrisesunset.info/>. [Online; accessed 07-June-2016].
- Rostra-Vernatherm. Thermally Activated Valves, 2014. URL http://www.vernatherm.com/thermal_valves.html#. [Online; accessed 07-June-2016].
- RS-Components. How to Select Your RS Solenoid. URL <http://docs-europe.electrocomponents.com/webdocs/001b/0900766b8001b732.pdf>. [Online; accessed 16-May-2016].
- Sigma-Netics. White Paper: Designing with Metal Bellows. 2015.
- Siddharth Srinivasan, Tinnokesh. Residential Solar Cooker with Enhanced Heat Supply. *International Journal of Scientific and Research Publications*, 3(10), 2013.
- Asfafaw Haileselassie Tesfay, Mulu Bayray Kahsay, and Ole Jørgen Nydal. Design and Development of Solar Thermal Injera Baking: Steam Based Direct Baking. *Energy Procedia*, 57:2946–2955, 2014.
- Therm-Omega-Tech. Thermal Actuator, Solid-Liquid Phase Change Actuators, 2014. URL <http://www.thermomegatech.com/wp-content/uploads/2014/10/Actuators.pdf>. [Online; accessed 07-June-2016].
- Elias Wagari and Abdulkadir Aman. Characterization and Experimental Investigation of nano3: Kno3 as Solar Thermal Energy Storage for Potential Cooking Application.

Part I

Appendices

Appendix A

The Liquids Inside The Bellows

The different liquids used inside the bellows were antifreeze, ethanol and the pure one-component liquid 1,2-Propylene glycol diacetate. Information about the different products can be studied in their safety data sheets, available in this appendix. For the antifreeze there has been attached two copies, as some information, e.g. the liquids vapor pressure at 20°C, was missing in the latest updated version of the safety data sheet. It would, however, be reasonable to assume that this information is reliable and correct, as the liquid still appears to be the same.

SIKKERHETS DATABLAD

FROSTVÆSKE KONSENTRAT

AVSNITT 1: Identifikasjon av stoffet/stoffblandingen og selskapet/foretaket

1.1 PRODUKTIDENTIFIKATOR

Handelsnavn FROSTVÆSKE KONSENTRAT
Handelsnavn 2 BS6580

1.2 RELEVANTE, IDENTIFISERTE BRUKSOMRÅDER FOR STOFFET ELLER BLANDINGEN, OG IKKE-ANBEFALT BRUK

Bruksområder Kjølevæske

1.3 DETALJER OM LEVERANDØREN PÅ SIKKERHETS DATABLADET

Kontaktperson Kjersti Ilebrekke - kjersti.ilebrekke@wilhelmsen.com
Produsent Wilhelmsen Chemicals AS
P.Box 15 , N-3141 Kjøpmannskjær, Norway
Tel: +47 33 35 15 00
Fax: +47 33 35 14 40
chemicals@wilhelmsen.com

1.4 NØDTELEFONNUMMER

Nødnummer Giftinformasjonssentralen - 24 timer - Tlf.: 22591300 Wilhelmsen Chemicals AS,
Tel.: 33 35 15 00

AVSNITT 2: Fareidentifikasjon

2.1 KLASSIFISERING AV BESTANDELER ELLER BLANDING

Farlig ved svelging.

Faresymboler



Inneholder

1,2-etandiol
Natrium 2-etylhexanoate

2.2 ETIKETTELEMENTER

Risikoesetninger

R-22 Farlig ved svelging.
Livstruende forgiftning eller nyreskade kan bli følgen dersom innholdet drikkes.

Sikkerhetssetninger

S-46 Ved svelging, kontakt lege omgående og vis denne beholderen eller etiketten.
S-24/25 Unngå kontakt med huden og øynene.
S-2 Oppbevares utilgjengelig for barn.

CLP

Farepiktogrammer



Signalord

Advarsel

Faresetninger

Acute Tox. 4: H302 Farlig ved svelging. STOT RE 2: H373 Kan forårsake organskader ved langvarig eller gjentatt eksponering .

Sikkerhetssetninger

P102 Oppbevares utilgjengelig for barn. P260 Ikke innånd støv/røyk/gass/tåke/damp/aerosoler. P264 Vask hendene grundig etter bruk.

Personbeskyttelse Bruk verneklær som beskrevet i punkt 8 i dette sikkerhetsdatabladet.

6.2 FORHOLDSREGLER FOR VERN AV MILJØ

Miljøbeskyttelse Ikke forurens vannkilde eller kloakk.

6.3 METODER OG MATERIALER FOR BEGRENSNING OG OPPRENSKNING

Opprenskningsmetoder Absorber i vermikulitt, tørr sand eller jord og fyll i beholdere. Forhindre utslipp av større mengder til avløp.

6.4 REFERANSE TIL ANDRE AVSNITT

AVSNITT 7: Håndtering og lagring

7.1. FORHOLDSREGLER FOR SIKKER HÅNDTERING

Forholdsregler ved bruk Unngå søl, hud- og øyekontakt.

7.2 FORHOLD FOR SIKKER LAGRING, INKLUDERT EV. UFORENLIGHET

Forholdsregler ved lagring Oppbevares på kjølig, tørt og ventilert lager og i lukkede beholdere.

7.3 SPESIFIKK SLUTTBRUK

Særlig(e) bruksområde(r) Kontakt leverandøren for ytterligere informasjon.

AVSNITT 8: Eksponeringskontroll/personlig beskyttelse

8.1. KONTROLLPARAMETERE

| Navn | CAS nr. | Referanse | Gj.snitt 8t.eksp. | Takverdi | Dato |
|--------------|----------|-----------|----------------------|------------|------|
| 1,2-etandiol | 107-21-1 | AN. | 52 mg/m ³ | 25 ppm, HT | |

8.2 EKSPONERINGSKONTROLL

Åndedrettsvern

Ingen spesielle anbefalinger er gitt, men bruk av åndedrettsvern kan være nødvendig under uvanlige forhold med sterk luftforurensning. Gassfilter A (organiske stoffer, brunt).

Håndvern

Bruk vernehansker av: Polyvinylklorid (PVC). Nitrilgummi. Naturgummi eller plast. Hanske må velges i samarbeid med hanskeleverandøren, som kan opplyse om hanskematerialets gjennomtrengningstid.

Øyevern

Ved fare for sprut, bruk godkjente vernebriller eller ansiktsskjerm.

Verneklær

Bruk hensiktsmessige verneklær for å beskytte mot mulig hudkontakt.

Hygieniske rutiner

Vask huden ved slutten av hvert skift og før spising, røyking og bruk av toalett. Vask straks hud som er blitt våt eller tilsølt. Skift arbeidsklær daglig hvis det er mulighet for at de er tilsølt.

AVSNITT 9: Fysiske og kjemiske egenskaper

9.1. INFORMASJON OM GRUNNLEGGENDE FYSISKE OG KJEMISKE EGENSKAPER

Form/konsistens Flytende. Væske.

Farge Blå.

Lukt Mild (eller svak).

Løselighetsbeskrivelse Lett oppløselig i vann. Lett oppløselig i: Alkoholer,

Kokepunkt (°C, intervall) 164 **Trykk:** 760mmHg

Smelte/frysepunkt (°C, intervall) - 18

Tetthet (g/cm³) 1,1 **Temperatur (°C):** 20

pH, konsentrert løsning 8,7

Flammepunkt (°C) 115 **Metode:** CC-Lukket kopp.

9.2 ANDRE OPPLYSNINGER AV BETYDNING FOR HELSE, MILJØ OG SIKKERHET

AVSNITT 10: Stabilitet og reaktivitet

10.1. REAKTIVITET

Ingen reaktive grupper.

10.2. KJEMISK STABILITET

Stabil under normale temperaturforhold og anbefalt bruk.

10.3 MULIGHET FOR SKADELIGE REAKSJONER

SIKKERHETSDATABLAD

FROSTVÆSKE BS

1. IDENTIFIKASJON AV STOFFET/STOFFBLANDINGEN OG SELSKAPET/FORETAKET

| | |
|--------------|--|
| Handelsnavn | FROSTVÆSKE BS |
| Bruksområder | Kjølevæske |
| Produsent | Wilhelmsen Chemicals AS P.Box 15 , N-3141 Kjøpmannskjær, Norway Tel: +47 33 35 15 00 Fax: +47 33 35 14 40 chemicals@wilhelmsen.com |
| Nødnummer | Giftinformasjonssentralen - 24 timer - Tlf.: 22591300 Wilhelmsen Chemicals AS, Tel.: 33 35 15 00 |

2. FAREIDENTIFIKASJON

Farlig ved svelging.

3. SAMMENSETNING/OPPLYSNINGER OM BESTANDDELER

Ingredienser

| Navn | EC-nr. | CAS-nr. | Innhold | Symbol | Klassifisering |
|---------------------|-----------|-----------|-----------|---------|------------------|
| 1,2-etandiol | 203-473-3 | 107-21-1 | 60-100 % | Xn | R-22 |
| Denatonium Benzoate | | 3734-33-6 | 10-30 ppm | Xn | R-20/22, R-52/53 |
| natrionnitritt | 231-555-9 | 7632-00-0 | <0,2 % | T ,O ,N | R-8, R-25, R-50 |

Se avsnitt 16 for setninger i fulltekst.

4. FØRSTEHJELPSTILTAK

| | |
|-----------|---|
| Innånding | Flytt straks den eksponerte til frisk luft. I lette tilfeller av illebefinnende: Hold pasienten under oppsyn og kontakt eventuelt lege. I alvorligere tilfeller: Bevisstløse legges i stabilt sideleie og holdes varme. Lege tilkalles. |
| Svelging | Gi rikelig med vann. Om mulig også aktivt kull (kullsuspensjon). Forsøk å fremkalle brekning. Gi straks 7-8 ss. (1 dl) etanol. Skaff øyeblikkelig legehjelp eller transport til sykehus. Gi vann og fremkall brekning hos våken person. Gi oppslemming av 50-100 gr. medisinsk kull i et glass vann, gjentas etter eventuell brekning. Deretter etanol ca. 40%, 30-50 ml (brennevin). Skaff øyeblikkelig legehjelp eller bring pasienten til syke- hus. |
| Hud | Vask straks huden med såpe og vann. Ta av gjennomfuktede klær. |
| Øyne | Skyll straks øyet med mye vann mens øyelokket løftes. Kontakt lege hvis ikke alt ubehag gir seg. |

5. BRANNSLOKKINGSTILTAK

| | |
|-----------------------|---|
| Brannsløkkingsmidler | Vann, Pulver, skum eller CO ₂ , |
| Brannbekjempelse | Bruk vann for å kjøle beholdere og spre damper. |
| Karakteristiske farer | Kan reagere voldsomt med oksidasjonsmidler. |

6. TILTAK VED UTILSIKTEDE UTSLIPP

Opprenskningsmetoder Absorber i vermikulitt, tørr sand eller jord og fyll i beholdere. Benytt nødvendig verneutstyr. Forhindre utslipp av større mengder til avløp.

7. HÅNDTERING OG LAGRING

Forholdsregler ved bruk Unngå søl, hud- og øyekontakt.

Forholdsregler ved lagring Oppbevares på kjølig, tørt og ventilert lager og i lukkede beholdere.

8. EKSPONERINGSKONTROLL/PERSONLIG BESKYTTELSE

| Navn | CAS nr. | Referanse | Gj.snitt 8t.eksp. | Takverdi | Dato |
|--------------|----------|-----------|-------------------|------------|------|
| 1,2-etandiol | 107-21-1 | AN. | | 25 ppm, HT | |

Åndedrettsvern Ingen spesielle anbefalinger er gitt, men bruk av åndedrettsvern kan være nødvendig under uvanlige forhold med sterk luftforurensning. Gassfilter A (organiske stoffer, brunt).

Håndvern Bruk vernehansker av: Neoprengummi. Naturgummi, neopren eller PVC.

Øyevern Ved fare for sprut, bruk godkjente vernebriller eller ansiktsskjerm.

Verneklær Bruk hensiktsmessige verneklær for å beskytte mot mulig hudkontakt.

Hygieniske rutiner Vask huden ved slutten av hvert skift og før spising, røyking og bruk av toalett. Vask straks hud som er blitt våt eller tilsølt. Skift arbeidsklær daglig hvis det er mulighet for at de er tilsølt.

9. FYSISKE OG KJEMISKE EGENSKAPER

| | | | |
|--|---|-----------------------------|-----------------|
| Form/konsistens | Flytende. Væske. | | |
| Farge | Blå. | | |
| Lukt | Søtlig. | | |
| Løselighetsbeskrivelse | Lett oppløselig i vann. Lett oppløselig i: Alkoholer, | | |
| Kokepunkt (°C, intervall) | > 155 | Trykk: | 760mmHg |
| Smelte/frysepunkt (°C, intervall) | - 17 | | |
| Tetthet (g/cm³) | 1,10 - 1,13 | Temperatur (°C): | 20 |
| Damptrykk | 0,01 mmHg | Temperatur (°C): | 20 |
| pH, fortynnet løsning | 10,2-10,8 | Konsentrasjon (%_M): | 50% |
| Viskositet (intervall) | 20 - 30 cSt | Temperatur (°C): | 20 |
| Flammepunkt (°C) | > 115 | Metode: | CC-Lukket kopp. |
| Selvantennelsestemp. (°C) | > 400 | | |
| Ekspløsjongrense (%) | 3 - 15 | | |

10. STABILITET OG REAKTIVITET

Stabilitet Normalt stabil.

11. TOKSIKOLOGISKE OPPLYSNINGER

Toksisk dose, LD 50 > 2000 mg/kg (oral-rotte) (MEG)

Helsefareinformasjon HUDKONTAKT. Opptas gjennom huden. ØYEKONTAKT. Irriterende. Sprut kan skade. SVELGING. Farlig ved svelging. Tas opp i mage/tarmsystemet. Kan gi lever- og/eller nyreskade. Etylenglykol tas opp i organismen fra mage- og tarmkanalen, mindre gjennom hud og ved innånding. Den omdannes bl.a. til oxalsyre i organismen og kan medføre skade på hjernen og nyrer. Forgiftning skjer ved svelging. Akutte symptomer: Rusvirkning, munterhet, ustøhet, deretter brekninger, bevisstap og åndedrettssvikt. Forsinkede symptomer etter et par timer: tiltakende hurtig ustøhet, ånde, hurtig puls, blodtrykkstigning, kramper, bevisstløshet, nyresvikt og død.

AVSNITT 1 IDENTIFIKASJON AV STOFFET/STOFFBLANDINGEN OG SELSKAPET/FORETAKET

1.1. Produktidentifikator

Produktnavn : KEMETYL RØDSPRIT
Artikel nr. : 4730, 300660

1.2. Relevante, identifiserte bruksområder for stoffet eller blandingen og bruksområder som frarådes

Bruksmåter : Konsument produkt (SU21). Rengjøringsmiddel (PC35).

1.3. Nærmere opplysninger om leverandøren av sikkerhetsdatabladet

Leverandør : Kemetyl Norge AS
Delitoppen 3
1540 Vestby, Norge
Telefon : +47 64 98 08 00
E-mail : msds@kemetyl.com
Hjemmeside : www.kemetyl.com

1.4. Nødtelefonnummer

NØDTELEFONNUMMER, bare for DOKTORER/BRANN BRIGADE/POLITI:

NO - Telefon : +47 64 98 08 00 (Bare i kontortiden)

NØDTELEFONNUMMER:

Giftinformasjonen : +47-22 59 13 00 (Døgnet rundt)

AVSNITT 2 FAREIDENTIFIKASJON

2.1. Klassifisering av stoffet eller blandingen

CLP klassifisering (EF) nr. : Brannfarlige væsker, kategori 2. Øyeirritasjon, kategori 2. Spesifikk målorgantoksisitet – enkelteksponering kategori 3. 1272/2008

Helsefare : Gir alvorlig øyeirritasjon. Kan forårsake døsighet eller svimmelhet.
Fysiske/kjemiske risiko : Meget brannfarlig. Holdes vekk fra antenneskilder - Røyking forbudt.
Miljøfarer : Ikke klassifisert som farlig ifølge gjeldende EU-direktiv.
Andre opplysninger : Oppbevares utilgjengelig for barn. Ved svelging, kontakt lege omgående og vis denne beholderen eller etiketten.

2.2. Etikettelementer

Etikett elementer ((EF) nr. 1272/2008):

Farepiktogrammer :



Signalord : Fare

H- og P-setninger : H225 Meget brannfarlig væske og damp.
H319 Gir alvorlig øyeirritasjon.
H336 Kan forårsake døsighet eller svimmelhet.
P101 Dersom det er nødvendig med legehjelp, ha produktets beholder eller etikett for hånden.

AVSNITT 9 FYSISKE OG KJEMISKE EGENSKAPER

9.1. Opplysninger om grunnleggende fysiske og kjemiske egenskaper

| | | |
|--|--------------------|---|
| Utseende | : Flytende. | |
| Farge | : Rosa. | |
| Lukt | : Karakteristisk. | |
| Luktterskel | : Ikke kjent. | |
| pH | : Ikke anvendelig. | Nesten vannfri. |
| Vannløselighet | : Løslig. | |
| Fordelingskoeffisient (n-oktanol/vann) | : Ikke kjent. | |
| Flammepunkt | : 12 °C | |
| Antennelighet (fast stoff, gass) | : Ikke anvendelig. | Flytende. Se flammepunkt. |
| Selvantennningstemperatur | : 425 °C | |
| Kokepunkt/kokeområde | : 78 °C | |
| Smeltepunkt/smelteområde | : < -20 °C | |
| Ekspljosjonsegenskaper | : Ingen kjent. | Inneholder ikke sprengstoff. |
| Ekspljosjonsegenskaper (i luft) | : Ikke kjent. | Nedre ekspljosjonsgrense i luft (%): 2 (Propan-2-ol) |
| | : | Øvre ekspljosjonsgrense i luft (%): 19 Etanol |
| Oksidasjonsegenskaper | : Ikke anvendelig. | Inneholder ikke oksiderende stoffer. |
| Nedbrytingstemperatur | : Ikke anvendelig. | |
| Viskositet (20°C) | : Ikke kjent. | |
| Viskositet (40°C) | : Ikke relevant. | Produktet inneholder < 10% stoffer med risiko for aspirasjon. |
| Damptrykk (20°C) | : > 2300 Pa | |
| Damptetthet (20°C) | : > 1 | (luft = 1) |
| Relativ tetthet (20°C) | : 0,8 g/ml | |
| Fordampningshastighet | : < 1 | (n-butylacetate = 1) |

AVSNITT 10 STABILITET OG REAKTIVITET

10.1. Reaktivitet

Reaktivitet : Se underavsnitt nedenfor.

10.2. Kjemisk stabilitet

Stabilitet : Stabil under normale omstendigheter.

10.3. Risiko for farlige reaksjoner

Reaktivitet : Ingen farlige reaksjoner er kjent.

10.4. Forhold som må unngås

Forhold som skal unngås : Se avsnitt 7.

10.5. Materialer som må unngås

Stoffer som skal unngås : Oppbevares adskilt fra oksiderende stoffer.

10.6. Farlige nedbrytningsprodukter



SAFETY DATA SHEET

according to Regulation (EC) No. 1907/2006

Revision Date 23.04.2015

Version 3.5

SECTION 1. Identification of the substance/mixture and of the company/undertaking

1.1 Product identifier

| | |
|---------------------------|--|
| Catalogue No. | 814588 |
| Product name | 1,2-Propylene glycol diacetate for synthesis |
| REACH Registration Number | A registration number is not available for this substance as the substance or its use are exempted from registration according to Article 2 REACH Regulation (EC) No 1907/2006, the annual tonnage does not require a registration or the registration is envisaged for a later registration deadline. |
| CAS-No. | 623-84-7 |

1.2 Relevant identified uses of the substance or mixture and uses advised against

| | |
|-----------------|---|
| Identified uses | Chemical for synthesis For additional information on uses please refer to the Merck Chemicals portal (www.merckgroup.com). |
|-----------------|---|

1.3 Details of the supplier of the safety data sheet

| | |
|------------------------|--|
| Company | Merck KGaA * 64271 Darmstadt * Germany * Phone:+49 6151 72-0 |
| Responsible Department | EQ-RS * e-mail: prodsafe@merckgroup.com |

1.4 Emergency telephone number Please contact the regional company representation in your country.

SECTION 2. Hazards identification

2.1 Classification of the substance or mixture

This substance is not classified as dangerous according to European Union legislation.

2.2 Label elements

Labelling (REGULATION (EC) No 1272/2008)

Not a hazardous substance or mixture according to Regulation (EC) No. 1272/2008.

2.3 Other hazards

None known.

SECTION 3. Composition/information on ingredients

3.1 Substance

| | |
|------------|--|
| Formula | C ₇ H ₁₂ O ₄ (Hill) |
| EC-No. | 210-817-6 |
| Molar mass | 160,16 g/mol |

Remarks No disclosure requirement according to Regulation (EC) No. 1907/2006.

SAFETY DATA SHEET
according to Regulation (EC) No. 1907/2006

Catalogue No. 814588
Product name 1,2-Propylene glycol diacetate for synthesis

The protective gloves to be used must comply with the specifications of EC Directive 89/686/EEC and the related standard EN374, for example KCL 706 Lapren® (full contact), KCL 741 Dermatril® L (splash contact).

The breakthrough times stated above were determined by KCL in laboratory tests acc. to EN374 with samples of the recommended glove types.

This recommendation applies only to the product stated in the safety data sheet (>,<) supplied by us and for the designated use. When dissolving in or mixing with other substances and under conditions deviating from those stated in EN374 please contact the supplier of CE-approved gloves (e.g. KCL GmbH, D-36124 Eichenzell, Internet: www.kcl.de).

Respiratory protection

required when vapours/aerosols are generated.

Recommended Filter type: Filter A (acc. to DIN 3181) for vapours of organic compounds

The entrepreneur has to ensure that maintenance, cleaning and testing of respiratory protective devices are carried out according to the instructions of the producer. These measures have to be properly documented.

Environmental exposure controls

Do not let product enter drains.

SECTION 9. Physical and chemical properties

9.1 Information on basic physical and chemical properties

| | |
|-----------------------------|------------------------------|
| Form | liquid |
| Colour | colourless |
| Odour | weak |
| Odour Threshold | No information available. |
| pH | No information available. |
| Melting point | No information available. |
| Boiling point/boiling range | 190 - 191 °C at 1.013 hPa |
| Flash point | 87 °C |
| Evaporation rate | No information available. |
| Flammability (solid, gas) | No information available. |
| Lower explosion limit | 2,8 %(V) |
| Upper explosion limit | 12,7 %(V) |
| Vapour pressure | < 1 hPa at 20 °C |
| Relative vapour density | No information available. |

SAFETY DATA SHEET
according to Regulation (EC) No. 1907/2006

Catalogue No. 814588
Product name 1,2-Propylene glycol diacetate for synthesis

| | |
|--|--|
| Density | 1,05 g/cm ³ at 20 °C |
| Relative density | No information available. |
| Water solubility | 90 g/l at 20 °C |
| Partition coefficient: n-octanol/water | log Pow: 0,82 (calculated) (Lit.) Bioaccumulation is not expected. |
| Auto-ignition temperature | No information available. |
| Decomposition temperature | > 170 °C |
| Viscosity, dynamic | 3,0 mPa.s at 20 °C |
| Explosive properties | Not classified as explosive. |
| Oxidizing properties | none |

9.2 Other data

Ignition temperature 431 °C

SECTION 10. Stability and reactivity

10.1 Reactivity

Forms explosive mixtures with air on intense heating.
A range from approx. 15 Kelvin below the flash point is to be rated as critical.

10.2 Chemical stability

The product is chemically stable under standard ambient conditions (room temperature) .

10.3 Possibility of hazardous reactions

Violent reactions possible with:
Strong oxidizing agents

10.4 Conditions to avoid

Strong heating.

10.5 Incompatible materials

no information available

10.6 Hazardous decomposition products

no information available

Appendix B

Duratherm 630

Duratherm 630 is the oil we have used throughout the experiments. It is a high performance fluid that is efficient as well as environmentally friendly. The properties of the oil together with its safety data sheet can be found in this appendix.

OVERVIEW

Duratherm 630 is a high performance, efficient and environmentally friendly fluid engineered for applications requiring high temperature stability to 630°F. Offering precise temperature control it's a great alternative to high temperature aromatic fluids, at a fraction of the cost.

It is ideal for a wide range of applications including, high temperature batch processing, chemical reactions, pharmaceutical and resin manufacturing among others.

APPLICATION

Duratherm 630 is a high performance, efficient and environmentally friendly fluid engineered for applications requiring high temperature stability to 630°F. Offering precise temperature control it's a great alternative to high temperature aromatic fluids, at a fraction of the cost.

It is ideal for a wide range of applications including, high temperature batch processing, chemical reactions, pharmaceutical and resin manufacturing among others.

THE DIFFERENCE

Our exclusive additive package, including a proprietary dual stage anti-oxidant, ensures long trouble free operation. Duratherm also incorporates metal deactivators, a seal and gasket extender, de foaming and particle suspension agents.

LASTS LONGER

In the heat transfer fluid industry cost is always a concern, however fluid longevity and resistance to harmful fouling are of equal importance. Air contact is normally detrimental to a fluid. Oxidation can cripple your system and if left unchecked will ultimately cause catastrophic failure. Unscheduled downtime due to oil failure has a high cost and negative effect on production.

The Duratherm product line was developed with this in mind. Most other fluids fall short in their protection from oxidation and can quickly foul a system. Duratherm is engineered to give unsurpassed levels of protection and service life.

RUNS CLEANER

In our effort to truly service the heat transfer industry, we have developed unique and specific heat transfer system cleaners.

Ranging from preventative maintenance system cleaners to emergency downtime system revivers, we have a cleaner that fits your needs and schedule.

ENVIRONMENTAL

Duratherm 630 is environmentally friendly, non-toxic, non-hazardous and non-reportable. Worker health and safety is of great concern, **Duratherm 630** poses no ill effect to worker safety. After its long service life it can easily be disposed of with other waste oils.

DURATHERM 630 PROPERTIES

| | | |
|---|--------------------------|----------------|
| Appearance: colorless, clear and bright liquid | | |
| Maximum Bulk/Use Temp.* | 630°F | 332°C |
| Flash Point ASTM D92 | 444°F | 229°C |
| Fire Point ASTM D92 | 472°F | 244°C |
| Autoignition ASTM E-659-78 | 693°F | 368°C |
| Viscosity ASTM D445 | | |
| cSt at 104°F / 40°C | 36.2 | |
| cSt at 212°F / 100°C | 7.0 | |
| cSt at 600°F / 316°C | 0.7 | |
| Pour Point ASTM D97 | -1°F | -18°C |
| Density ASTM D1298 | | |
| | lb/ft³ | g/ml |
| at 100°F / 38°C | 52.8 | 0.845 |
| at 500°F / 260°C | 43.4 | 0.695 |
| at 600°F / 316°C | 41.2 | 0.658 |
| Average Molecular Weight | | |
| | 395 | |
| Carbon Residue ASTM D189 | 0.005 | % Mass |
| Sulphur Content X-RAY | <.001 | weight % |
| CU Strip Corrosion ASTM D130 | 1a | |
| Thermal Expansion Coefficient | | |
| | 0.0562 %/°F | 0.1011 %/°C |
| Thermal Conductivity | | |
| | BTU/hr F ft | W/m.K |
| at 100°F / 38°C | 0.082 | 0.141 |
| at 500°F / 260°C | 0.075 | 0.130 |
| at 600°F / 316°C | 0.074 | 0.128 |
| Heat Capacity | | |
| | BTU/lb F | kJ/kg K |
| at 100°F / 38°C | 0.471 | 1.971 |
| at 500°F / 260°C | 0.645 | 0.645 |
| at 600°F / 316°C | 0.685 | 2.876 |
| Vapor Pressure ASTM D2879 | | |
| | psia | kPa |
| at 100°F / 38°C | 0.00 | 0.00 |
| at 500°F / 260°C | 0.83 | 2.68 |
| at 600°F / 316°C | 1.64 | 11.30 |
| Distillation Range ASTM D2887 | | |
| | 10% | 727°F (386°C) |
| | 90% | 902°F (483°C) |
| *Maximum Film Temp. | 670°F | 354°C |

The values quoted are typical of normal production. They do not constitute a specification.

Material Safety Data Sheet

according to 1907/2006 EC, Article 31

Duratherm 630 High Temperature Heat Transfer Fluid

Revision Date: 02/2013
 Revision #: 1

1. IDENTIFICATION OF THE SUBSTANCE / PREPARATION AND THE COMPANY

| | |
|----------------------------|--|
| Product Name | Duratherm 630 - High Temperature Heat Transfer Fluid |
| Company Name | Duratherm Extended Life Fluids P.O. Box 563, Lewiston, NY 14092 |
| Telephone | 800-446-4910 |
| Fax | 905-984-6684 |
| Website | www.heat-transfer-fluid.com |
| Emergency telephone number | 800-446-4910 |

2. HAZARDS IDENTIFICATION

| | |
|--------------------|--|
| Physical State | Viscous Liquid |
| Odor | Very slight hydrocarbon odor |
| HMIS (Canada) | Not controlled under HMIS (Canada) |
| OSHA/HCS Status | This material is not considered hazardous by OSHA Hazard Communication Standard (29 CFR 1910.1200. Refer to and retain this MSDS for safety and handling information |
| Emergency Overview | No specific hazard |
| Routes of Enter | Dermal contact, eye contact, inhalation, ingestion |

Potential Acute Health Effect

| | |
|------------|--|
| Inhalation | No known significant effects or critical hazards |
| Ingestion | No known significant effects or critical hazards |
| Skin | No known significant effects or critical hazards |
| Eyes | No known significant effects or critical hazards |

Potential Chronic Health Effect

| | |
|---------------------|--|
| Chronic Effects | No known significant effects or critical hazards |
| Carcinogenicity | Not listed as a carcinogenic by OSHA, NTP, or IARC |
| Mutagenicity | No known significant effects or critical hazards |
| Teratogenicity | No known significant effects or critical hazards |
| Development Effects | No known significant effects or critical hazards |
| Fertility Effects | No known significant effects or critical hazards |

| | |
|---|--|
| Medical Conditions Aggravated by Overexposure | Repeated or prolonged exposure with spray or mist may produce chronic eye irritation and severe skin irritation. Repeated skin exposure can produce local skin destruction or dermatitis |
|---|--|

3. COMPOSITION / INFORMATION ON INGREDIENTS

Name: Mixture of severely hydrotreated and hydrocracked hydrocarbons **CAS#:** 178603-65-1

There are no additional ingredients present which, within the current knowledge of the supplier and in the concentrations applicable, are classified as hazardous to health or the environment and hence require reporting in this section

4. FIRST AID MEASURES

| | |
|--------------|--|
| Skin contact | Wash affected areas thoroughly with soap and water. Wash contaminated clothing before reuse. See medical attention if irritation or symptoms persist |
| Eye contact | Flush with clean, lukewarm water (low pressure) occasionally lifting eyelids. Seek physician assessment if eyes are inflamed. |
| Inhalation | Avoid breathing oil mists. Remove to fresh air. Give artificial respiration if not breathing. Oxygen may be given by qualified personnel if breathing is difficult. Get medical attention. |
| Ingestion | Do not induce vomiting. Force fluid. Has laxative effect. |

5. FIRE FIGHTING MEASURES

| | |
|----------------------|--|
| Extinguishing media | For small fires: Carbon dioxide (CO2) Dry chemical. Foam. Water spray. |
| Fire hazards | LOW FIRE HAZARD - Do not cut, drill, or weld empty containers |
| Protective equipment | Wear suitable respiratory equipment when necessary. |

6. ACCIDENTAL RELEASE MEASURES

| | |
|---------------------------|---|
| Personal precautions | Ensure adequate ventilation of the working area. |
| Environmental precautions | Do not allow product to enter drains. Prevent further spillage if safe. |
| Clean up method | Absorb with inert, absorbent material. Transfer to suitable, labelled containers for disposal. Clean spillage area thoroughly with plenty of water. |

7. HANDLING AND STORAGE

| | |
|----------|--|
| Handling | Avoid contact with eyes and skin. Ensure adequate ventilation of the working area. Adopt best Manual Handling considerations when handling, carrying and dispensing. |
| Storage | Keep in a cool, dry, well ventilated area. Keep containers tightly closed. Store in correctly labelled containers. Store at a maximum of 40°C. |

8. EXPOSURE CONTROLS / PERSONAL PROTECTION

| | |
|------------------------------|--|
| Engineering measures | Ensure adequate ventilation of the working area. |
| Occupational exposure contd. | Keep away from food, drink and animal feed. |
| Respiratory protection | Normally not necessary. If mist is generated, wear approved organic vapor respirator suitable for oil mist areas with sufficient oxygen. |
| Skin/Hand Protection | Normally none required, for direct contact of more than 2 hours, PVC, Viton, or Nitrile gloves are recommended. |
| Eye protection | Normally none required, chemical goggles if splashing is likely or high pressure systems are used. |
| Ventilation | General ventilation |
| Exposure limits | <u>Practically non-toxic</u> ACGIH TL (United States). Notes: (Oil Mist) TWA: 5mg/m ³ , 8 hour(s) / STEL: 10 mg/m ³ 15 minute(s) |
| Protective equipment | Protect clothing from contact with the product. |

9. PHYSICAL AND CHEMICAL PROPERTIES

| | |
|------------------------|------------------------------|
| Description | Liquid |
| Color | Clear liquid |
| Odor | Very slight hydrocarbon odor |
| Boiling point | >570°F (>298°C) |
| Flash point | >430°F (>221°C) |
| Vapor pressure | <0.003 kPa @ 25°C |
| Specific Gravity | 0.84 - 0.92 |
| Volatiles, % Volume | 0% |
| Solubility in water | Negligible |
| Evaporation rate | Nil |
| Viscosity @40 °C (cSt) | Varies depending on grade |

10. STABILITY AND REACTIVITY

| | |
|--------------------------|---|
| Stability | Stable under normal conditions. |
| Hazardous polymerization | Will not occur |
| Materials to avoid | Strong oxidizing agents. |
| Decomposition products | Analogous compounds evolve, carbon monoxide, carbon dioxide, and other undefined fragments. |

11. TOXICOLOGICAL INFORMATION

| | |
|---------|--|
| General | <p>Acute Toxicity (LD₅₀): LD₅₀ (oral, rabbit): > 5000 mg/kg LD₅₀ (dermal, rat): > 2000 mg/kg LD₅₀ (inhalative, rat): > 2500 mg/kg/4h</p> |
| Other | <p>In case of inhalation: no data available Skin contact: no data available Eye contact: no data available Ingestion: no data available Irritation: skin and eye irritating Sensitization: no sensitizing effects known Subacute toxicity: Intensive or prolonged exposition. Repeated or prolonged exposure with spray or mist may product chronic eye irritation and severe skin irritation. Repeated skin exposure can produce local skin destruction or dermatitis. Chronic Toxicity: not available Subchronic Exposure: not available Specific symptoms observed in animal studies: no data available CMR Effects: Carcinogenity: no data available Reproductive toxicity: no data available Mutagenicity: no data available Summarized evaluation of the CMR properties: not available</p> |

12. ECOLOGICAL INFORMATION

| | |
|------------------------|---|
| Ecological Information | <p>Do not allow to enter sewer/soil/surface or ground water Check with local laws and regulations regarding disposal Ecological Information: LC50 (Rainbow Trout): > 100 000 MG/1/96 h Mobility: no data available Persistence and biodegradation: Inherently biodegradable in aerobic conditions. Check with local laws and regulations regarding disposal Bioaccumulation potential: no data available Results of PBT assessments: no data available Other adverse side effects: no data available</p> |
|------------------------|---|

13. DISPOSAL CONSIDERATIONS

| | |
|---------------------|--|
| General information | <p>Used product must be disposed of in accordance with Federal, State, and Local environmental control regulations. Incineration is preferred. DO NOT HEAT OR CUT EMPTY CONTAINER WITH ELECTRIC OR GAS TORCH.</p> |
|---------------------|--|

14. TRANSPORTATION INFORMATION

| | |
|---------------------|--|
| Technical Name | Paraffinic Hydrocarbon |
| D.O.T. hazard class | Not regulated |
| U.N. N.A. # | Not regulated |
| Product label | Duratherm 630 - Duratherm High Temperature Heat Transfer Fluid |

15. REGULATORY INFORMATION

| | |
|-------------------|--|
| EU Risk phrases | NSH - No Significant Hazard This product is not classified according to EU regulations |
| HMIS | Not controlled under HMIS (Canada) |
| EC Classification | Not classified as dangerous under EC classifications |
| EC Symbols | Not classified |
| OSHA status | Non Hazardous under 29 CFR 1910.1200 |
| TSCA status | All components are listed on TSCA Inventory |
| RCRA status | If discarded in its purchased form this product would not be a hazardous waste either by listing or characteristic. However it is the responsibility of the product user to determine at the time of disposal, whether the material being disposed of is a hazardous waste (40 CFR 261.20-24). |
| Other Information | Environmental Protection Act 1990 (as amended). Health and Safety at Work Act 1974. Consumers Protection Act 1987. Control of Pollution Act 1974. Environmental Act 1995. Factories Act 1961. Carriage of Dangerous Goods by Road and Rail (Classification, Packaging and Labelling) Regulations. Chemicals (Hazard Information and Packaging for Supply) Regulations 2002. Control of Substances Hazardous to Health Regulations 1994 (as amended). Road Traffic (Carriage of Dangerous Substances in Packages) Regulations. Merchant Shipping (Dangerous Goods and Marine Pollutants) Regulations. Road Traffic (Carriage of Dangerous Substances in Road Tankers in Tank Containers) Regulations. Road Traffic (Training of Drivers of Vehicles Carrying Dangerous Goods) Regulations. Reporting of Injuries, Diseases and Dangerous. Other Regulations. Health and Safety (First Aid) Regulations 1981. Personal Protective Equipment (EC Directive) Regulations 1992. Personal Protective Equipment at Work Regulations 1992. |

HMIS status

| | |
|---------------------|---|
| Health Hazard | ① |
| Fire Hazard | ① |
| Reactivity | ① |
| Personal Protection | Ⓑ |

NFPA (U.S.A.)



Rating 0= Insignificant,
1=Slight,
2=Moderate,
3= High,
4= Extreme

16. OTHER INFORMATION

| | |
|---------------------|---|
| Further information | This information is furnished without warranty, expressed or implied, except that it is accurate to the best knowledge of Duratherm Extended Life Fluids. The data on this sheet related only to the specific material designed herein. Duratherm Extended Life Fluids assumes no legal responsibility for the use or reliance upon these data. |
|---------------------|---|

Appendix C

Weldon Racing Pumps

The pump used in the oil circulating system setup was a Weldon racing pump. It is an oil transfer pump from the 9200-A series, designed to handle high oil temperatures. Further information regarding the pump and its features is available in this appendix.



NEW PRODUCT RELEASE

Weldon Racing Pumps introduces the 9200-A series external oil transfer pump.



Weldon's 9200-A oil transfer pump circulates hot oil in transmissions and differentials and has been designed to meet the demanding rigors of racing and OEM applications. They have been manufactured using the same stringent quality requirements and exacting specifications as Weldon's aerospace fuel pumps.

Although very few are willing to divulge the information, the 9200-A is presently being used on a number of front runners' superspeedway cars in Cup and Nationwide series. In fact, it is the only pump known to be used in circle track racing for transmission and differential cooling.

Product Features:

- 1) Internal Relief Valve prevents system damage. The valve is designed to lift sufficiently to relieve fluid pressure build-up over setting. These valves help protect vessel and piping system damage from over pressurization. To ensure that oil pressure does not exceed the rated maximum, a spring-loaded pressure relief valve routes oil back to its source once pressure exceeds a preset limit.
- 2) Pumps are 100 percent serviceable/repairable
- 3) Internal components are 100 percent metallic—no plastics or composite materials are used
- 4) Compatible with all types of hot oils
- 5) Resistant to contamination
- 6) Blades self-compensating for wear
- 7) Flow rate for the 9200-A is 30 gallons per hour of 300-degree F 80-90W differential gear oil or ATF
- 8) Current draw of only 5.5 amps
- 9) Compact and lightweight: weighs 3 pounds and measures 2.50x5.40-inches



Price: The Weldon 9200-A fluid pump retails for \$390

Availability: Ready for immediate delivery.

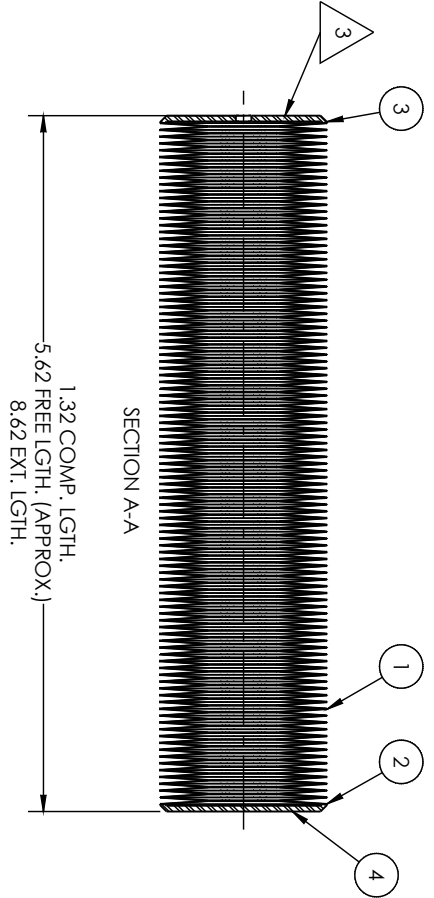
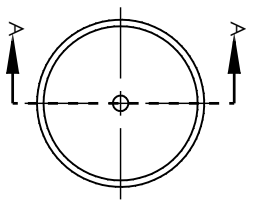
Applications: Approved for use by GM in export C5 and C6 Corvettes destined for warmer climates. Weldon is also working on a prototype high-temperature oil transfer pump for the new Cadillac CTS-V. This pump can be found in the GM Motorsports catalog under PN 12480080.

For further information contact: Weldon Racing Pumps 640 Golden Oak Parkway, Oakwood Village, Ohio 44146 Telephone (440) 232-2282 or visit www.WeldonRacing.com

Appendix D

The Bellows

A technical drawing of the bellows is available in this appendix.



| BELLAWS DATA | |
|--------------|---------|
| DIE | 9196 |
| O.D. | 1.350 |
| I.D. | .540 |
| MATL | 347 SST |
| THK. | .003 |
| CONVS | 100 |
| STROKE | 7.30 |

- ASSEMBLY NOTES:**
- LEAK CHECK ASS'Y TO 1X10-9 STD CC/SEC. OF He.
 - LIFE: 10,000 CYCLES W/ VACUUM, INTERNAL AND ATMOSPHERE, EXTERNAL.
 - ELECTROETCH: METAL FLEX, P/N, (DATE), USA, AND JOB NO..
 - BELLAWS CORE TO BE WELDED PER METAL FLEX SPEC S-6000.

CONTROLLED

THE INFORMATION CONTAINED IN THIS DRAWING IS THE SOLE PROPERTY OF METAL FLEX, INC. ANY REPRODUCTION IN PART OR AS A WHOLE WITHOUT THE WRITTEN PERMISSION OF METAL FLEX, INC. IS PROHIBITED. THIS DOCUMENT SHALL BE RETURNED UPON REQUEST.

| ITEM NO. | DESCRIPTION | QTY. | MATERIAL |
|----------|-------------------------|------|----------|
| 1 | BELLAWS CORE (SEE DATA) | 1 | 347 SST |
| 2 | DBL'S | 2 | 347 SST |
| 3 | BORED B-STYLE | 1 | 304 SST |
| 4 | B-STYLE | 1 | 304 SST |

| | | |
|---------|-----|-----------|
| DRAWN | MRC | 5/18/2015 |
| DESIGN | JLR | 5/19/2015 |
| CHECK | DEH | 5/19/2015 |
| APPROV. | RTG | 5/19/2015 |

UNLESS OTHERWISE SPECIFIED:

DIMENSIONS ARE IN INCHES
 DECIMALS ±.010
 DECIMALS .XXX ±.005
 FRACTIONAL 1/64
 ANGULAR 1°

CUSTOMER: NORWEGIAN UNIVERSITY OF SCIENCE AND TECHNOLOGY
 CUST. P/N DWG NO. 13554BB-10 (MOD.)

MEX NO.

FED. ID. NO.: THS33

SCALE: 1:1 OR AS NOTED



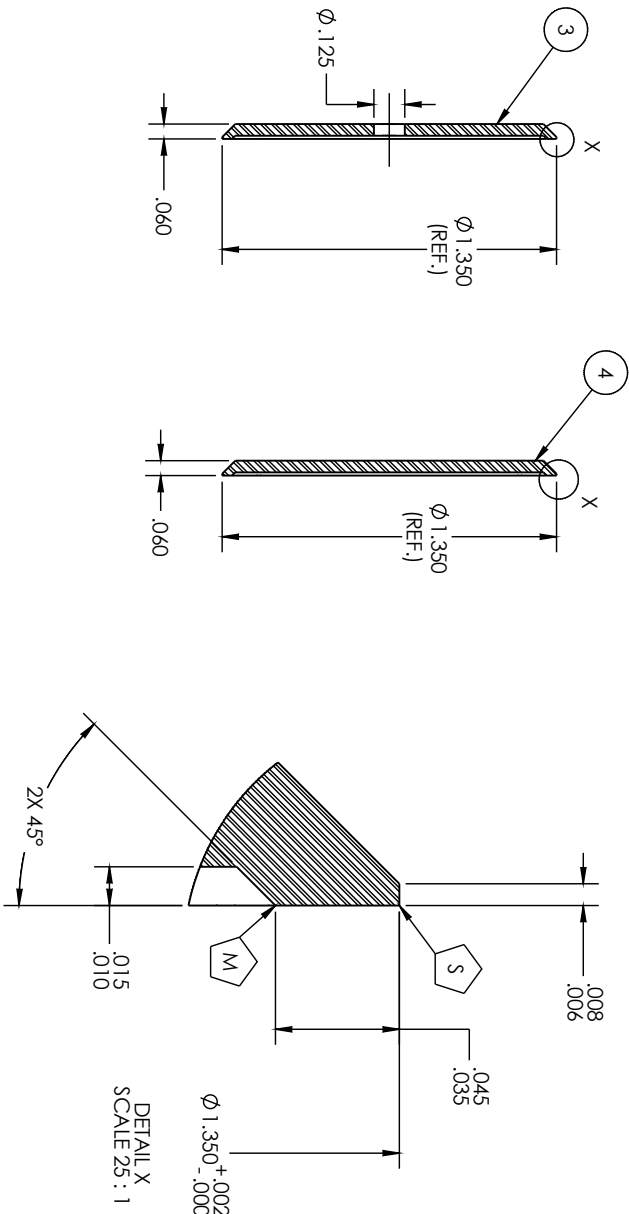
8 7 6 5 4 3 2

WEIGHT (LBS) :

MAX SIZE B Sheet 1 OF 2

B 30656
 DWG. NO.

REV.



- MACHINE NOTES:
 (UNLESS OTHERWISE SPECIFIED)
- BREAK EDGES .010/.020
 - FILLETS .005/.030
 - DIAMETERS .005 TIR.
 - FACES .005 //.
 - S** SHARP CORNER, NO BURR .001 R MAX.
 - B** BREAK .005/.010.
 - M** BREAK .005 MAX.
 - R** .003/.005 R
6. MACHINE SURFACES TO $\sqrt{32}$ FINISH EXCEPT WHERE NOTED.
7. PARTS TO BE FREE OF ALL OILS AND CHIPS UPON COMPLETION OF MACHINING PROCESS.
8. SEALING SURFACE, PROTECT FROM NICKS, DENTS, AND SCRATCHES.

| ITEM NO. | DESCRIPTION | QTY. | MATERIAL |
|----------|---------------|------|----------|
| 3 | BORED B-STYLE | 1 | 304 SST |
| 4 | B-STYLE | 1 | 304 SST |

| | | |
|---------|-----|-----------|
| DRAWN | MRC | 5/18/2015 |
| DESIGN | JLR | 5/19/2015 |
| CHECK | DEH | 5/19/2015 |
| APPROV. | RTG | 5/19/2015 |

UNLESS OTHERWISE SPECIFIED:

DIMENSIONS ARE IN INCHES
 DECIMALS TO $\pm .010$
 FRACTIONAL $1/64$
 ANGULAR 1°

CUSTOMER: NORWEGIAN UNIVERSITY OF SCIENCE AND TECHNOLOGY
 CUST. P/N DWG. NO. 13554BB-10 (MOD.)

MEX. NO.

FED. ID. NO.: TH533

SCALE: 2:1 OR AS NOTED



CONTROLLED

THE INFORMATION CONTAINED IN THIS DRAWING IS THE SOLE PROPERTY OF METAL FLEX, INC. ANY REPRODUCTION IN PART OR AS A WHOLE WITHOUT THE WRITTEN PERMISSION OF METAL FLEX, INC. IS PROHIBITED. THIS DOCUMENT SHALL BE RETURNED UPON REQUEST.

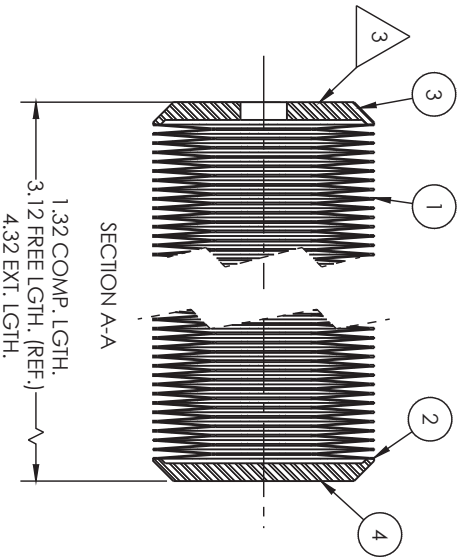
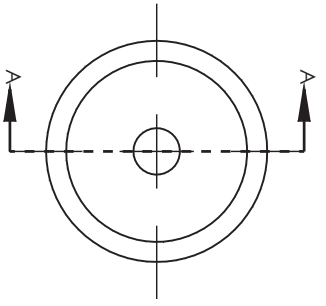
WEIGHT (LBS) :

8 7 6 5 4 3 2 1

Appendix E

The Gas Bellows

A technical drawing of the gas bellows is available in this appendix.



| BELLOWS DATA | |
|----------------|---------|
| DIE | 172 |
| O.D. | .595 |
| I.D. | .258 |
| MATL | 347 SST |
| THK. | .0025 |
| CONV'S | 120 |
| FULL STROKE | 3.00 |
| WORKING STROKE | 1.20 |

- ASSEMBLY NOTES:**
1. LEAK CHECK ASS'Y TO 1X10-9 STD CC/SEC. OF He.
 2. LIFE: 10,000 CYCLES W/ VACUUM TO 2 PSID, INTERNAL AND ATMOSPHERE, EXTERNAL.
 3. VIBROPEEN: JOB NO..
 4. BELLOWS CORE TO BE WELDED PER METAL FLEX SPEC S-6000.

CONTROLLED

THE INFORMATION CONTAINED IN THIS DRAWING IS THE SOLE PROPERTY OF METAL FLEX, INC. ANY REPRODUCTION IN PART OR AS A WHOLE WITHOUT THE WRITTEN PERMISSION OF METAL FLEX, INC IS PROHIBITED. THIS DOCUMENT SHALL BE RETURNED UPON REQUEST.

WEIGHT (LBS) :

| ITEM NO. | DESCRIPTION | QTY. | MATERIAL |
|----------|-------------------------|------|----------|
| 1 | BELLOWS CORE (SEE DATA) | 1 | 347 SST |
| 2 | DBL S | 2 | 347 SST |
| 3 | BORED B-STYLE | 1 | 304 SST |
| 4 | BLANK B STYLE | 1 | 304 SST |

| | | |
|---------|-----|-----------|
| DRAWN | MRC | 2/18/2016 |
| DESIGN | JRH | 2/22/2016 |
| CHECK | DEH | 2/22/2016 |
| APPROV. | RTG | 2/22/2016 |

UNLESS OTHERWISE SPECIFIED:

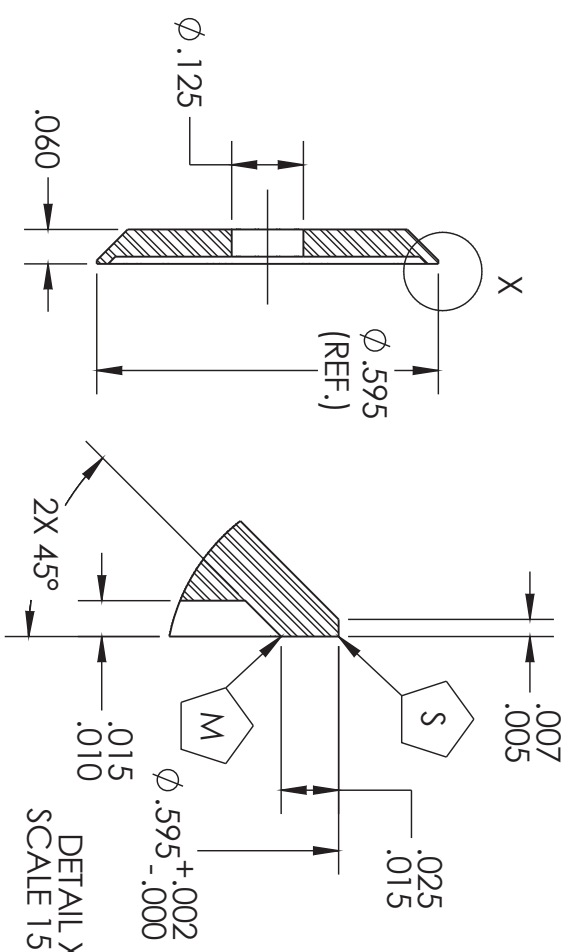
DIMENSIONS ARE IN INCHES
 DECIMALS TO **±.010**
 DECIMAL XXX **±.005**
 FRACTIONAL **1/64**
 ANGULAR **1°**

CUSTOMER: NORWEGIAN UNIVERSITY OF SCIENCE AND TECHNOLOGY
 CUST. P/N DWG NO. 059268BB-12 (MOD.)

METAL FLEX
 WEIDED BELLOWS, INC.
 NEWPORT, VT 05855 www.metalflexbellows.com

FED. ID. NO.: THS33
 MEX NO.
 SCALE: 3:1 OR AS NOTED

MAX SIZE B Sheet 1 OF 3



DETAIL X
 SCALE 15 : 1

- MACHINE NOTES: (UNLESS OTHERWISE SPECIFIED).
1. BREAK EDGES .010/.020
 2. FILETS .005/.030.
 3. DIAMETERS .005 TIR.
 4. FACES .005 //.
 5. **S** SHARP CORNER, NO BURR .001 R MAX.

- B** BREAK .005/.010.
- M** BREAK .005 MAX.
- R** .003/.005 R
- U** UNDERCUT RADIUS TO ACCEPT SHARP CORNER.

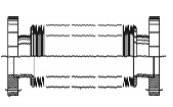
6. MACHINE SURFACES TO \sqrt{c} FINISH EXCEPT WHERE NOTED.
7. PARTS TO BE FREE OF ALL OILS AND CHIPS UPON COMPLETION OF MACHINING PROCESS.

| ITEM NO. | DESCRIPTION | QTY. | MATERIAL |
|----------|---------------|------|----------|
| 3 | BORED B-STYLE | 1 | 304 SST |

| | | |
|---------|-----|-----------|
| DRAWN | MRC | 2/18/2016 |
| DESIGN | JJR | 2/22/2016 |
| CHECK | DEH | 2/22/2016 |
| APPROV. | RTG | 2/22/2016 |

UNLESS OTHERWISE SPECIFIED:

DIMENSIONS ARE IN INCHES
TOLERANCES:
 DECIMAL .XX ±.010
 DECIMAL .XXX ±.005
 FRACTIONAL 1/64
 ANGULAR 1°



METAL FLEX
WELDED BELLOWS, INC.
 NEWPORT, VT 05855 www.metalflexbellows.com

CUSTOMER NORWEGIAN UNIVERSITY OF SCIENCE AND TECHNOLOGY

CUST. P/N/DWG. NO. 05926BB-12 (MOD.)

MFX NO.

FED. ID. NO.: 1HS33

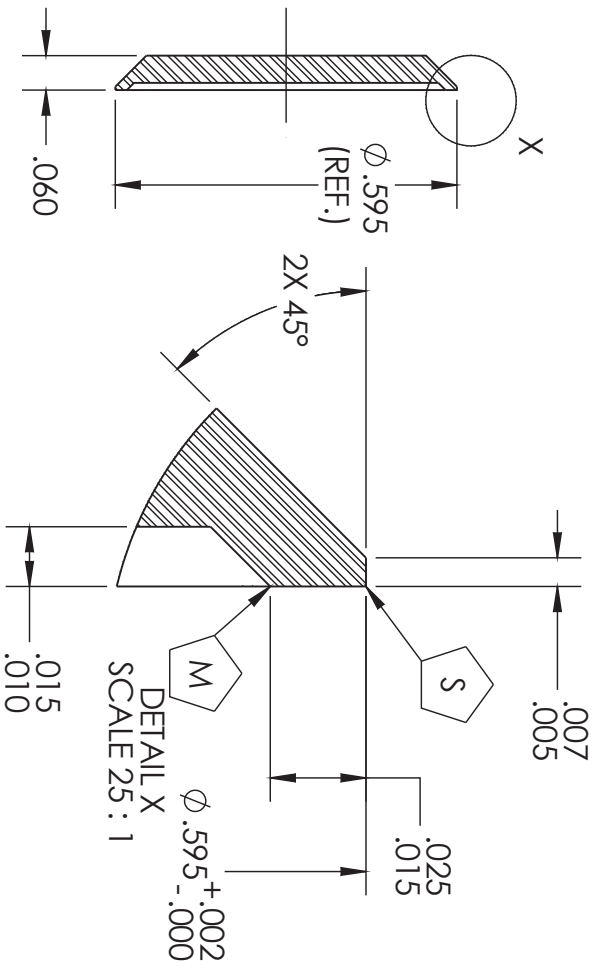
31499-3

WG. NO

REV.

CONTROLLED

WEIGHT (LBS) :
 THE INFORMATION CONTAINED IN THIS DRAWING IS THE SOLE PROPERTY OF METAL FLEX INC. ANY REPRODUCTION IN PART OR AS A WHOLE WITHOUT THE WRITTEN PERMISSION OF METAL FLEX INC. IS PROHIBITED. THIS DOCUMENT SHALL BE RETURNED UPON REQUEST.



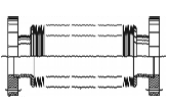
1. MACHINE NOTES: (UNLESS OTHERWISE SPECIFIED).
2. BREAK EDGES .010/.020
3. FILETS .005/.030.
4. DIAMETERS .005 TIR.
5. FACES .005 //.
6. **S** SHARP CORNER, NO BURR .001 R MAX.
7. **B** BREAK .005/.010.
8. **R** BREAK .003/.005 R.
9. **M** BREAK .005 MAX.
10. **U** UNDERCUT RADIUS TO ACCEPT SHARP CORNER.
11. MACHINE SURFACES TO $\sqrt{32}$ FINISH EXCEPT WHERE NOTED.
12. PARTS TO BE FREE OF ALL OILS AND CHIPS UPON COMPLETION OF MACHINING PROCESS.

| ITEM NO. | DESCRIPTION | QTY. | MATERIAL |
|----------|---------------|------|----------|
| 4 | BLANK B STYLE | 1 | 304 SST |

| | | |
|---------|-----|-----------|
| DRAWN | MRC | 2/18/2016 |
| DESIGN | JJR | 2/22/2016 |
| CHECK | DEH | 2/22/2016 |
| APPROV. | RTG | 2/22/2016 |

UNLESS OTHERWISE SPECIFIED:

DIMENSIONS ARE IN INCHES
TOLERANCES:
 DECIMAL .XX ±.010
 DECIMAL .XXX ±.005
 FRACTIONAL 1/64
 ANGULAR 1°



METAL FLEX
WELDED BELLOWS, INC.
 NEWPORT, VT 05855 www.metalflexbellows.com

CUSTOMER NORWEGIAN UNIVERSITY OF SCIENCE AND TECHNOLOGY

CUST. P/N/DWG. NO. 05926BB-12 (MOD.)

MFX NO.

FED. I.D. NO.: 1HS33

1499-4

G. NO

REV.

CONTROLLED

WEIGHT (LBS) :

THE INFORMATION CONTAINED IN THIS DRAWING IS THE SOLE PROPERTY OF METAL FLEX INC. ANY REPRODUCTION IN PART OR AS A WHOLE WITHOUT THE WRITTEN PERMISSION OF METAL F PROHIBITED. THIS DOCUMENT SHALL BE RETURNED UPON REQUEST.

5

4

A

B

C

A

B

C

Appendix F

The Solenoid

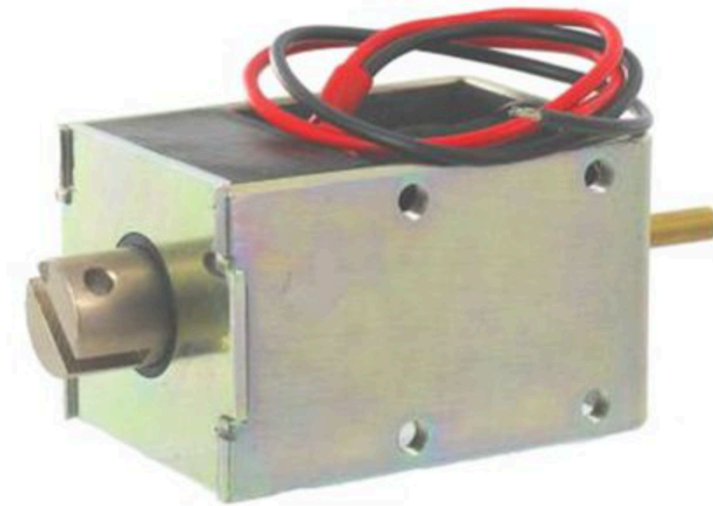
Further information regarding the solenoid can be found available in this appendix.

Push Pull Action DC D-Frame Solenoid, 20mm Stroke, 80W, 12 V dc

RS-lagernummer **307-3708**

Produsent **Mecalectro**

Producentens varenummer **8.MB5 02 29 12 VCC 80W**



Produktdetaljer

8.MB series maintained linear electromagnets

3 sizes available, each in several versions.

Pulse supply. Core activates when powered up (+ red wire); held in retract position by magnetic locking, with power off. Unlocks by reverse polarity with a minimum pulse of 50 → 100 ms.

Linked to a return system (spring, earth, etc.), this type of electromagnet ensures 2 stable positions with the power off (bistable).

Recommended for applications requiring 2 stable states without consumption. For example: mechanical memory function, improving the service life of battery-powered systems.

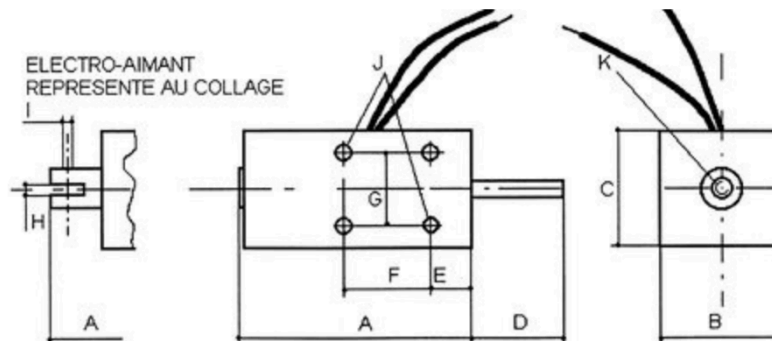
| |
|-------------------------|
| Thermal class B (130°C) |
|-------------------------|

| |
|---|
| Connected by 2 x 200-mm long insulated cables |
|---|

| Stock | | release | power | Travel C | F to C nom. |
|----------|-----------|---------|----------------|-----------|-------------|
| no. | Model | rating | Inrush/outrush | max./nom. | / holding |
| 379-4051 | Pull/push | 12 V dc | 15 W/0.5 W | 9/5 mm | *1 N/3.5 N |
| 379-4067 | Pull/push | 24 Vdc | 15 W/0.5 W | 9/5 mm | *1 N/3.5 N |
| 307-3657 | Pull/push | 12 V dc | 40 W/2.5 W | 13/5 mm | 12.5 N/35 N |
| 307-3663 | Pull/push | 24 Vdc | 40 W/2.5 W | 13/5 mm | 12.5 N/35 N |
| 307-3708 | Pull/push | 12 V dc | 80 W/2 W | 25/10 mm | 26 N/60 N |
| 307-3714 | Pull/push | 24 Vdc | 80 W/2 W | 25/10 mm | 26 N/60 N |

*Electromagnet fitted with a return spring whose force should be deducted from the values shown

| Stock | dimensions (mm) | | | | | | | | | | |
|----------|-----------------|------|------|----|-----|------|------|-----|-----|-------|----|
| no. | A | B | C | D | E | F | G | H | W | J | K |
| 379-4051 | 36 | 12.7 | 10 | 9 | 6.5 | 17 | 6 | - | - | M2 | M3 |
| 379-4067 | 36 | 12.7 | 10 | 9 | 6.5 | 17 | 6 | - | - | M2 | M3 |
| 307-3657 | 55 | 31.8 | 25.4 | 26 | 7.7 | 19 | 17.4 | 3.6 | 3.2 | M4 to | - |
| 307-3663 | 55 | 31.8 | 25.4 | 26 | 7.7 | 19 | 17.4 | 3.6 | 3.2 | M4 to | - |
| 307-3708 | 79.5 | 48.8 | 41.3 | 25 | 11 | 28.6 | 31.7 | 3.6 | 4 | M5 to | - |
| 307-3714 | 79.5 | 48.8 | 41.3 | 25 | 11 | 28.6 | 31.7 | 3.6 | 4 | M5 to | - |



Appendix G

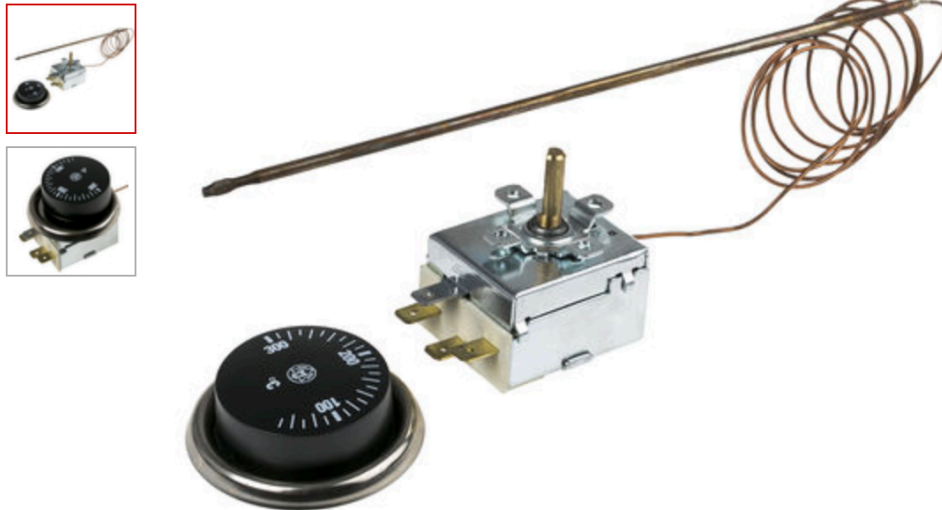
Capillary Thermostat

Further information regarding the capillary thermostat that can be used together with the solenoid is available in this appendix.

RS Pro SPDT 16 A Thermostat, +50°C +300°C

RS Stock No. 733-4729

Brand RS Pro



Product Details

Adjustable Capillary & Safety Limit Thermostats

Capillary Thermostats which operate from a remote bulb linked with a 1m capillary, changeover contacts (SPDT) enable use with both heating and cooling loads. Supplied with chrome mounting bezel and knob
0 to 300 °C Thermostat also has an OFF position

Safety Limit Thermostat (stock no. 733-4735) with manual reset and positive cut-off activated when capillary breaks (SPDT contact)

Suitable for domestic/commercial applications

| | |
|------------------------------------|-----------------|
| Capillary length | 1000 mm |
| Min. capillary bend radius | 5mm |
| Temp. rate of change | 1°K/min |
| Contact rating (SPDT) | 250 Vac 16 A |
| Body dimensions W x L x H | 32 x 44 x 36 mm |
| Overall size (excluding capillary) | 32 x 44 x 60 mm |

Appendix H

Risk Assessment

A risk assessment was conducted and carried out according to the procedures of the Department of Energy and Process Engineering. The risk assessment was documented and approved in advance of the experimental work. Due to the size of the document, only the front page with signatures have been attached.

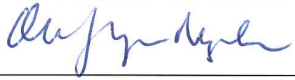
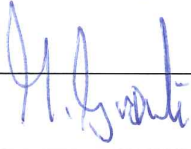
Risk Assessment Report

Oil-based Rig

| | |
|----------------------------|---|
| Prosjektnavn | Concentrated Solar Thermal Energy: experiment on oil-based system with heat storage |
| Apparatur | Oil-based Rig |
| Enhet | NTNU |
| Apparaturansvarlig | Ole Jørgen Nydal |
| Prosjektleder | Ole Jørgen Nydal |
| HMS-koordinator | Morten Grønli |
| HMS-ansvarlig (linjeleder) | Olav Bolland |
| Plassering | EPT – Varmeteknisk Lab |
| Romnummer | Rom C082 - Kjeller FlerfaseLab |
| Risikovurdering utført av | Silje Fosseng Duley |

Approval:

| | |
|---|--|
| Apparatur kort (UNIT CARD) valid for: | |
| Forsøk pågår kort (EXPERIMENT IN PROGRESS) valid for: | |

| Rolle | Navn | Dato | Signatur |
|----------------------------|------------------|------------|---|
| Prosjektleder | Ole Jørgen Nydal | 16/10/15 |  |
| HMS koordinator | Morten Grønli | 16/10-2015 |  |
| HMS ansvarlig (linjeleder) | Olav Bolland | | |